DOCUMENT RESUME

ED 182 115 SE 029 671

AUTHOR Astill, Kenneth N.
TITLE Elementary Experiments in Mechanical Engineering.
INSTITUTION New York Univ., Bronx. Dept. of Mechanical Engineering.
SPONS AGENCY National Science Foundation, Washington, D.C.
PUB DATE Feb 71
GRANT NSF-GY-2467
NOTE 138p.; Contains occasional light and broken type

EDRS PRICE MF01/PC06 Plus Postage.
DESCRIPTORS College Science; Curriculum Development; *Engineering Education; Higher Education; *Instructional Materials; *Laboratory Procedures; *Mechanics (Physics); Science Course Improvement Project; *Science Experiments; Undergraduate Study

ABSTRACT

Fourteen basic experiments in mechanical engineering, intended for use at the sophomore level, are presented. The experiments are described as open-ended in order to give students the opportunity to discover the importance of stable operating conditions. The concept of experimentation is introduced and there is an interrelation between theory and experiment. The experiments allow for modifications and some of these are given with the exercise. Each experiment does not depend on the previous one, but stands by itself. Sample results, curves, data, and calculations are also included. (Author/SA)

ELEMENTARY EXPERIMENTS IN MECHANICAL ENGINEERING

Kenneth N. Astill
Department of Mechanical Engineering
Tufts University

Sponsored by the National Science Foundation under Grant No. GY-2467
to Prof. Fred Landis of New York University

February 1971

ELEMENTARY EXPERIMENTS IN MECHANICAL ENGINEERING

Prepared by

Kenneth N. Astill
Professor of Mechanical Engineering
Tufts University
Medford, Massachusetts 02155

under Grant No. GY-2467 from the National Science Foundation

February 1971

This booklet is one in a series to provide resource material for Freshman-Sophomore courses. This work is being coordinated by Professor Fred Landis, Department of Mechanical Engineering, New York University, who serves as Project Director.

Additional copies may be obtained at $2.75 per copy from Professor Fred Landis
Department of Mechanical Engineering, New York University, Bronx, N.Y. 10453

Preface

The present booklet describes fourteen elementary experiments in Mechanical Engineering, of which more than half can be readily incorporated into a sophomore course. The book differs significantly from most laboratory manuals in its philosophy towards both the student and the instructor.

The student is introduced to the concepts of experimentation, to the inter-relation of theory and experiment, to the use of dimensionless quantities and to the vagaries of instrumentation with a minimum of prior theoretical background. Some of the experiments are open-ended so that students can learn early in their college career that a slight change in operating conditions can shift a problem from the trivial to the challenging. Perhaps most important is that many of the experiments involve transient situations; all too rarely are students introduced to the idea that the real world does not correspond to the steady state which is usually set up in the laboratory.

The instructor should appreciate the underlying simplicity of the experiments; little is demanded in terms of manufacturing and erection, and the instruments called for should be available in any undergraduate laboratory. Where needed, construction details are given in full. Furthermore sample results are presented; all experiments have been pretested with student groups.

In terms of required background knowledge, little is assumed for experiments 6, 7 and 12 which can be offered at any time during the sophomore year and may even be included in a freshman engineering course. Some knowledge of differential equations is desirable for experiments 1 through 5 with a dynamics course recommended for 2 and 3 and strength of materials for 1 and 4. Experiments 8 through 11, 13 and 14 are probably best offered during the junior year although for exceptional students or for special projects they might be suitable on the sophomore level.

Hopefully this set of experiments will make an impact in a field where all too long stereotyped performance tests have ruled the curriculum and where experimentation has been driven from the lower division years. If it can provide only a modicum of excitement about mechanical engineering problems and supplement the analytical diet of which so many sophomore complain, it will have served its purpose.

This booklet has been prepared under the sponsorship of the National Science Foundation (Grant No. GY-2467) and the continued assistance and patience of the Foundation is gratefully acknowledg

One free copy is being distributed to each accredited Mechanical Engineering Department. Additional copies will be available at nominal cost from the project director.

F. Landis, Chairman
Mechanical Engineering Department
New York University
Project Director

February 1971

Introduction

The objective of this work is to bring together a series of experiments in mechanical engineering which are understandable to students in their first and second years of the undergraduate program. While an effort has been made to maintain this level, it is to be expected that some sections will be too advanced for freshmen and sophomores. This is most apt to occur in the theoretical development, and in sections where one might expect this to happen there are notations in the text. Each experiment is relatively simple to construct and operate, and can be done using instrumentation normally available in undergraduate laboratories. There is no attempt to prepare a structured laboratory program. The order of experiments is arbitrary except in so far as they are grouped according to fields of study.

Each experiment is written in sufficient detail to be useful to the instructor or the student. Primarily, the text is designed as an instructor's manual. Theory is developed with considerable detail when that is necessary, and usually references are given for two sources where additional pertinent information can be found. Drawings are given of special equipment as well as diagrams for the experimental set-ups.

Each experiment has been executed successfully by undergraduates in the Department of Mechanical Engineering at Tufts University. Sample results, curves, data and calculations are given. Data can not always be guaranteed to be precise, but it is safe to say it is the best available from several sets of results. An object statement precedes each experiment. An effort has been made to insure that each description will stand by itself. It is not necessary to read the experiments that precede a particular experiment in order to understand it.

An objective of any experiment for the engineering undergraduate is to motivate the student and call on him to use his imagination and to be creative. All of the experiments can be modified so that the same apparatus can be used to do several distinct experiments or a succession of experiments. It would be improper to use the same experiment repeatedly for a succession of students, and that plainly is not the intent of setting these down. Some modifications are given in each of the experiments. A useful technique for introducing modifications is to have one group of students start an experiment, letting groups that follow build on the results of those who precede. In this way, the development of the experiment follows the pattern of long-term research programs. It also provides incentive for each group to present its results in a manner easily understood by the succeeding group. In the author's opinion, these experiments are best done with three students in a group.

In addition to the people cited in the text, I should like to acknowledge with appreciation the speoial contributions of several: Professor Fred Landis, for his confidence in me which he showed by asking me to undertake this task; Peter Boyce, a Tufts undergraduate, for preparing the drawings; Mrs. Irma Wallace and Mrs. Betty Steel for typing drafts and final copy; and to the students too numerous to list who performed the experiments so well.

Kenneth N. Astill
Tufts University
Medford, Mass.
1 February 1971

Table of Contents

Experiment No. 1

The Torsional Pendulum

The object of this experiment is to measure the frequency of a torsional pendulum and determine the stiffness of the system.

A simple, but useful piece of laboratory equipment is a length of music wire about six feet long with screw fasteners brazed on each end, Fig. 1-1a. One end is clamped in the ceiling, while the other is fastened to an object to form a torsional pendulum. A torsional pendulum oscillates about an axis, in this case the wire, as shown in Fig. 1-1b. Several interesting experiments can be developed from this system, but first the wire stiffness must be determined.

Wire calibration

To be useful, the stiffness of the wire must be known. For small oscillations, with negligible air resistance, the motion of a torsional pendulum can be described by the equation

$$I \frac{d^2\theta}{dt^2} + k\theta = 0 \qquad 1\text{-}1$$

where
- I = mass moment of the object about the axis of rotation
- θ = the angle of oscillation
- t = time
- k = the stiffness of the wire, radians per unit of torque

From the solution of this equation which is $\theta = A \sin(\omega_n t + \alpha)$ it is seen that the displacement is sinusoidal with a frequency, called the natural frequency, of $\omega_n = \sqrt{\frac{k}{I}}$, radians/second. (See ref. 1). In this expression, A is the amplitude and α a phase angle, found using the initial conditions. Using this information it is apparent that if we measure the frequency of the oscillation for an object of known inertia, we can calculate the stiffness k.

A calibration disc, Fig. 1-1c, was made from a solid cylinder of metal (aluminum). Its mass moment of inertia about its axis of rotation is

$$I = \frac{mR^2}{2} \qquad 1\text{-}2$$

where m is the mass of the disc and R its radius. Measuring the period of oscillation of the pendulum, the stiffness of the wire, k, can be determined from the expression for ω_n. There is a discussion of units included with sample results in the next section.

An assumption has been made that the mass-moment of inertia of the wire is negligible when compared to the inertia of the calibration disc. Each section of the wire turns through an angle between 0 and θ depending on its distance from the fastening point in the ceiling. Normally an "equivalent inertia" is defined as the inertia which would be added to the disc to produce the same effect as the inertia of the wire. As the wire turns through an angle less than θ, this is bound to be smaller than the inertia of the wire, I_{wire}. This equivalent inertia could be found experimentally. If, instead of I in eq. (1-1), we add

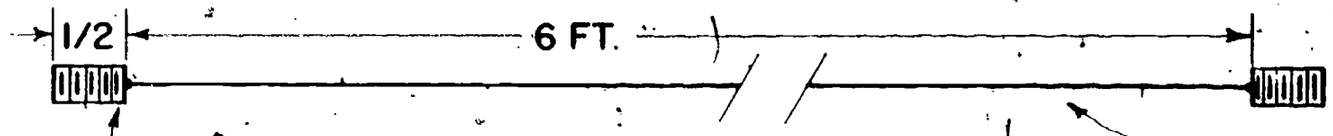

FIG. I-1a MUSIC WIRE

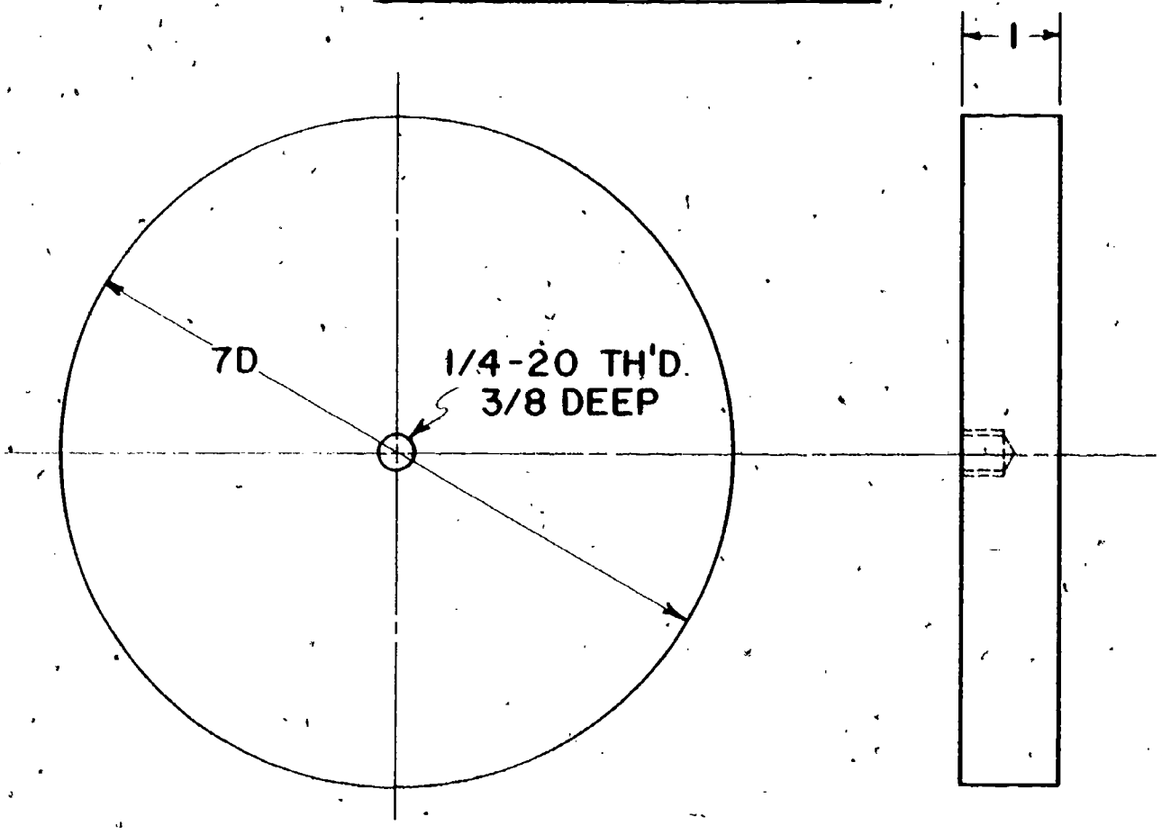

FIG. I-1c CALIBRATION DISC — ALUMINUM
HALF SCALE

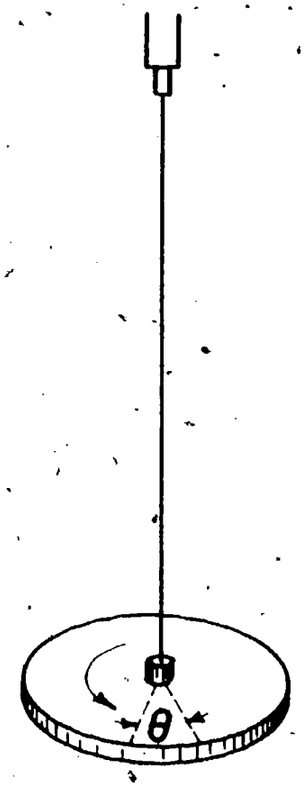

FIG. I-1b TORSIONAL
PENDULUM

the equivalent inertia to that of the calibration disc, I, then

$$\omega_1 = \sqrt{\frac{k}{I_1 + I_e}} \qquad 1\text{-}3$$

Now ω_1 can be measured, I can be computed from eq. 1-2, leaving two unknowns, I_e and k. Using a second disc of known inertia I_2 and repeating the measurement for ω_2, produces a second equation in k and I_e, which can be solved simultaneously with eq. (1-3). It is possible that the effect of I_e on the frequency is too small to measure accurately, as is quite likely the case here. It is a simple matter to determine I_e analytically for a wire or shaft of circular cross section (reference 2). The result is

$$I_e = \frac{I_{wire}}{3} \qquad 1\text{-}4$$

An assumption has been made in this analysis that the angular deflection of the wire is proportional to its distance from the point of attachment.

If is possible to compute k from the properties of the music wire using the shear modulus for the wire $G = s/\gamma$, in lbf/in^2.

where s = shear stress and γ = shear strain.

Let ℓ = length of wire

ϕ = angle of twist per unit length of ϕ/ℓ

A = cross-sectional area of the wire

r = radius of wire

then the moment required to twist a unit length of wire through an angle ϕ is

$$M = \int_A r \; s dA$$

$$= \int_A r \; G\gamma dA$$

$$\gamma = r\phi$$

Hence $$M = \int_{r_1}^{r_2} \phi r^2 \; G dA$$

$$M = \phi G J$$

Where J is the polar moment of inertia of the wire cross section

Now $k = \frac{M}{\theta}$, torque per angle of twist, where θ is the angle through which the end of the wire is twisted. In terms of θ, the deflection of each element is

$$\phi = \theta/\ell$$

Hence $$k = \frac{\phi G J}{\ell \phi} = \frac{GJ}{\ell} \qquad 1\text{-}5$$

Sample results

An experiment was conducted to determine the wire stiffness.

Dimensions of calibration disc:

mass: $m = 1671$ gm or 3.681 lbm

radius: $R = 9$ cm $\pm$ 0.1 cm or 0.295 ft

$I = 1/2 mR^2 = 1/2 (1671)(9)^2 = 6.77 \times 10^4$ gm-cm^2

or, in English units $I = (1/2)(3.68)(0.295)^2 = 0.160$ lbm-ft^2.

For five measurements of the period made with a stop watch, the average was

$\tau = 18.4$ sec. which corresponds to frequency of

$$\omega_n = \frac{2\pi}{\tau} = 0.34 \text{ radians/second}$$

$$k = \omega_n^2 I = (0.34)^2(6.77 \cdot 10^4)$$

$$= 0.783 \times 10^4 \text{ dyne-cm/rad.}$$

or

$$k = (.34)^2 \frac{(0.160)}{32.2}(12) = 0.00689 \text{ lbf-in/rad.}$$

This calculation required introduction of the two conversion factors

$g_o = 32.2$ lbm-ft/lbf-sec^2

and 12 in/ft to produce the units ordinarily used for k.

A value of k can be found using eq. (1-5). For the wire:

length: $\ell = 148$ cm$\pm$0.1 cm or
58.27 in $\pm$0.04 in

diameter: $d = 6.10 \times 10^{-2}$ cm or
2.4×10^{-2} in

$$J = \frac{\pi d^4}{32} = \frac{\pi(6.10)^4 10^{-8}}{32} \text{ cm}^4 \text{ or}$$

$$\frac{\pi(2.4)^4 10^{-8}}{32} \text{ in}^4$$

Shear modulus for music wire:

$G = 12.5 \times 10^6$ lbf/in^2 or

$(12.5 \times 10^6 \text{ lbf/cm}^2)(4.45 \times 10^5 \text{dynes/lbf})(0.155 \text{ in}^2/\text{cm}^2)$

$$= 8.62 \times 10^{11} \frac{\text{dynes}}{\text{cm}^2}$$

From eq. (1-5)

In cgs:

$$k = \frac{Gj}{\ell} = \frac{(8.62 \times 10^{11})\pi(6.0)^4 10^{-8}}{(148)(32)}$$

$$= 0.792 \times 10^4 \text{ dyne-cm/rad}$$

In English units:

$$k = \frac{(12.5 \times 10^6)\pi(2.4)^4 10^{-8}}{(59)(32)}$$

$$= 0.00690 \text{ lbf-in/rad.}$$

The experimental value is within 1% of these predictions.

To determine the effect of the mass-moment of inertia of the wire first compute

$$I_{wire} = \frac{(m_{wire})(r_{wire})^2}{2}$$

For this we require the

$$\text{Mass of the wire: } m_{wire} \approx \left(\frac{\pi d^2}{4}\ell\right)(\text{density}) = \frac{\pi(2.4)^2 10^{-4} 59(500)}{4\,(1728)}$$

$$= 7.72 \times 10^{-3} \text{ lbm}$$

The density chosen for the steel wire was 500 lbm/ft^3.

$$I_{wire} = \frac{(7.72)(1.2)^2 10^{-4}}{(2)} = 5.558 \times 10^{-4}$$

Then determine the effect on the inertia by introducing

$$I_e = \frac{I_{wire}}{3} = 1.85 \times 10^{-4}$$

The corrected inertia including this is

$$I_1 = I + I_e = 0.160 + .0002 = 0.1602$$

which is a change in the value of k of about 0.1%. This is small enough to neglect.

References

1. Church, A. H., Mechanical Vibrations, John Wiley and Sons, Inc., New York (1963) p23.
2. Crossley, F.R.E., Dynamics in Machines, The Ronald Press, New York (1954), p119.

Experiment No. 2

Damping a Torsional Pendulum

An electric galvanometer consists of a cylindrical core suspended on a filament. When the core moves, it carries an indicator such as a needle or mirror. It is necessary to damp the system so that it does not oscillate when the reading is changed, but comes to rest at the proper position. One suggestion is to immerse part of the core in a fluid so that the shear force between the fluid and the walls of the cylinder will provide damping.

> The object of this experiment is to obtain a relation between the geometry and the damping, as well as between fluid properties and damping. In addition, a second experiment will be proposed to examine the effect of a stationary concentric cylindrical wall on the damping.

Experiment No. 2A

Effect of Fluid Properties

A model of the system is shown in Fig. 2-1. It consists of a hollow cylinder, 3.867 in. diameter, 4 11/64 in. long. It is capped with a threaded hole to receive the end of the music wire. The cylinder weight is 2.321 lbm. A drawing with dimensions is given in Fig. 2-2. A paper is cemented on the top surface, having markings on the outer edge in degrees. This will be used to measure the angle of oscillation, by matching the lines with a stationary indicator at each end of the oscillation.

Using the music wire, the cylinder is allowed to oscillate in air and its period of oscillation determined. From the method described in Experiment 1 (which assumes air damping to be negligible) the inertia of the cylinder is found.

The pendulum is then allowed to oscillate in a liquid, as illustrated in Fig. 2-1, and the angular displacement measured as a function of time. For the fixed geometry of the cylinder, the variables of interest are: the kind of fluid used; the depth of immersion; and the distance between the cylinder wall and the container wall. In the practical case it was the last effect that was of most interest.

Development of theory

The objective was to determine the damping ratio for the damped single-degree system. This can be expressed in terms of the logarithmic decrement, δ, or the ratio of damped frequency, ω_d, to the natural frequency, ω_n. Damping ratio is the ratio between the coefficient of viscous damping, c, and the critical damping coefficient c_c. The development of these expressions can be found in any elementary book on vibrations, e.g., ref. 1 or 2.

To summarize this analysis briefly, begin with a statement of Newton's second law for the system. Equating the time rate of change of angular momentum ($I\ddot{\theta}$) to the sum of the resisting moments due to the spring ($-k\theta$) and the damping ($-c\dot{\theta}$) results in the governing differential equation

$$I\ddot{\theta} + c\dot{\theta} + k\theta = 0 \qquad 2\text{-}1$$

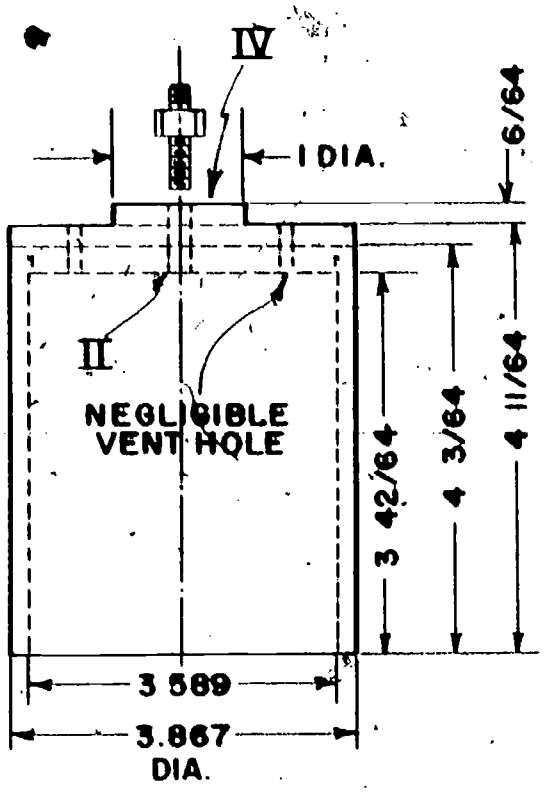

FIG. 2-2 HOLLOW CYLINDER

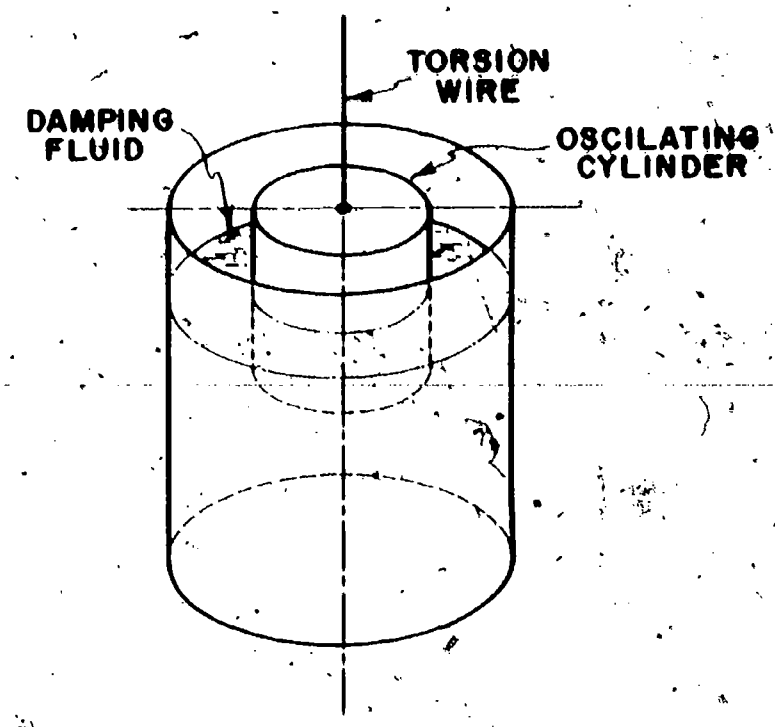

FIG. 2-1 EXPERIMENTAL MODEL OF GALVANOMETER DAMPING DEVICE.

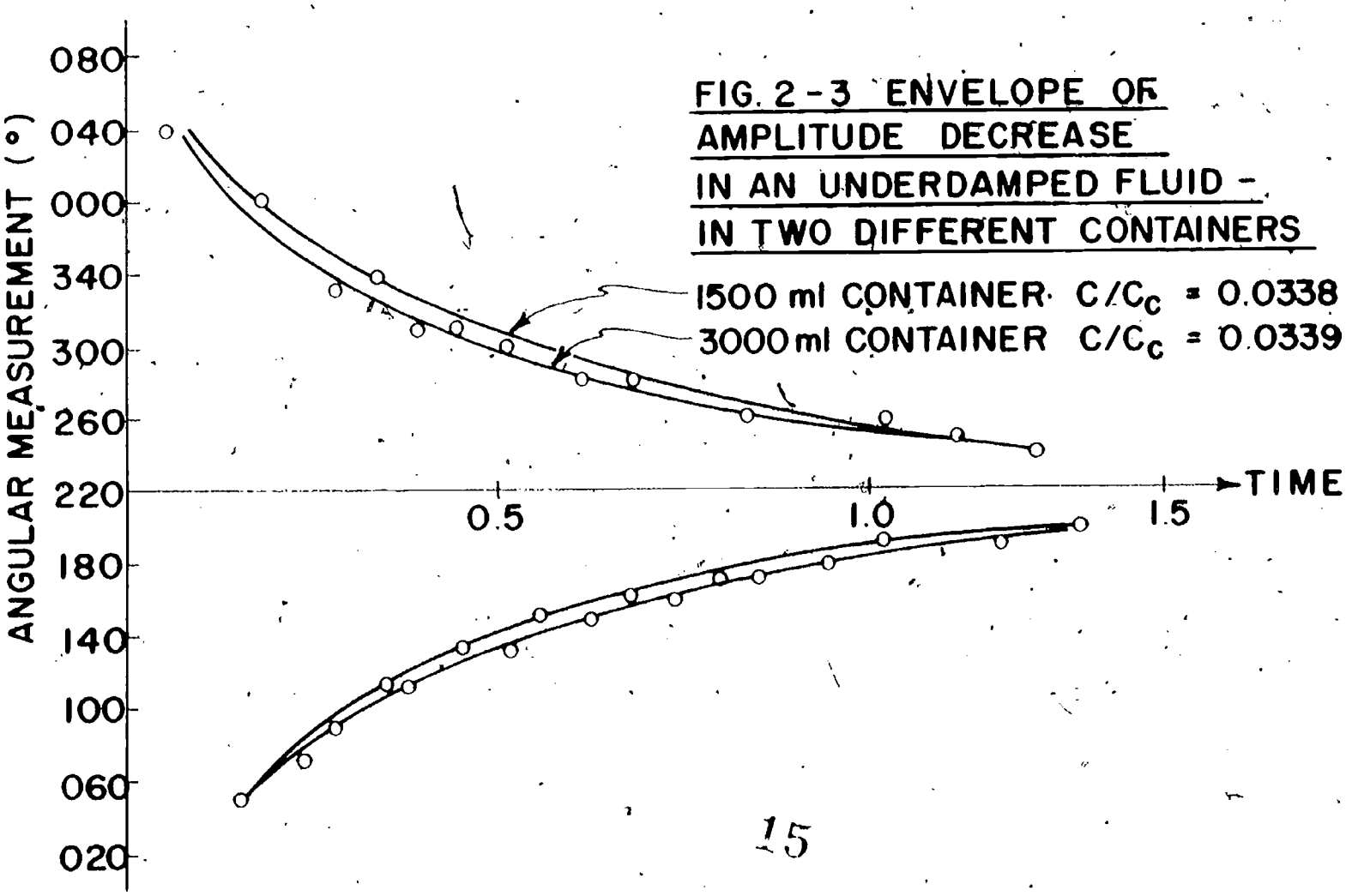

FIG. 2-3 ENVELOPE OF AMPLITUDE DECREASE IN AN UNDERDAMPED FLUID - IN TWO DIFFERENT CONTAINERS

where the dotted θ's are the second and first derivatives with respect to time. Introducing a trial solution of the form

$$\theta = Ae^{pt} \qquad 2\text{-}2$$

leads to the solution

$$\theta = A_1 e^{p_1 t} + A_2 e^{p_2 t} \qquad 2\text{-}3$$

where

$$p_1 = -\frac{c}{2I} + \sqrt{\left(\frac{c}{2I}\right)^2 - \frac{k}{I}} \qquad 2\text{-}4$$

and

$$p_2 = -\frac{c}{2I} - \sqrt{\left(\frac{c}{2I}\right)^2 - \frac{k}{I}}$$

The form of the solution depends on the nature of the term in the radical. When it is zero,

$$\frac{c}{2I} = \sqrt{\frac{k}{I}} \qquad 2\text{-}5$$

The system is said to be critically damped and the critical damping factor is

$$c_c = 2\ kI \qquad 2\text{-}6$$

This can be introduced into the expressions for p, by multiplying and dividing by

$$\omega_n = \sqrt{\frac{k}{I}} \qquad 2\text{-}7$$

The result is

$$p_{1,2} = \left[-\frac{c}{2\sqrt{kI}} \pm \sqrt{\frac{c^2}{4\ kI} - 1}\right]\sqrt{\frac{k}{I}} \qquad 2\text{-}8$$

$$= \left[-\frac{c}{c_c} \pm \sqrt{\left(\frac{c}{c_c}\right)^2 - 1}\ \right]\omega_n$$

The ratio c/c_c is sometimes expressed as ζ.

When $c/c_c > 1$, the system is said to be overdamped, and does not oscillate. Instead the amplitude decays exponentially from the initial state. Light damping or underdamping occurs when $c/c_c < 1$. Then the root is imaginary and the solution has the form of a damped sine wave.

$$\theta = \theta_o \frac{\omega_n}{\omega_d} e^{-\left(\frac{c}{c_c}\right)\omega_n t} \sin\left[\sqrt{1 - \left(\frac{c}{c_c}\right)^2}\,\omega_n t + \phi\right] \qquad 2\text{-}9$$

Here θ_o is the initial amplitude which decays in time according to the exponential expression $e^{-\left(\frac{c}{c_c}\right)\omega_n t}$. The frequency is called the damped frequency, ω_d, and is defined to be

$$\omega_d = \sqrt{1 - \left(\frac{c}{c_c}\right)^2}\ \omega_n \qquad 2\text{-}10$$

This is the actual frequency of the damped system, and can be measured. Finally, the phase angle ϕ can be determined from initial conditions.

Solving the expression for the damped frequency provides a means of determining the

damping ratio experimentally as

$$\frac{c}{c_c} = \sqrt{1 - \left(\frac{\omega_d}{\omega_n}\right)^2} \qquad 2\text{-}11$$

If ω_n is the frequency of the pendulum in air (undamped) and ω_d the measured frequency in the damping fluid, then c/c_c can be computed.

While the preceding procedure can be employed where damping is significant, it is difficult to determine c/c_c experimentally when damping is small because ω_d is approximately equal to ω_n. An alternate procedure is to measure the amplitude of the oscillation, θ, on two successive oscillations, θ_1 and θ_2. Let two swings be at times t_1 and $t_1 + \tau$ where τ is the period of the damped pendulum. Then since the sine part of the expression is the same in each case, the ratio of the two amplitudes is

$$\frac{\theta_1}{\theta_2} = \frac{e^{-\frac{c}{c_c}\omega_n t_1}}{e^{-\frac{c}{c_c}\omega_n (t_1+\tau)}} = e^{\frac{c}{c_c}\omega_n \tau} \qquad 2\text{-}12$$

The logarithmic decrement δ is defined as the logarithm of the ratio of successive amplitudes, or

$$\delta = \ln \frac{\theta_1}{\theta_2} = \left(\frac{c}{c_c}\right)\omega_n \tau \qquad 2\text{-}13$$

For a more accurate experimental determination of δ, it is better to compare two peak amplitudes that are several oscillations apart, say n. Then it is easy to show that the logarithmic decrement between the ith peak and the $(i + n)$th peak becomes

$$\delta = \frac{1}{n} \ln \frac{\theta_i}{\theta_{i+n}} \qquad 2\text{-}14$$

But the period is related to the damped frequency by the expression

$$\tau = \frac{2\pi}{\omega_d} = \frac{2\pi}{\omega_n \sqrt{1 - \left(\frac{c}{c_c}\right)^2}} \qquad 2\text{-}15$$

With this substituted in the expression for the logarithmic decrement, the damping ratio can be expressed as

$$\frac{c}{c_c} = \frac{\delta}{\sqrt{4\pi^2 + \delta^2}} \qquad 2\text{-}16$$

Sample results

For the cylinder oscillating in air, the damping was too small to determine the amplitude change, so the value of δ was assumed to be small and ω set as ω_n. For the system tested $\omega_n = 58.4$ rad/min. The inertia of the cylinder was found to be 4.46 lbm-in^2, using the music wire calibrated in Experiment 1.

In one experiment water and glycerin were compared. It was found that for water, the damping was small and it was more accurate to measure amplitude, while changes in frequency of the glycerin-damped system were more accurately obtained. Some results are given in the

following table for tests in containers of several sizes. The effect of the container wall is evident in the results.

Fluid	Container	δ	ω	c/c$_c$
Air	None	-	58.1	
Water	5 qt. pail	.213	-	.0340
	1500 ml beaker	.201	-	.0338
	3000 ml beaker	.197	-	.0339
Glycerin	5 qt. pail	-	31.9 rad/min	.837
	1500 ml beaker	-	20.2 rad/min	.938

The glycerin is a more effective damping fluid than water and the effect of the wall is more pronounced. The smaller gap (1500 ml beaker) produced more effective damping than the larger (5 qt. pail). Curves of amplitude and the envelope of the amplitude are shown in Fig. 2-3 for the 1500 ml beaker.

Experiment 2B

Effect of a Concentric Wall

In the proposed galvanometer system, a concentric wall will be employed to improve the damping. The object of this experiment is to determine the relation between damping and wall location. The cylinder is allowed to oscillate in glycerin in a large container. A concentric wall is introduced as shown in Fig. 2-1. In this case the wall can be made from a sheet of thin aluminum so it can be adjusted to several diameters. As the cylinder is 3.867 in. in diameter, the gap will be half the difference between wall diameter and 3.867. Tests then can be made by determining amplitude as a function of time for the torsional oscillation, for several wall diameters.

Some results

Damping in these tests was more severe than in those for Experiment 2A. It was overdamped so that the pendulum did not oscillate. Amplitude was ready by several observers at intervals and recorded. A more accurate measure would be to use stroboscopic light and record the position by multiple exposures on camera film. The angular displacements could then be taken from photographs.

Curves of displacement versus time (Fig. 2-4) show the interesting result of an optimum wall diameter of 5 inches. Larger diameters lead to a partial oscillation while smaller diameters are so heavily damped that the cylinder requires too much time to come to rest.

References

1. Church, A. H., Mechanical Vibrations, John Wiley & Sons, Inc., New York City (1963), pp 69-92.
2. Thomson, W. T., Vibration Theory and Applications, Prentice-Hall, Inc., Englewood Cliffs, N. J. (1965), pp 36-47.

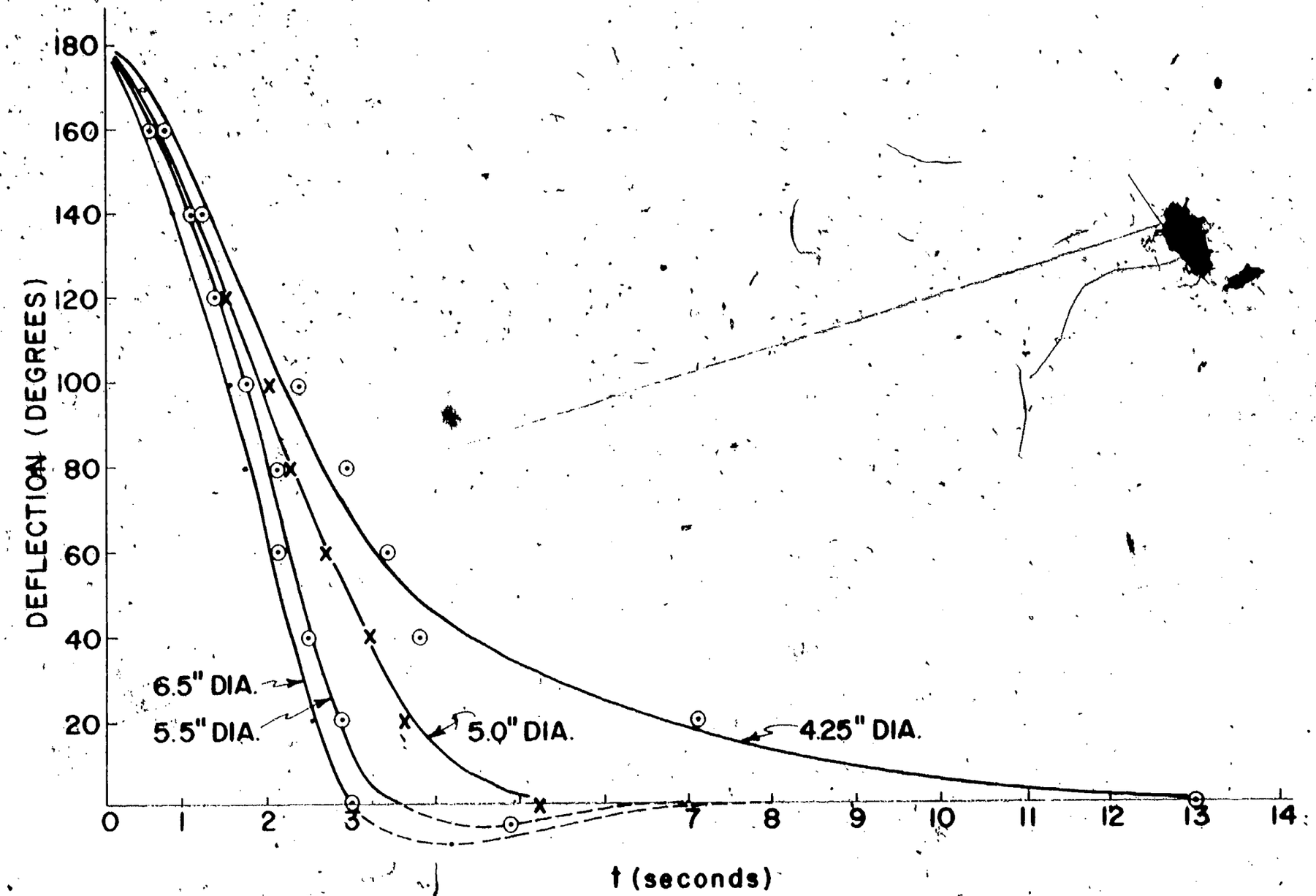

FIG. 2-4 EFFECT OF A CONCENTRIC WALL ON THE DAMPING OF A TORSIONAL PENDULUM. THE FLUID IS GLYCERINE. WALL DIAMETERS ARE SHOWN ON THE CURVES. CYLINDER DIAMETER = 3.867 in.

Experiment No. 3

The Effect of Fluid Forces on Oscillating Systems

The object of this experiment is to investigate the effect a sloshing fluid has on a dynamic system.

Introduction

In the previous experiments the pendulum was a solid mass, and the position of each element in the mass was fixed with respect to each other. If, during the oscillation, the pendulum interacts with a fluid, the fluid will be set in motion through viscous interaction and pressure forces. The fluid will then move at a speed which is different from the speed of the pendulum. In solving equations of motion, the mass of the fluid, so excited, will increase the mass or inertia term as well as contribute to the damping term. But as the velocities of the fluid and solid surface are different, the effective increase in inertia will be different from the actual mass or inertia of the fluid. It can be described as an equivalent mass or inertia. This is a difficult problem to analyze but experimental results will be useful in understanding the behavior. In addition, these experiments provide an opportunity to examine dimensionless numbers.

Dimensionless numbers allow generalization from an experimental result. For example, if one says a measured length is accurate to within one foot, it may not carry much meaning, as it would be good or poor depending on the length measured. If, instead, the error was one foot in a length of 4000 feet, then one can express this error as a dimensionless number, 1/4000, which gives an indication of the accuracy. A more complicated expression is the drag coefficient of a body moving through a fluid medium. This is the ratio of the resistance force created by the fluid to the force equivalent of the velocity pressure $\frac{\rho v^2}{2}$. Using C_D to represent the drag coefficient and A, a projected frontal area of the body, this is traditionally written

$$C_D = \frac{\text{Drag}}{(\frac{\rho v^2}{2})\, A} \qquad 3\text{-}1$$

In dimensions of force (F), mass (M), length (L) and time (T) we see that

$$\begin{aligned} \text{Drag} &= \text{force, } F \\ \rho &= \text{density of the fluid, } M/L^3 \\ v &= \text{velocity, } L/T \\ A &= \text{area, } L^2 \end{aligned}$$

and

$$C_D = \frac{F}{(\frac{M}{L^3})(\frac{L}{T})^2} L^2 = \frac{F\text{-}T^2}{ML} \qquad 3\text{-}2$$

There is a redundancy here as we know that force, mass, length and time are related by Newton's law as

$$F = M\frac{L}{T^2}$$

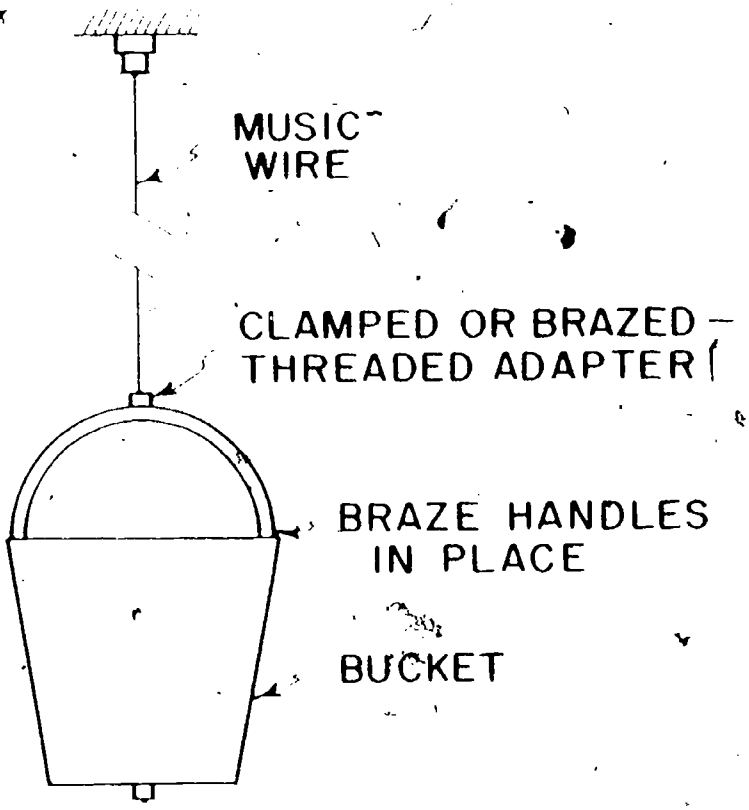

FIG. 3-1 A TORSIONAL PENDULUM USING A BUCKET

Consequently

$$C_D = \frac{ML}{T^2}\left(\frac{T^2}{ML}\right) = \text{dimensionless.}$$

Reynolds number

$$\frac{\rho v D}{\mu} \qquad 3\text{-}3$$

with

D = a length (L)

μ = viscosity ML/T

is another useful dimensionless expression in fluid mechanics. Experimental results for the fluid drag on bodies, such as a sphere, show that a curve of C_D versus Re is independent of the size of the sphere or the properties of the fluid. Thus results from a single experiment can be applied to other similar systems.

Experiment 3A

Fluid Mechanics in a Torsional Bendulum*

A simple but effective experiment can be made using a common bucket as a torsional pendulum. The handles of the bucket are brazed to prevent swinging, and a clamp of some sort fastened to the handle. Fitting the clamp with a 1/4-20 thread allows it to be attached to the music wire of Experiment 1 to form a torsional pendulum. This is illustrated in Fig. 3-1. Having calibrated the stiffness of the wire, the mass-moment of inertia of the pail can be determined using the procedure of Experiment 1.

Next, the bucket can be filled to different levels with sand or other granular material. The inertia can be determined using the music wire, and might be graphed against the mass of the sand in the bucket. It is possible to separate the contribution to the total inertia due to the sand. It would be best if a granular substance having the density of water were used to compare these results to the next part of the experiment using water.

A more interesting experiment results when the bucket is filled with liquid. This problem is a difficult one, but it offers an opportunity for the student to select dimensionless variables and determine their appropriateness. One can define a linear damping factor, c, from eq. (2-1). Using inertia determined from the sand experiments, and the wire stiffness evaluate c as in Experiment 2. It is found from the experiment that this is very nearly constant for any given run. The damping factor can be related to a characteristic Reynolds number and compared graphically to determine if this is a suitable scaling parameter for the damping factor. Variations in Reynolds number can be obtained by using fluids of different viscosity or density and by filling the bucket to different depths.

A Reynolds number in this case can be defined as the ratio of the torque at the wall due to the fluid momentum divided by the wall torque due to viscous forces at the wall.

Then

$$\text{Re} \equiv \frac{(\text{mass of fluid})\,(\text{velocity at wall})\,(\text{wall diameter})}{(\text{viscous stress})\,(\text{wall area})\,(\text{wall diameter})}$$

*This experiment was based on one by Professor William C. Reynolds, of Stanford University which appears in ref. 1.

Introducing the properties from this problem the Reynolds number is

$$Re = \frac{\rho\dot{\theta}D^2}{\mu}$$

D = bucket diameter

μ = viscosity of liquid

ρ = density of liquid

$\dot{\theta}$ = angular velocity of bucket

As we require a single value for $\dot{\theta}$, we can recognize that.

$$\dot{\theta} = A\omega \sin \omega t \qquad 3\text{-}4$$

where A is an amplitude and ω the frequency of the oscillation.

Then

$$Re = \frac{\rho\omega D^2}{\mu} \text{ or } \frac{\rho A\omega D^2}{\mu} \qquad 3\text{-}5$$

Whether or not the initial displacement or amplitude should enter is a question to be examined experimentally.

This experiment provides a good example of a very difficult problem in which dimensional analysis is a profitable tool to employ. In fact, by experimental measurement, the rather long list of important variables can be narrowed. For example, the ratio of spring constant to moment of inertia is important, but not these individual quantities. Fluids of differing viscosity and density can be used. In addition, the spring constant can be changed by shortening or lengthening the wire, and the moment of inertia changed by adding mass external to the bucket, so that the dimensionless parameters can be varied in a number of ways, and the scaling laws given a thorough test.

Technique is not too important. With periods of the order of 5-10 seconds it is an easy matter to measure the amplitude at the zero velocity points by marking on polar graph paper, and noting the time on a stop watch. One must be careful in locating the clamp to have it above the center of mass of the bucket, lest lateral swinging motions be excited when the torsional pendulum is allowed to oscillate. With water in a one gallon bucket, the amplitude is down about 50 percent after about six swings, so the experiments go rapidly. A three-man group can get more data than it can process in a matter of an hour or two.

The flow patterns during the oscillation can be observed by introducing dye near the wall and along the bottom of the bucket. Through these patters, the relationship between the motion of the bucket and the motion of the liquid can be examined.

Experiment 3B

A Torsional Pendulum with Two Degrees of Freedom

It is simple to modify this experiment to one having two degrees of freedom by connecting a second bucket similar to the first with a second music wire as shown in Fig. 3-2. This is said to be a system of two degrees of freedom because it requires two independent coordinates to describe the position of elements of the system. In this case, it is the angular position of each bucket with respect to the ground. This system has two natural frequencies,

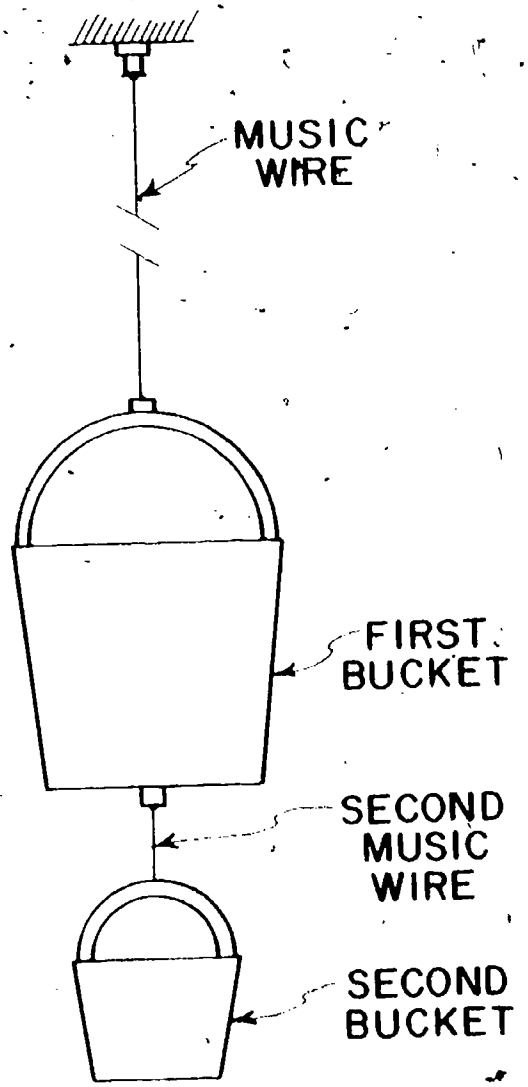

FIG. 3-2 TORSIONAL PENDULUM

which can be observed if the oscillation is started in just the right way. Normally the motion will be the result of combinations of the two "modes" of oscillation associated with the two natural frequencies. Analyses and examples of free vibration (no damping) for systems of two degrees of freedom are given in most elementary texts in vibration such as refs. 2 and 3.

Results are better if the two wires have the same or nearly the same stiffness. It will be necessary to determine the stiffness of both wires by the method of Experiment 1 as well as the moment of inertia of each mass. The attractive aspect of this system is that the inertia of either mass can be changed by simply changing the amount of sand added to each bucket. The motion will follow the behavior predicted by the vibration analysis quite well and can be related to the inertia of the two masses and the stiffness of the two wires; that is, to the natural frequency of each individual pendulum,

$$\sqrt{\frac{k}{I}}$$

To produce a more complex system, damping can be introduced by adding water to the buckets instead of sand. This system is too complicated to attempt to analyze but provides an opportunity to study the motion through experiment.

Experiment 3C

Fluid Mechanics in a Simple Pendulum

> The objective is to determine the effects on damping of a simple pendulum resulting when the mass of the pendulum oscillates through a liquid.

A design calls for damping the motion of a simple pendulum by allowing the weighted end to oscillate in a liquid. An experimental model was constructed as shown in Fig. 3-3. It consisted of a pendulum oscillating on a hardened steel knife edge taken from an old weighing balance. The pendulum bob was rectangular in cross section. It was constructed so the pendulum bob could be in the position shown or at right angles to it. A large tub was filled with water and placed under the pendulum so that the bob was submerged for small angles of oscillation. Tests were then made to measure the frequency and logarithmic decrement in an effort to evaluate the effect on the motion produced by the water.

For a simple pendulum with a mass, m, assumed to be concentrated at a length ℓ from the fulcrum, the restoring force due to gravity, g, is $-mg\ell \sin\theta$. These forces are shown in the illustration, Fig. 3-4. Expressing Newton's law for the pendulum,

$$m\ell^2 \frac{d^2\theta}{t^2} = -mg\ell \sin\theta \qquad 3\text{-}6$$

For small deflections, $\theta \approx \sin\theta$ eq. (3-6) becomes

$$\frac{d^2\theta}{dt^2} + \frac{g}{\ell}\theta = 0 \qquad 3\text{-}7$$

for which the natural frequency, ω_n, is

$$\omega_n = \sqrt{\frac{g}{\ell}} \qquad 3\text{-}8$$

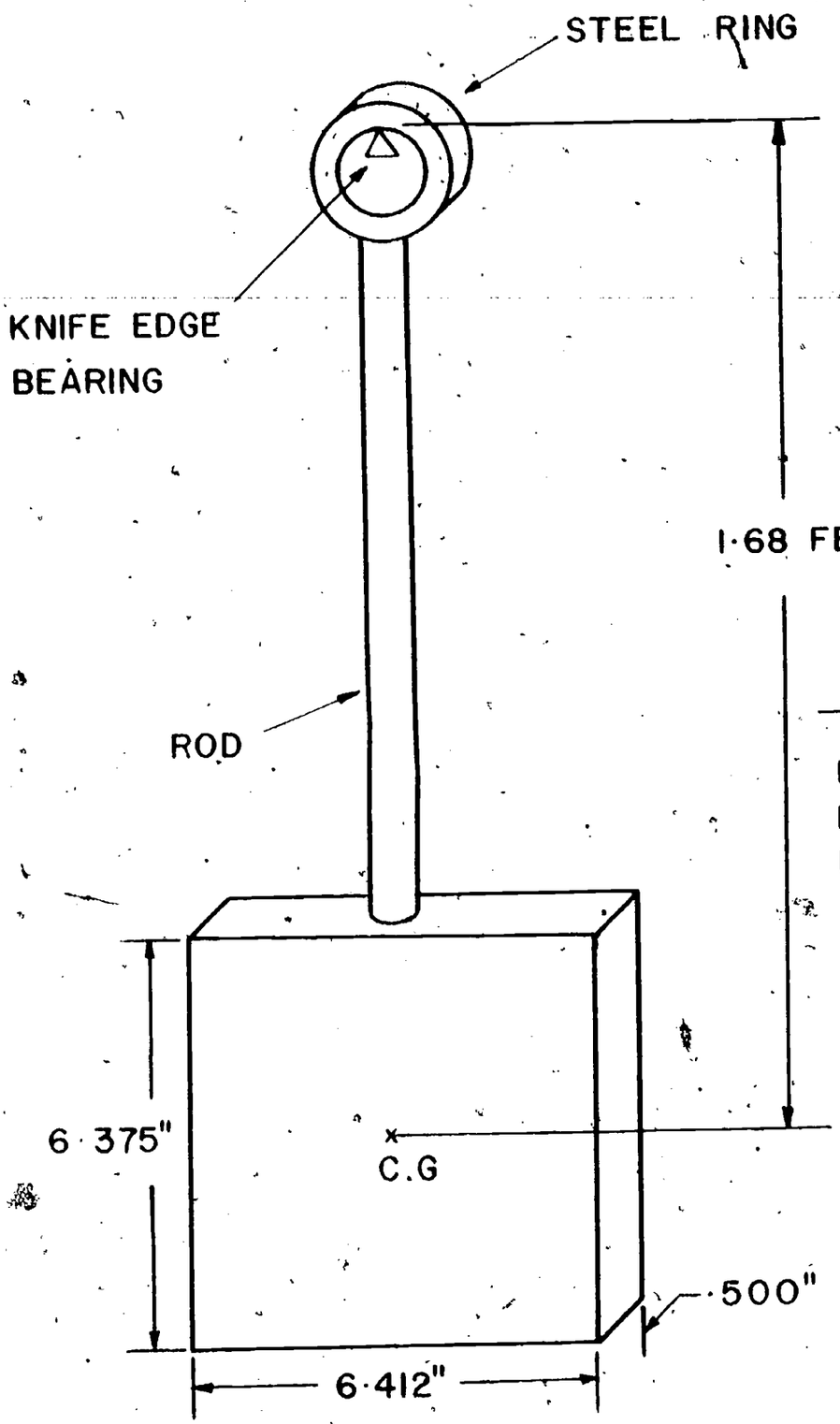

FIG. 3-3 DIAGRAM OF APPARATUS

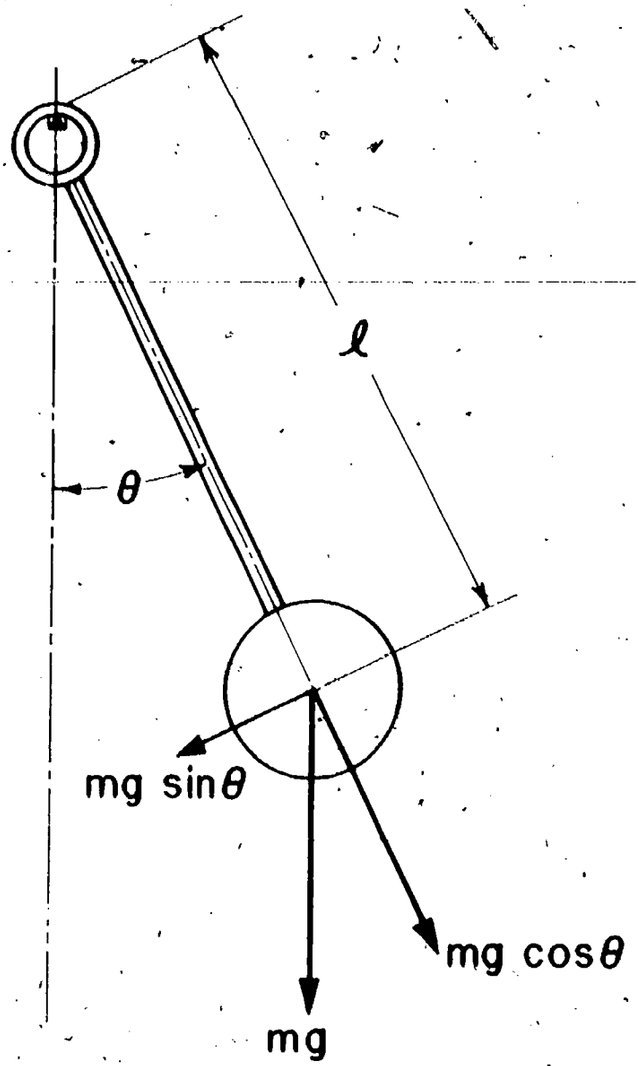

FIG. 3-4 FORCES IN A SIMPLE PENDULUM

and the period

$$\tau = 2\pi\sqrt{\frac{\ell}{g}} \qquad 3\text{-}9$$

The development of this solution directly parallels that for eq. (1-1) (see also ref. 4). This expression for the period can be compared experimentally to the period of the pendulum measured in air. For the pendulum of Fig. 3-3, the mass is not concentrated at a point which will result in a slightly different period from that given by eq. (3-9).

When the pendulum oscillates in the water, damping will result due to the resistance of the water. In addition, the pendulum will induce some of the water to move with the pendulum, which adds to the mass in the equation of motion. The liquid will also affect the restoring force. Consequently eq. (2-1) will be written in terms of equivalent mass, damping and restoring force, M_e, c_e, K_e respectively. Assuming that the equivalent mass is concentrated a distance ℓ from the fulcrum, the moment of inertia about the fulcrum is $M_e\ell^2$ and eq. (2-1) becomes, for small θ,

$$M_e\ell^2\ddot{\theta} + C_e\dot{\theta} + K_e\theta = 0 \qquad 3\text{-}10$$

Now we can express the equivalent mass as the mass of the pendulum M plus the equivalent mass effect of water, e,

$$M_e = (M + e) \qquad 3\text{-}11$$

Damping is caused by the resistance of the water to the pendulum motion. This can be expressed in terms of the drag coefficient, which is known for flat plates, see ref. 5 or 6. Referring back to eq. (3-1) for the definition of drag coefficient, C_D, and recognizing that each term in eq. (3-10) must be a moment about the fulcrum, then

$$C_e\dot{\theta} = (\text{Drag}) \cdot \ell = \frac{C_D\rho v^2}{2} A \cdot \ell$$

A is the area of the pendulum normal to the direction of motion. But the velocity of the pendulum bob is

$$v = \ell\dot{\theta}$$

Hence

$$C_e\dot{\theta} = C_D\frac{\rho\dot{\theta}^2 A\ell^3}{2}$$

from which we conclude that

$$C_e = \frac{C_D\rho\dot{\theta}\ell^3 A}{2} \qquad 3\text{-}12$$

Finally the restoring torque involves not only the weight of the pendulum but the bouncy effect due to the liquid. Hence the restoring moment for small θ,

$$K_e\theta = \left[mg - (At)\rho g\right]\theta$$

and

$$K_e = \left[mg - At\rho g\right]\ell \qquad 3\text{-}13$$

It is important to verify that each term in eq. (3-10) has the same dimensions, i.e. ML^2T^{-2}.

To relate the quantities expressed above to measurable quantities, we can use several expressions from Experiment 2. Defining, for convenience,

$$\frac{c}{c_c} = \zeta$$

equation 2-10 for the damped frequency is

$$\omega_d = \sqrt{1 - (\zeta)^2}\ \omega_n \qquad 3\text{-}14$$

Combining eqs. (2-13), (2-14) and (2-15),

$$\delta = \frac{1}{n} \ln \frac{\theta_i}{\theta_{i+n}} = \frac{2\pi\zeta}{\sqrt{1-(\zeta)^2}} \qquad 3\text{-}15$$

with eq. (3-10), eq. (3-11) is

$$\delta = 2\pi \sqrt{\left(\frac{\omega_n}{\omega_d}\right)^2 - 1} \qquad 3\text{-}16$$

Referring now to the expression for c_c, eq. (2-6), the damping factor can be written as

$$C_e = c_c \zeta = 2\sqrt{K_e I_e}\ \zeta$$

Noting that $\omega_n = \sqrt{K_e / I_e}$

$$C_e = 2\zeta \frac{K_e}{\omega_n} \qquad 3\text{-}17$$

and

$$I_e = \frac{C_e}{2\zeta\omega_n} = \frac{K_e}{(\omega_n)^2} \qquad 3\text{-}18$$

The experiment-

The specific objectives of the experiment are to evaluate the equivalent mass of the liquid and the equivalent damping from measurements on the pendulum. Simple physical measurements were made to determine the pendulum mass, area and volume. The pendulum was allowed to swing in the water. A Polaroid camera was used and the shutter opened for a swing of the pendulum. After several measured swings (n) the camera shutter was opened again. The exposure in each case was long enough to record the extreme position of the pendulum. This showed quite clearly as the arm came to rest at that point. During this interval, the damped frequency was measured counting swings with a stop watch. The experiment can be run with the bob as shown in Fig. 3-3 or at right angles to it.

The procedure for determining the equivalent mass and damping were:

1. With liquid properties determined, the equivalent stiffness, K_e, can be found from eq. (3-13).
2. Measuring θ at the two exposures δ was calculated from eq. (3-15).

3. Knowing δ and having measured ω_d, ω_n was computed from eq. (3-16).

4. Now ζ was calculated from eq. (3-14) or (3-15) as

$$\zeta = \sqrt{1 - \left(\frac{\omega_d}{\omega_n}\right)^2}$$

5. Having found ζ, K_e and ω_n, the equivalent damping was found with eq. (3-17).

6. With K_e and ω_n eq. (3-18) was solved for I_e.

7. From the relation

$$I_e = (M + e)\,\ell^2$$

a value for the equivalent mass of the water was found.

Sample results

Step 1. For the pendulum shown in Fig. 3-3 oscillating in water (ρ=62.4 lbm/ft^3), the equivalent stiffness is

$$K_e = [5.75 - (.018)(62.4)]\,(32.2)(1.68)$$

$$= 250\ \frac{\text{lbm-ft}^2}{\text{sec}^2}$$

(Note: if K_e is divided by the conversion factor $g_o = 32.2\ \frac{\text{lbm-ft}}{\text{lbf-sec}^2}$, the result is 7.77 lbf-ft, which is properly torque.)

Step 2. Experiments were made with the pendulum mass as shown in Fig. 3-3 and with the broad edge of the pendulum normal to the path of the arc. For the latter case, the damped frequency was 25 cycles per minute and the logarithmic decrement measured from the photographs was 1.20.

Step 3. From equation (3-16),

$$\left(\frac{\omega_n}{\omega_d}\right)^2 = \left[\left(\frac{\delta}{2\pi}\right)^2 + 1\right] = \left(\frac{1.20}{2\pi}\right)^2 + 1 = 1.101$$

$$\omega_n = \sqrt{1.101}\cdot 25 = 26.2 \text{ cycles/in}$$

or 2.75 rad/sec.

Step 4. The damping ratio, equation (3-15) is

$$\zeta = \sqrt{1 - \frac{1}{1.101}} = 0.303$$

Step 5. From (3-17), the equivalent damping was

$$C_e = \frac{(2)(0.303)(250)}{2.75} = 55.1\ \frac{\text{lbm-ft}^2}{\text{sec}^2}$$

$$\text{or } \frac{55.1}{32.2} = 1.71 \text{ lbf-ft-sec}$$

Step 6. The equivalent inertia, I_e is from eq. (3-18)

$$I_e = \frac{K_e}{(\omega_n)^2} = \frac{250}{(2.75)^2} = 33.1 \text{ lbm-ft}^2$$

which is equivalent to a mass of

$$M_e = \frac{33.1}{(1.68)^2} = 11.71 \text{ lbm.}$$

Step 7. Mass equivalent of the water is

$$d = 11.71 - 5.75 = 5.96 \text{ lbm}$$

Based on the results of Stelson and Mairs (ref. 7) the equivalent mass, M_e, should have been 13.6 lbm. This is 14% larger than that determined above.

An equivalent drag coefficient can be estimated for the plate using eq. (3-12) and the computed damping coefficient 1.71 lbf-ft-sec. A velocity is required and the average was assumed to be $\omega_d/\sqrt{2}$.

Then

$$C_D = \frac{(1.71)(32.2)}{(62.4)(1.68)^3}(0.272)\left(\frac{2.75}{1.414}\right)$$

$$= 0.351$$

This is about 1/3 of what one might anticipate for the drag coefficient from experimental results (ref. 5 or 6). This discrepancy could be examined by further experiment. It is quite likely that a more appropriate way of selecting "average velocity" could be made.

Two additional observations can be made regarding the experiments. Results for the pendulum turned with its narrow edge normal to the motion were comparable to the above in their agreement with ref. 7, and in the magnitude of the discrepancy in determining C_D. Several tests were made for each case, varying θ at the start of the test from 5° to 22°. The damped frequency was unaffected for this variation in the starting condition.

References

1. Landis, F. L. et al, Laboratory Experiments and Demonstrations in Fluid Mechanics and Heat Transfer, New York University, New York, New York (1964), p.24.
2. Church, A. H., Mechanical Vibrations, John Wiley and Sons, New York, N. Y. (1963), pp. 221-256 and p. 289.
3. Thomson, W. T., Vibration Theory and Applications, Prentice-Hall, pp. 159-171 (particularly problems 1 and 2, p. 200).
4. Church, A. H., (op. cit.), p. 28.
5. Street, V. L., Fluid Mechanics, 5th ed., McGraw Hill, New York, New York (1971), p. 271.
6. Hunsaker, J. C. and R. G. Rightmire, Engineering Applications of Fluid Mechanics, McGraw Hill, New York, New York (1947), p. 198.
7. Stelson, T. E. and F. T. Mairs, "Virtual mass and acceleration in fluids", Trans. of ASME, vol. 122, (1957), p. 518.

Experiment No. 4

Internal Damping in Structural Material

Prepared by Robert Greif
Associate Professor of Mechanical Engineering
Tufts University

The object of this experiment is to define analytically and measure experimentally the internal damping properties of structural materials.

Introduction

This experiment brings together, in a laboratory setting, some concepts in materials and dynamics that the student learns during his first two years of engineering education. Some of the more pertinent aspects are

i) modeling a beam as an equivalent spring

ii) modeling material damping behavior in terms of equivalent viscous damping

iii) clear determination of the relative damping properties of various common engineering materials and the possible variation of this damping effect with frequency.

Nomenclature:

- m - mass of cantilever beam
- M - mass of tip load
- y - deflection of tip mass
- ℓ - length of beam
- I - moment of inertia of cross-section
- E - elastic modulus of beam
- t - time
- K - equivalent spring constant; $K = 3EI/\ell^3$
- c - damping constant
- c_c - critical damping associated with viscous damping, $c_c = 2M\omega_n$
- ω_n - undamped natural frequency; $\omega_n = \sqrt{K/M}$
- ω_d - damped natural frequency; $\omega_d = \omega_n \sqrt{1-\zeta^2}$
- ζ - dimensionless damping ratio; $\zeta = c/c_c$
- η - material damping factor (dimensionless)
- δ - logarithmic decrement

Discussion

The basic experiment involves the free transverse vibration of a tip loaded cantilever beam and the measurement of the resultant amplitude decay. The first step in the analysis is to model the cantilever as an equivalent single degree of freedom mass spring system Fig. 4-1.

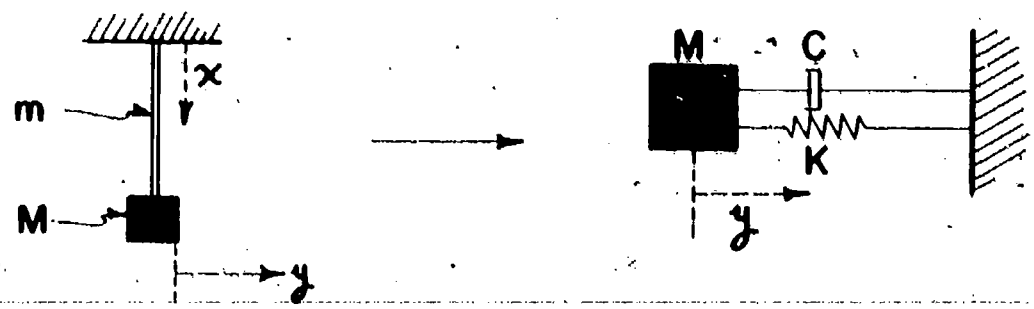

$M \gg m$

$K = 3EI/L^3$

FIG. 4-1 EQUIVALENT SINGLE DEGREE OF FREEDOM SYSTEM

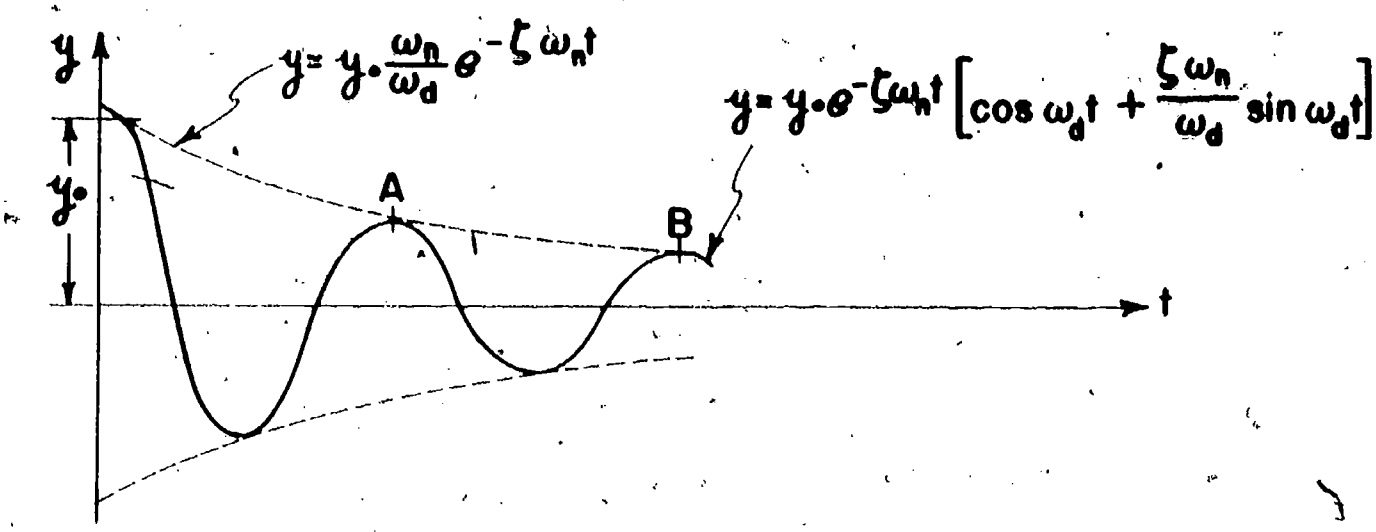

FIG. 4-2 RESPONSE OF DAMPED SYSTEM WITH INITIAL DISPLACEMT. y_0

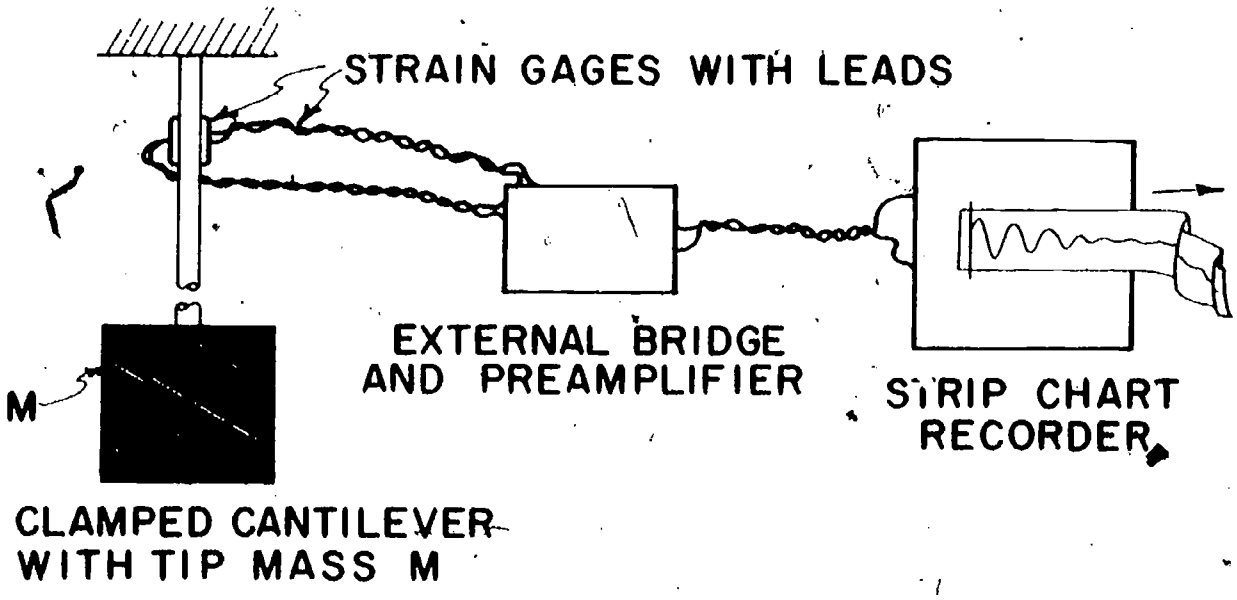

FIG. 4-3 EXPERIMENTAL SETUP FOR DAMPING EXPERIMENT

In the following, it will be assumed that $M>>m$ so that the beam is essentially acting as a spring for the tip mass M.[1] The stiffness, or spring constant, K may be derived from "strength of materials" considerations for a cantilever subjected to a tip load. This load, divided by the deflection at the tip $(x = \ell)$ due to this load, gives the following value of K (ref. 1)

$$K = 3EI/\ell^3 \ [\text{lbf/in}] \qquad 4\text{-}1$$

The quantity c is not the usual constant associated with the viscous damping of a dashpot but is related to the material damping factor η that we are seeking to find in this experiment. However, for the time being we shall take c as a constant; application of Newton's law to the single degree of freedom system of Fig. 4-1 then leads to the following second order, linear ordinary differential equation, with constant coefficients, (ref. 2).

$$M\frac{d^2y}{dt^2} + \frac{cdy}{dt} + ky = 0 \qquad 4\text{-}2$$

Normally, this equation is put in more useful engineering form by introducing the following terms: c_c, the critical damping associated with viscous damping $(=2M\omega_n)$; ζ, the dimensionless damping ratio $(=c/c_c)$; and ω_n the undamped natural frequency. Then eq. (4-2) becomes

$$\frac{d^2y}{dt^2} + 2\zeta\omega_n\frac{dy}{dt} + \omega_n^2 y = 0 \qquad 4\text{-}3$$

and its solution for a system with an initial displacement $y(o) = y_o$ but with zero velocity $(dy/dt)_{t=o} = 0$, in an underdamped situation of $\zeta<1$, is (ref. 2).[2]

$$y = y_o e^{-\zeta\omega_n t}\left[\cos \omega_d t + \frac{\zeta\omega_n}{\omega_d}\sin \omega_d t\right] \qquad 4\text{-}4$$

where ω_d is the "damped natural frequency" $(=\omega_n\sqrt{1-\zeta^2})$. This solution represents a damped periodic function which schematically looks like Fig. 4-2.

The higher the damping constant c (or equivalently ζ since $\zeta = c/c_c$), the steeper the exponential envelope, and consequently the vibration takes less cycles to die down. The rate at which this vibration decays is of importance and, indeed, is the quantity that is

---

[1] For a more accurate model which takes the mass m of the beam into account, it follows from ref. 5, pg. 430, that the equivalent mass in the single degree of freedom system may be taken as $(M + .23m)$.

[2] By making use of trigonometric identities, it may be shown that this solution can also be written as

$$y = y_o\frac{\omega_n}{\omega_d}e^{-\zeta\omega_n t}\sin(\omega_d t + \phi), \quad \phi = \tan^{-1}\frac{\omega_d}{\zeta\omega_n}$$

measured in this experiment. Consider the two local maxima y_A and y_B in Fig. 4-2[3] in which the amplitude changes from $y_A = y_o \frac{\omega_n}{\omega_d} e^{-\zeta\omega_n t_A}$ to $y_B = y_o \frac{\omega_n}{\omega_d} e^{-\zeta\omega_n (t_A + \frac{2\pi}{\omega_d})}$. Note that y_B is a constant factor $e^{-2\pi\zeta\omega_n/\omega_d}$ times y_A. This factor is the same for any two consecutive peaks. Therefore, in general for any two adjacent peaks, y_n and y_{n+1}, the following relationship holds,

$$\frac{y_n}{y_{n+1}} = e^{2\pi\zeta\omega_n/\omega_d} \qquad 4\text{-}5$$

Taking the natural logarithm of both sides of this equation introduces the logarithmic decrement δ

$$\delta \equiv \ln \frac{y_n}{y_{n+1}} = \frac{2\pi\zeta\omega_n}{\omega_d} = \frac{2\pi\zeta}{\sqrt{1-\zeta^2}} \qquad 4\text{-}6$$

The magnitudes of the adjacent peaks may be picked off the response curve Fig. 4-2 and the logarithmic decrement calculated; substitution into 4-6 will then yield ζ, which is a measure of the damping in the system.

As will be seen from actual experimental output, the adjacent peaks are so close together for small damping ($\zeta \ll 1$) that it is quite difficult to obtain accurate results. A better technique is to use two peaks y_1 and y_{n+1} that are separated by enough cycles so that an accurate measurement can be made. It is easy to show(ref.2), that for this case the logarithmic decrement δ is

$$\delta \equiv \frac{1}{n} \ln \frac{y_1}{y_{n+1}} = \frac{2\pi\zeta}{\sqrt{1-\zeta^2}} \qquad 4\text{-}7$$

Finally, for small damping $\zeta \ll 1$, we may approximate eq. (4-7) by

$$\zeta \approx \frac{1}{2\pi}\delta \qquad \zeta \approx \frac{1}{2\pi n} \ln \frac{y_1}{y_{n+1}} \qquad 4\text{-}8$$

As has been mentioned previously, the damping involved in this experiment is basically due to the inherent internal friction property of materials and is not associated with any external mechanisms.[4] We may now write the dissipation term $c\frac{dy}{dt}$ in eq. (4-2) explicitly

---

[3] We may assume for engineering purposes that these local peaks y_A and y_B are tangent to the envelope curve

$$y = y_o \frac{\omega_n}{\omega_d} e^{-\zeta\omega_n t}$$

[4] Comments on some possible energy loss associated with clamping procedures and also air damping is discussed in the following "Experiment" section.

for the material damping property that will be measured in this experiment. From previous experiments on typical engineering materials it has been observed that the energy dissipated in a typical engineering material per cycle of forced sinusoidal vibration is independent of the frequency and is proportional to the square of the amplitude. Consequently, we model the material damping force as independent of frequency and proportional to amplitude,

$$\text{material damping force} = -\frac{k\eta}{\omega}\frac{dy}{dt} \qquad 4\text{-}9$$

where η is the (dimensionless) material damping factor, and ω is the frequency. The damping force, as expressed by eq. (4-9), is obviously independent of frequency since for forced sinusoidal vibration the velocity dy/dt is directly proportional to the frequency ω. We may now carry these concepts over to the present free vibration problem and replace the damping constant c in (4-2) in terms of an "equivalent viscous damping" based on (4-9)

$$\frac{Md^2y}{dt^2} + c\frac{dy}{dt} + Ky = 0 \qquad 4\text{-}10a$$

$$\frac{Md^2y}{dt^2} + \frac{K\eta}{\omega_d}\frac{dy}{dt} + Ky = 0 \qquad 4\text{-}10b$$

Introducing terms in a similar fashion to that used in going from (4-2) to (4-3) and assuming $\omega_n \approx \omega_d$, yields

$$\frac{d^2y}{dt^2} + 2\zeta\omega_n\frac{dy}{dt} + \omega_n{}^2y = 0 \qquad 4\text{-}11a$$

$$\zeta = \eta/2 \qquad 4\text{-}11b$$

Combining (4-11b) and (4-8), the damping ratio ζ is eliminated giving a relationship between η and two peak amplitudes y_1 and y_{n+1}.

$$\eta = \frac{1}{\pi n}\ln\frac{y_1}{y_{n+1}} \qquad 4\text{-}12$$

Equation (12) is the relation that is used to calculate the material damping factor η.

Experiment

The basic experiment involve the monitoring of the free vibrations of a cantilever beam carrying a heavy mass at its tip. The material damping factor η is then determined from eq. (4-12). It is also of interest to determine possible variations of η with frequency of vibration. This frequency variation is obtained experimentally by changing the magnitude of the tip mass[5] or shortening the length of the beam. It is inherent in the discussion involving eq. (4-9) that η is independent of frequency. (Experimental results

[5] From a study of gravity effects it may be shown that decreasing the frequency by increasing the tip load will yield accurate results as long as $g/\ell < \frac{K}{M}$, i.e., the beam frequency is greater than the frequency associated with pendulum motion. This equation serves to put a lower limit on the frequency range.

on engineering materials at low frequency, i.e. between 2 and 100 cycles per second tend to confirm this frequency independence, (ref. 3)).

A schematic of the apparatus used to obtain data is shown in Fig. 4-3.

The cantilever is clamped securely to a massive structure so that losses due to this connection are minimized. Some researchers have reported good results, (ref. 6), using a beam with an enlarged end which is then clamped to a massive structure. Strain gages are glued to both sides of the beam near the clamped end (BLH SR-4 gages with Eastman 910 adhesive produces good results). The gage leads are attached to a bridge circuit so that the (strain produced) change in the resistance of the gage can be measured with precision. Although self-temperature-compensating gages are the most desirable, temperature compensation may be attained by attaching the leads from the gages to the two adjacent arms of a four arm bridge, (ref. 4). This set-up also has the advantage of eliminating strains associated with longitudinal stresses (as opposed to bending stresses). The deflection $y(t)$ at the tip of the beam and the strain $\varepsilon(t)$ from the gages are both linearly proportional to tip load, and hence linearly proportional to each other.[6] The strains are then amplified and sent to a strip chart recorder so that a "hard copy" of strain versus time can be recorded. A very convenient device that combines both a bridge and an amplifier circuit, and is specifically built to accept strain gage input, is a Type Q Plug-In Unit for use with Tektronix oscilloscopes. This unit minimizes problems associated with calibration, balancing, linearity, etc. The typical chart recorder that accepts the amplified signals records on heat sensitive paper. Chart speed is variable so that maximum accuracy can be attained in reading relative amplitudes. Good results have been obtained using a Sanborn chart recorder, Model 322 Dual Channel DC Amplifier-Recorder.

It should be noted that for metals, which typically have small values of η, the damping associated with air resistance can be of importance. For accurate results one then has to consider a vacuum enclosing system around the beam. A typical device would be a long glass tube around the beam and base with an attachment leading to a pump. The vibration may be initiated by using a bar magnet outside the tube to attract a strip of iron attached to the beam. Another way to start the motion is by displacing the end of the beam with a thin conducting wire and then sending a high current through the wire (using a battery source); a high enough current will melt the wire and start the beam vibrating.

A typical specimen is a wood (pine) cantilever 7" in length and 3/4" by 5/32" in cross-section. The natural frequency is about 70 cycles/second (simply let it vibrate without any mass at the tip and count the cycles on the chart paper). Shown in Fig. 4-4 are actual test results for the beam with response frequencies of 16 and 30 cycles/second, respectively (the chart speed is 100mm/sec). It may be seen that it takes about 20 cycles for the amplitude to drop 50%; substitution into eq. (4-12) leads to a value of .011 for the structural damping factor η. It is sometimes difficult to read the curves if the zero point is slightly off line, as in Fig. 4-4b. To alleviate this difficulty one can read the double amplitude (on both

[6] The actual constant of proportionality are irrelevant since only the ratios of strain (or displacement) amplitudes are necessary in the calculation of the material damping factor η.

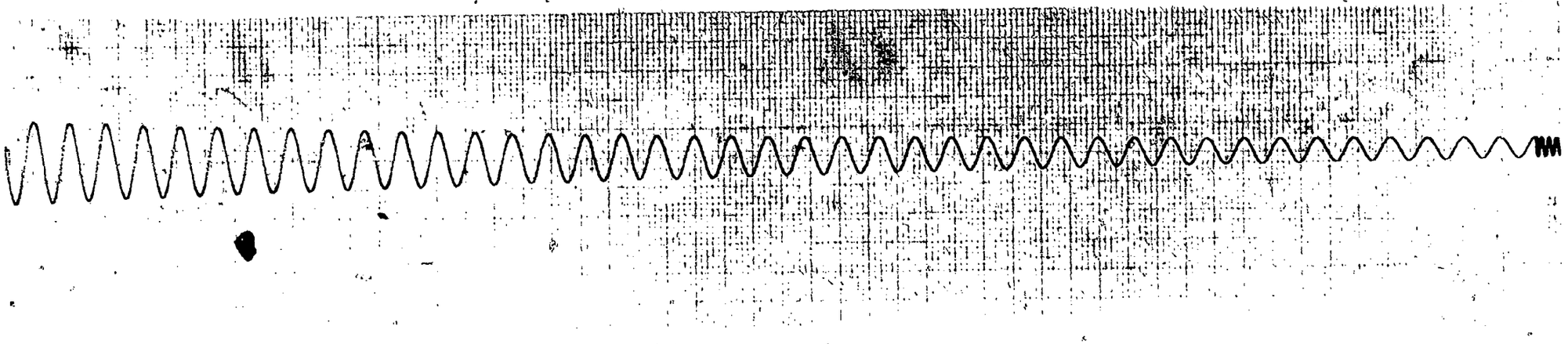

(a) 16 cycles/sec.

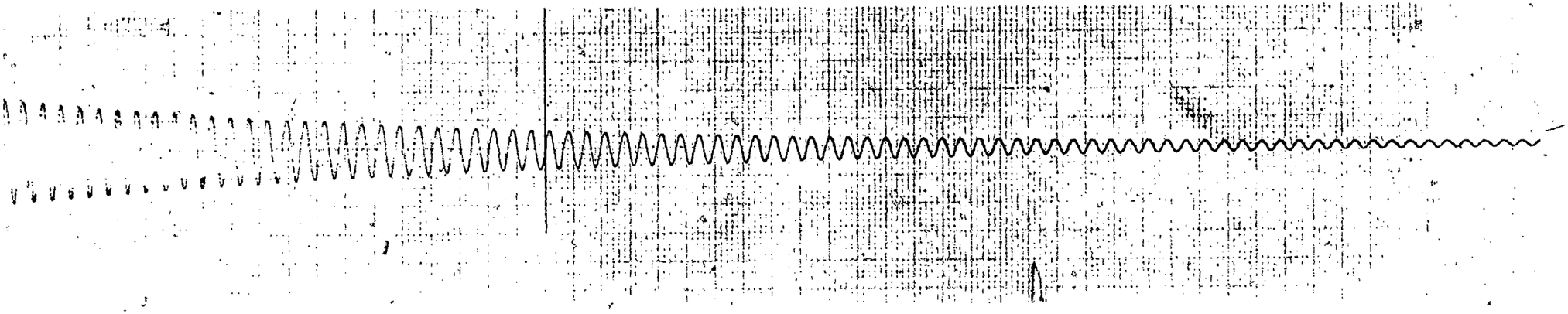

(b) 30 cycles/sec.

Fig. 4-4 Strip chart records of damped oscillations

TABLE A

TYPICAL VALUES OF η REF. [3]

STEEL	η	= .0006
COPPER	η	= .001
WOOD (WALNUT)	η	= .009
LUCITE	η	= .04 to

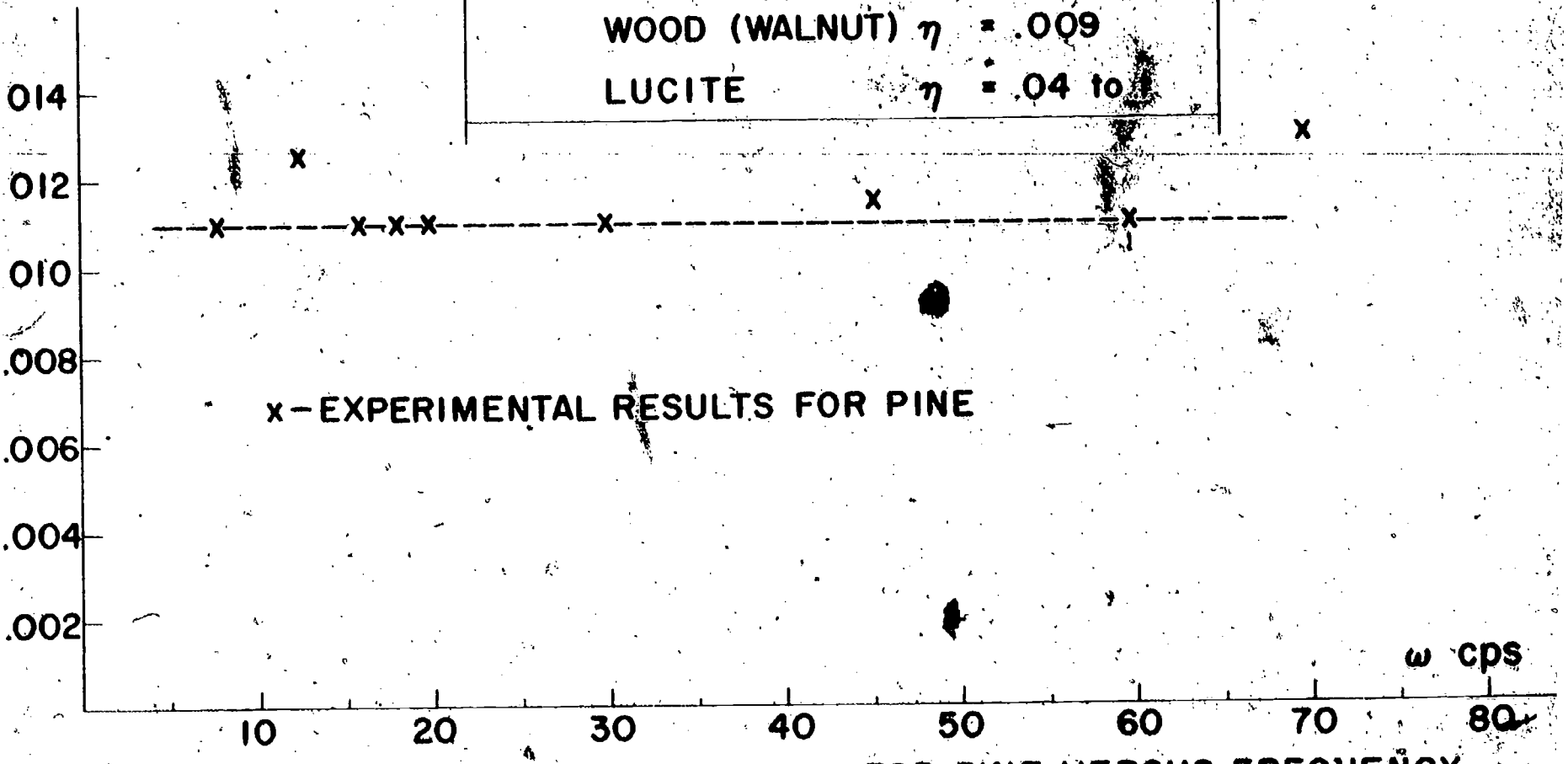

FIG. 4-5 MATERIAL DAMPING FACTOR η FOR PINE VERSUS FREQUENCY ω

sides of the zero). Further testing with different end masses verified that this result was roughly independent of frequency. These results are plotted in Fig. 4-5 and agree with published values in ref. 3.

To get results at higher frequency the specimen should be cut down. Since the stiffness varies as ℓ^{-3} eq. (4-1) cutting the beam in half increases the frequency by a factor of $2^{3/2} = 2.8$. The values of η for common metals such as steel and copper would fall about an order of magnitude below this value for wood (thereby necessitating a partial vacuum environment to maintain accuracy) while a hard "viscoelastic" substance such as polymethylmethacrylate (lucite, plexiglass) would have η about 5 to 10 times as high as the value for wood. Some typical values of η taken from experiments and ref. 3, are shown in Fig. 4-6. It should be pointed out that viscoelastic materials such as lucite are quite sensitive to environmental conditions, in particular, the temperature. This leads to some difficulty in reproducing results for different specimens under different conditions, but it should be of interest to the students to try to quantify these effects.

References

1. Flugge, W. (Editor), Handbook of Engineering Mechanics, McGraw-Hill (1962), Chapter 32.
2. Church, A. H., Mechanical Vibrations; John Wiley & Sons (1963).
3. Lazan, B. J., Damping of Materials and Members in Structural Mechanics, Pergamon Press (1968).
4. Dove, R. C. and P. H. Adams, Experimental Stress Analysis and Motion Measurement, Charles E. Merrill Books (1964).
5. Dan Hartog, J. P., Mechanical Vibrations, 4th Edition, McGraw-Hill (1956).
6. Plunkett, R., "Measurement of Damping", section 6 of Structural Damping, J. E. Ruzicka (Editor), ASME Publication (1959).

Experiment No. 5

Oscillations in a Manometer Fluid

Introduction

One of the problems encountered with manometers is the oscillations that can occur when the pressure being measured is changed suddenly. Instead of coming to rest, the fluid oscillates, until the natural damping causes it to come to rest. In this experiment we propose to examine the relation between fluid viscosity and the damping.

Consider the simple manometer shown in Fig. 5-1. A column of liquid of length ℓ and having density ρ is contained in the manometer as shown. In the analysis it will be assumed that both ends of the U-tube are open to air. We shall neglect the mass and damping of the air. For the present we shall also neglect the damping in the liquid. The illustration shows the fluid oscillating with the distance from the equilibrium level to the liquid level equal to h.

The mass of liquid oscillating is

$$m = \frac{\pi d^2 \ell \rho}{4} \qquad 5\text{-}1$$

where d is the inside diameter of the tube.

If we consider the pressure on the surface of each leg equal, the force due to the difference in levels, 2h, which tends to restore the liquid to a level state is

$$\frac{2h\pi d^2 \rho g}{4} \qquad 5\text{-}2$$

Writing Newton's second law for this use, using $\ddot{h} = \frac{d^2h}{dt^2}$ as the rate of acceleration of the liquid, we obtain the expression

$$\frac{\pi d^2 \ell \rho}{4} \ddot{h} + \frac{2\pi d^2 \rho}{4} h = 0 \qquad 5\text{-}3$$

or more simply

$$\ddot{h} + 2\frac{g}{\ell} h = 0 \qquad 5\text{-}4$$

For more detail about the development of the equation and its solution see ref. 1. The solution of the equation indicates that the oscillation is sinusoidal with a frequency, ω_n, the natural frequency. For an initial displacement h_o, the motion is

$$h = h_o \sin \omega_n t \qquad 5\text{-}5$$

where $\omega_n = \sqrt{\frac{2g}{\ell}}$

The liquid contributes damping due to the viscous action along the tube wall. Assuming this to be viscous damping, which means that the damping force is proportional to velocity, $\dot{h}$, such that the damping force equals $c\dot{h}$, Newton's second law becomes

$$\ddot{h} + \frac{c}{m}\dot{h} + \frac{2g}{\ell} h = 0 \qquad 5\text{-}6$$

For a discussion of the solution see ref. 2 or 3, and Experiments 2 and 4. For damping less

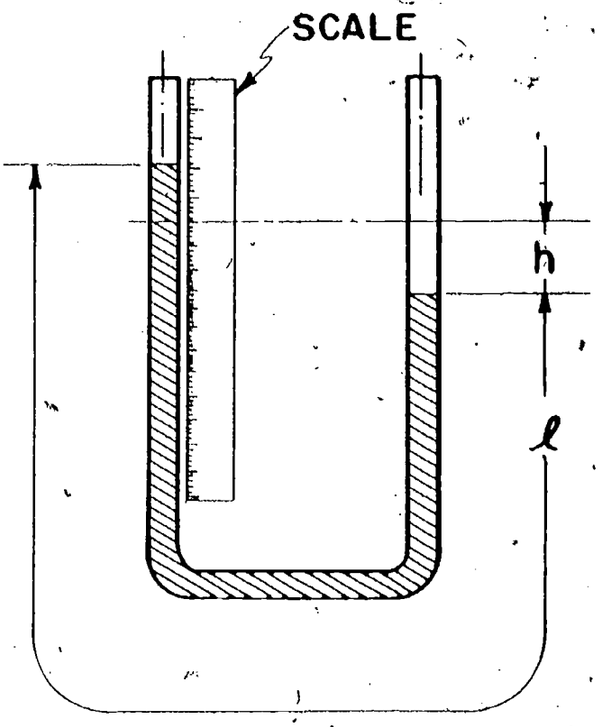

FIG. 5-1 U-TUBE MANOMETER MODEL SHOWING PRINCIPAL DIMENSIONS

than critical, the damping ratio can be expressed as

$$\zeta = \frac{c}{c_c} = \sqrt{1 - \left(\frac{\omega d}{\omega n}\right)^2} \qquad 5\text{-}7$$

where $c_c = 2m\omega_n$, the critical damping factor

ω_d = frequency of damped system

ω_n = frequency of undamped system (the natural frequency) $\omega_n = \sqrt{\frac{2g}{\ell}}$

Referring to Experiments 2 or 4, it is possible to measure the logarithmic decrement, δ, and compute ζ from it, as

$$\delta = \frac{1}{n} \ell n \frac{h_i}{h_{i+n}} = \frac{2\pi\zeta}{\sqrt{1-\zeta^2}} \qquad 5\text{-}8$$

The choice of procedures will depend upon the amount of damping. For very light damping, ω_n and ω_d are nearly the same, making precise evaluation of eq. (5-7) difficult.

Having found ζ, it is possible to determine the damping factor c by evaluating ω_n eq. (5-5) then c_c.

Experiment 5A

Effect of Manometer Geometry on Damping Factor

> The objective of this experiment is to determine the effect on the oscillation of liquid in a manometer produced by changes in the length and diameter of the liquid column.

This experiment will involve a single liquid in an open ended U-tube. Water is suitable. Now apply a pressure to one leg and release it suddenly. This will cause the column to vibrate. The tube will be filled with different amounts of liquid, thus changing ℓ. For each ℓ, the frequency, ω_d, will then be measured and the natural frequency ω_n computed from the expression developed above. From this information values of c/c_c and c can be computed. Now plot, versus liquid length ℓ, ω_n, c/c_c and c. Try to establish some relationship for $c(\ell)$.

For low frequency and large damping it may be practical to evaluate ω_d with a stop watch; then to determine the damping ratio from eq. (5-7). For other cases it will be necessary to determine the logarithmic decrement which will require determining the amplitude at specific times. Optical measurements provide an accuracy with no disturbance to the dynamics. This requires that glass tubing be used with colored (or opaque fluid). Dye can be added to clear fluids. One technique is to use a photo-electric cell, mounted so it may be moved vertically. When the fluid is between the light source and cell the signal will be interrupted. By positioning the system so that it is just interrupted by the fluid at the top of its oscillation, the point can be detected when the fluid stops interrupting the beam, and this height measured. Quickly relocating the cell, and counting oscillations, n, a second point, h_{n+i} can be measured and δ calculated.

Using a Polaroid camera (or better still, video tape) with 3000 film, exposure can be made at two successive times. This will require advancing the film for each exposure. Exposures must be made by opening the lens near the top of the oscillation for sufficient time for the fluid to reach its maximum height. With a scale mounted beside the manometer the height of the oscillation can be measured from each photograph. With video tape the recorded pictures can be replayed frame by frame to determine the maximum height at two different times. Close-up lenses on the video camera will improve the accuracy of the measurement. In either case, better definition can be obtained by lighting with high frequency stroboscopic light.

Another problem which should be examined is the effect of fluids which wet the wall. Non-wetting fluids will behave more like the model. It may be possible to treat the inner wall of the tube to reduce wetting with water.

An alternative experiment might be performed by repeating this experiment for tubes of three different diameters, and to establish the effect of the tube diameter on the several variables.

What might be of more interest is to relate the damping c to the wetted area of the manometer tube, $\pi d\ell$. Plot the results of all tests with damping as the ordinate and wetted surface area as the abscissa. Does there appear to be a consistant relationship between them?

Experiment 5B

The Effect of Liquid Viscosity on Damping in a U-tube

> The object is to evaluate the effect of fluid viscosity on the damping of oscillations in a U-tube manometer.

In Experiment 5A, the objective was to determine if damping could be related to the tube geometry, and in particular, the wetted surface area. Our next objective is to evaluate the effect of fluid viscosity on the viscous damping. To accomplish this, fluids of different viscosity will be caused to oscillate in the U-tube, and the damped frequency or logarithmic decrement measured. Tube diameter and length of liquid, ℓ , should be kept constant for each of the fluids. This will establish a single value for ω_n and wetted surface area. From separate measurements or tabulated values, ρ and the viscosity, μ , can be found. Now determine the damping factor c. Fluids should be used with less than critical damping. Try mercury, and silicone oil. Select fluids for which μ is known. Graphs can be drawn of damping factor versus viscosity. Once again, the question is: Can a relationship between these properties be established? If so, what is it? Furthermore, can a relationship be established for damping which includes both wetted surface and viscosity? Measurements can be made with various ℓ and α for several fluids in order to evaluate this relation.

An additional exercise can be done with the more viscous fluid. That is to try, by extrapolation and experiment to reach critical damping. Now compare the result to the expression for c_c,

$$c_c = 2m\omega_n$$

Experiment 5C

Modification of the System to Increase Damping

The objective is to introduce damping with a small restriction to the flow, and to evaluate its effect on the oscillation of fluid in a U-tube manometer.

One way to increase damping in the U-tube manometer is to introduce an orifice into the system. The restriction imposed on fluid movement will reduce the response of the instrument, but will also provide additional damping. An orifice might be used in the base of the U-tube to restrict fluid flow from one leg to the other. In this experiment, the restriction will be placed in the opening to atmosphere on one leg. Consequently, air displaced from one leg by the fluid must pass through the orifice to escape or return.

We seek, experimentally, answers to several questions.

1. What is the effect of orifice opening on the time for the manometer to respond to a pressure change? A variable orifice or valve should be used, with response time measured and plotted versus some measure of the valve setting or orifice opening. What is really needed here is to minimize the time required to come to an equilibrium state when a change in pressure is made, and it is that which should be measured. It may be that too much damping will cause this time to increase. Is there an optimum? Use water as the fluid.

2. What is the effect on response time of the size of the air column of the restriction?

3. What effect is observed by changing the length of liquid in the U-tube?

Devise a method for evaluating the response in terms of these variables, and conceive methods of expressing the relationships among them in a clear way.

References

1. Thomson, W. T., Vibration Theory and Application, Prentice Hall, England Cliffs, N. Y. (1965), pp 3-11.
2. Ibid, pp 39-41.
3. Church, A. H., Mechanical Vibrations, John Wiley & Sons, N. Y., N. Y. (1957), pp 46-58.

Experiment No. 6

Acceleration of a Spinning Disc

A machine is to be designed in which a disc is to revolve in free air. It is necessary to determine the power required to drive the disc as a function of the speed of the disc. To make this evaluation an experiment will be conducted using the model shown in Fig. 6-1. A circular disc is mounted on a shaft. The shaft is supported by two bearings, with the disc overhanging as shown. Finally the system is mounted to a firm table.

Experiment No: 6A

Determination of Frictional Effects

The object of this experiment is to measure the frictional resistance on the disc and then to express it as a function of speed.

The test will involve bringing the disc to some angular speed, then allowing it to decelerate due to the air resistance and bearing friction. The rate of deceleration is proportional to the torque applied by these resistive forces, according to Newton's law:

$$I\alpha = c_1(\omega) \qquad 6\text{-}1$$

where I = the mass moment of inertia of the system about the axis of rotation

α = the angular deceleration

c_1 = torque due to friction forces, a function of the angular speed, ω.

Inertia of the disc and shaft can be found by calculations, knowing the geometry and density of the disc and shaft, or it can be measured by means of the calibrated torsion wire of Experiment 1. Express it in $lbm_m inches^2$. It is necessary to measure the acceleration. This is more difficult to do than to measure angular velocity, and it is known that acceleration is the time rate of change of velocity. In terms of infinitesimals, it is the derivative of velocity with respect to time:

$$\alpha = \frac{d\omega}{dt} \qquad 6\text{-}2$$

where ω = angular velocity

t = time

One soon learns that derivatives are difficult to evaluate experimentally or graphically as these usually entail measurements at discrete time intervals, or approximating tangents to graphs. It is now a question of making accurate measurements of angular velocity, either at discrete time intervals or continuously in time.

Procedure suggestions

Some measuring schemes come to mind quickly which extract excessive amounts of energy from the sytem. Thus, the instrument contributes to the resistance giving a false result. Instruments in this category include mechanical or electric tachometers. A simple revolution counter can be made by attaching a small manget to the shaft, which will pass a pick-up coil with each revolution of the shaft. As it does, an electric impulse is induced in the coil by the magnet which can be used to drive an electronic impulse counter, or to produce Lissajous

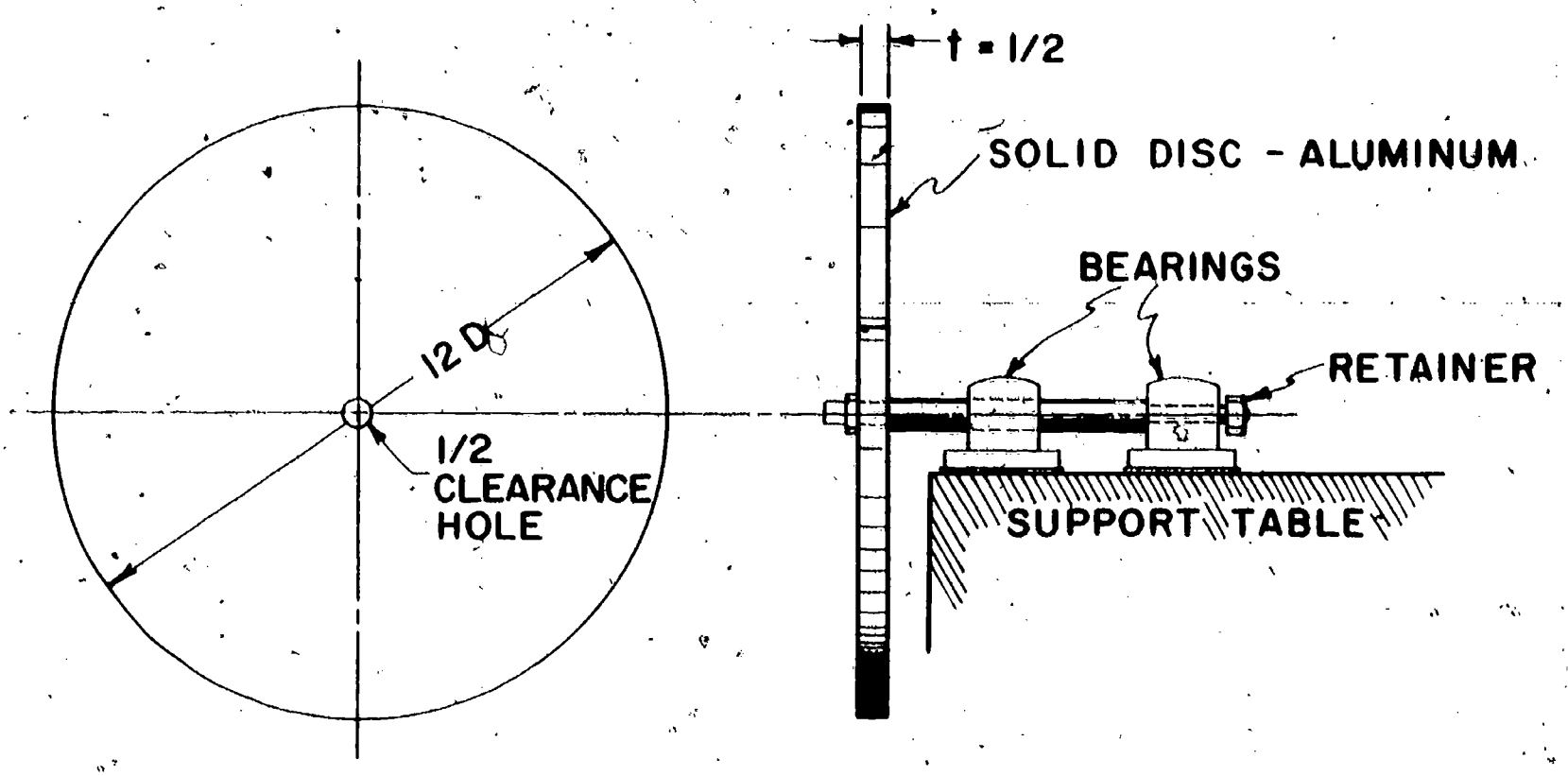

FIG. 6-1 ROTATING DISC ASSEMBLY

patterns on an oscilliscope (ref. 1 and 3).

Another simple speed-measuring technique which can be employed is to use a Strobotac to bring a mark on the wheel to an apparently stopped condition. One soon learns it is better to set the frequency of the strobotac and measure the time at which the wheel speed becomes synchronous, rather than trying to measure the time-varying speed at a given instant of time. This is best done by setting the strobotac to a frequency, say 600 flashes per minute, then marking the time that the mark on the disc appears to be stationary. A single mark will appear at 600 rpm. There will be two marks at 300 rpm; four at 150 rpm and so on. This has the advantage of spacing the readings more closely in the low speed range. Repeating the test with the light set at 400 flashes per minute, will allow measurement at 200 rpm, 100 rmp, etc.

Determination of resistance

It is now necessary to determine α from the time-velocity data. This can be done by approximating the derivative by a finite difference approximation

$$\frac{d\omega}{dt} \approx \frac{\omega_2 - \omega_1}{t_2 - t_1} \qquad 6\text{-}3$$

where the subscripts refer to successive measurements. As an alternative, data can be plotted and tangents $(\frac{d\omega}{dt})$ measured. An improved technique would be to fit a second degree polynomial through three successive data points expressing ω (t) as

$$\omega = A_o + A_1 t + A_2 t^2 \qquad 6\text{-}4$$

With the coefficients A_1 and A_2 determined

$$\frac{d\omega}{dt} \approx A_1 + 2A_2 t \qquad 6\text{-}5$$

for a value of t in the center of the two-step interval.

Now the value of c_1 in eq. (6-1) can be found for several values of speed ω, and a graph c_1 vs. ω can be constructed. It might look like Fig. 6-3. Notice that for the units of c_1 (ω) are in lbf-ft., which requires that the inertia of the shaft and disc, I, be converted to slugs-ft^2 (lbf-sec^2-ft) and α to be expressed in radians/sec^2.

Sample results

An experiment was conducted using a solid aluminum disc 12 inches in diameter having two 9/16 inch thick annular rings fastened with screws to the front and back faces. These rings had an outside diameter of 12 inches and an inside diameter of 8 inches. The disc assembly was fastened to the shaft of the apparatus, Fig. 6-1, and a pulley was fastened to the back end. The assembled rotating parts had a mass moment of inertia of 0.0751 lbf-ft-sec^2 or 2.419 lbm-ft^2. Using an electric motor and a v-belt drive, the system was brought to a speed of about 1000 rpm and the belt slipped off the pulley. Using a strobotac, and the technique described, the time required to decelerate was determined. It is shown graphically in Fig, 3-2.

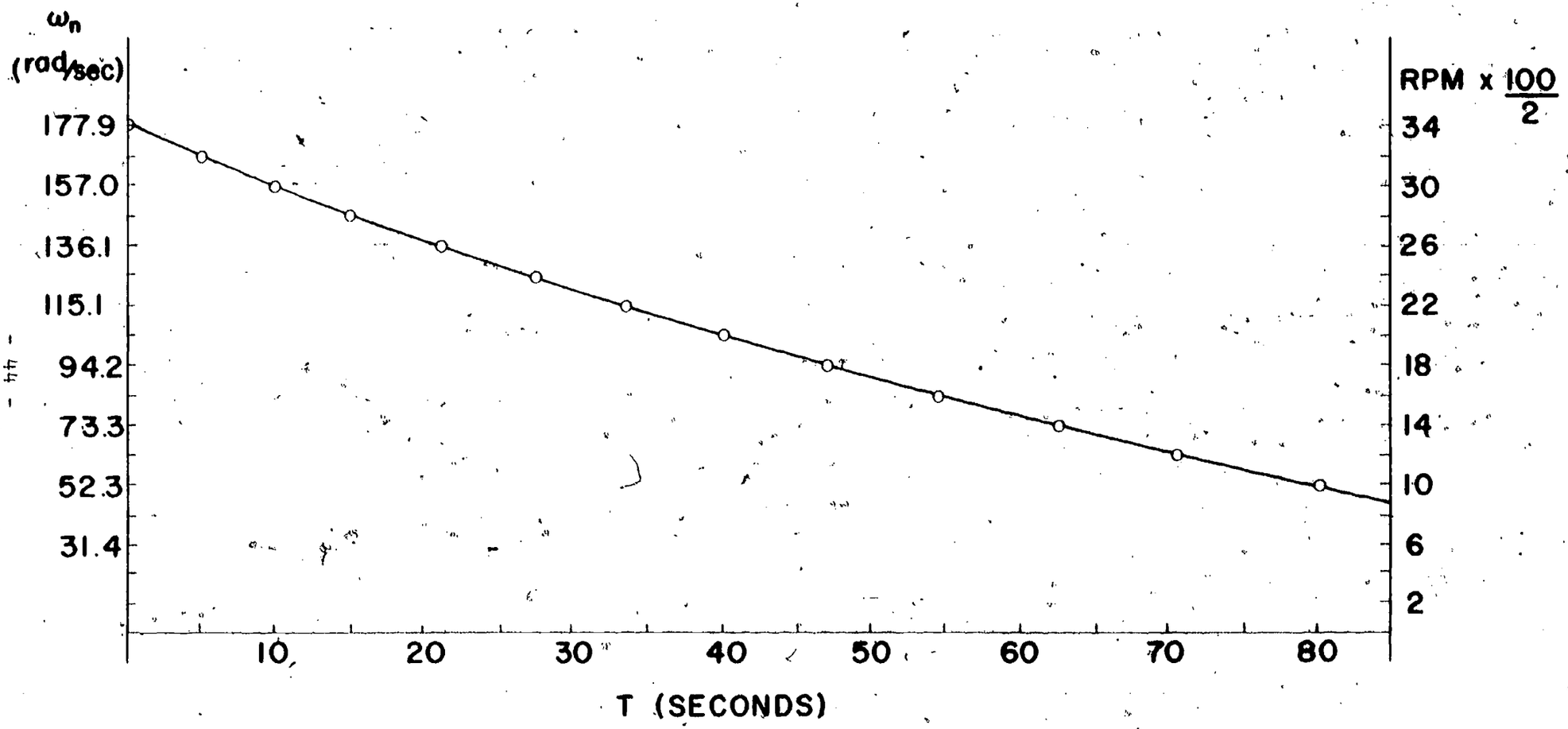

FIG. 6-2 DECAY OF VELOCITY WITH TIME FOR A SPINNING DISC

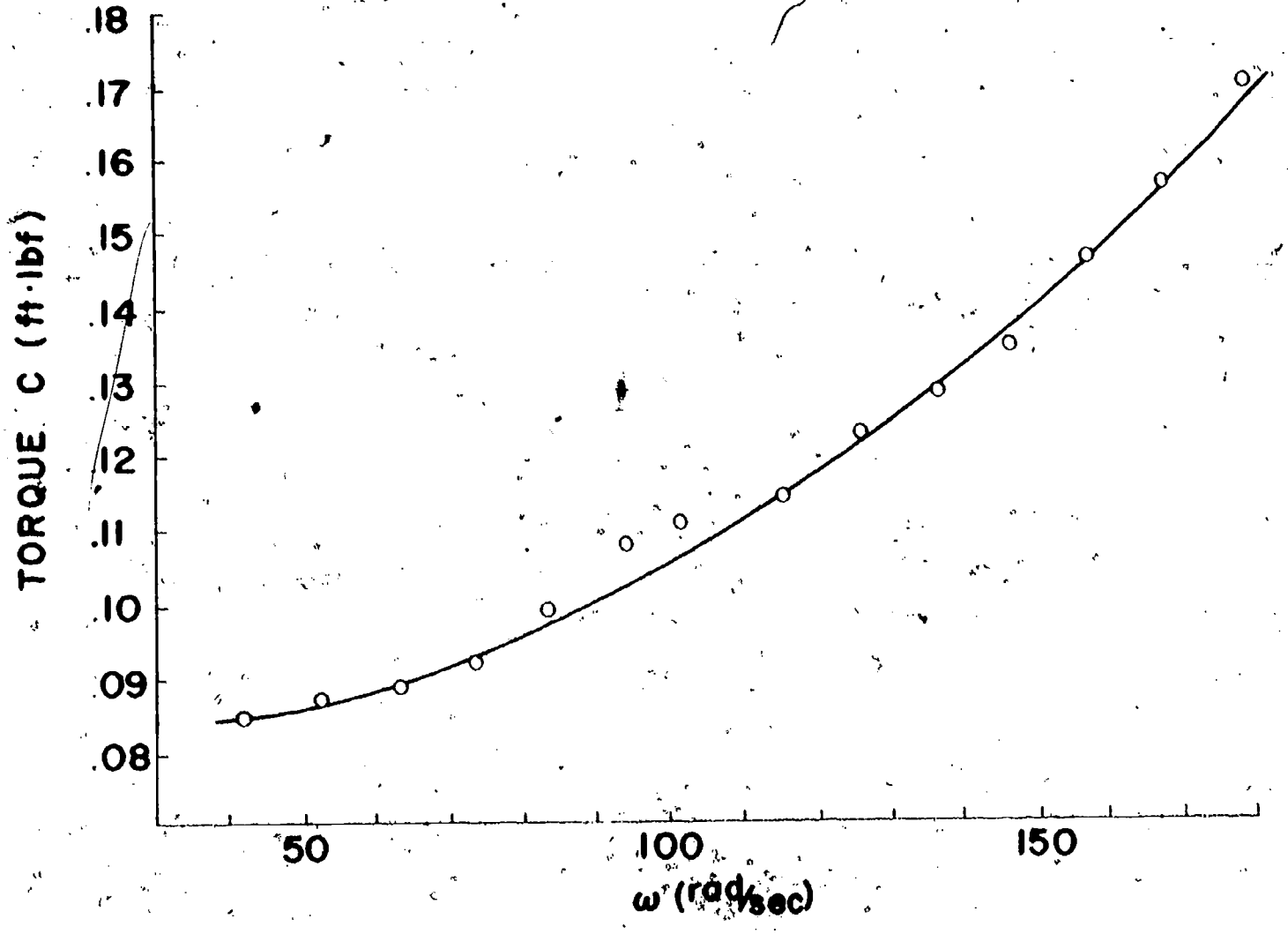

ANGULAR FREQUENCY

FIG. 6-3

From points on the curve, the acceleration was computed by eq. (6-3). Putting I and α in eq. (6-1) $c(\omega)$ was calculated. Results for $c(\omega)$ are shown plotted vs. speed in Fig. 6-3. For $I = 0.0751$ lbf-ft-sec^2 and α in rad/sec^2, $c(\omega)$ is expressed in lbf-ft.

Experiment No. 6B

A Least Squares Curve Fit

The object now is to use the data for $c_1(\omega)$ from the previous experiment and express the functional relationship as a polynomial of degree two using the method of least squares.

The form of the polynomial is

$$c_1(\omega) = a_o + a_1\omega + a_2\omega^2 \qquad 6\text{-}6$$

The method of least squares is described in refs. 2, 4 and 5, and involves a selection of the coefficients a_o, a_1 and a_2 such that the quantity

$$\sum_{k=o}^{n} (a_o + a_1\omega_k + a_2\omega_k^2 - c_{1k})^2 \qquad 6\text{-}7$$

is a minimum. Here the c_{1k} are the values of c_1 computed from the test results at the ω_k. There are a total of n such points. The method requires the solution of a set of simultaneous algebraic equations, linear in the unknowns a_o, a_1 and a_2.

$$\begin{aligned} na_o + a_1\sum_{k=o}^{n}\omega_k + a_2\sum_{k=o}^{n}\omega_k^2 &= \sum_{k=o}^{n} c_{1k} \\ a_o\sum_{k=o}^{n}\omega_k + a_1\sum_{k=o}^{n}\omega_k^2 + a_2\sum_{k=o}^{n}\omega_k^3 &= \sum_{k=o}^{n} c_{1k}\omega_k \qquad 6\text{-}8 \\ a_o\sum_{k=o}^{n}\omega_k^2 + a_1\sum_{k=o}^{n}\omega_k^3 + a_2\sum_{k=o}^{n}\omega_k^4 &= \sum_{k=o}^{n} c_{1k}\omega_k^2 \end{aligned}$$

The procedure then is to take the computed values of c_{1k} and the corresponding ω_k and determine the "best" fit according to the criterion of least squares. The values of a_o, a_1 and a_2 will be found using the eq. (6-8). These will then be substituted in eq. (6-6) to give the second-degree polynomial having the "best" fit.

Sample results

For the data plotted in Fig. 6-3, the expression for $c_1(\omega)$ was found to be

$$c_1(\omega) = 7.6 \times 10^{-2} + 7.5 \times 10^{-5}\,\omega + 2.05 \times 10^{-6}\,\omega^2$$

Experiment No. 6C

Evaluation of the Effect of Air Resistance

The objective here is to determine the effect a given area change has on air resistance, and to determine how the coefficients of the resistance equation (Experiment 6B) are affected.

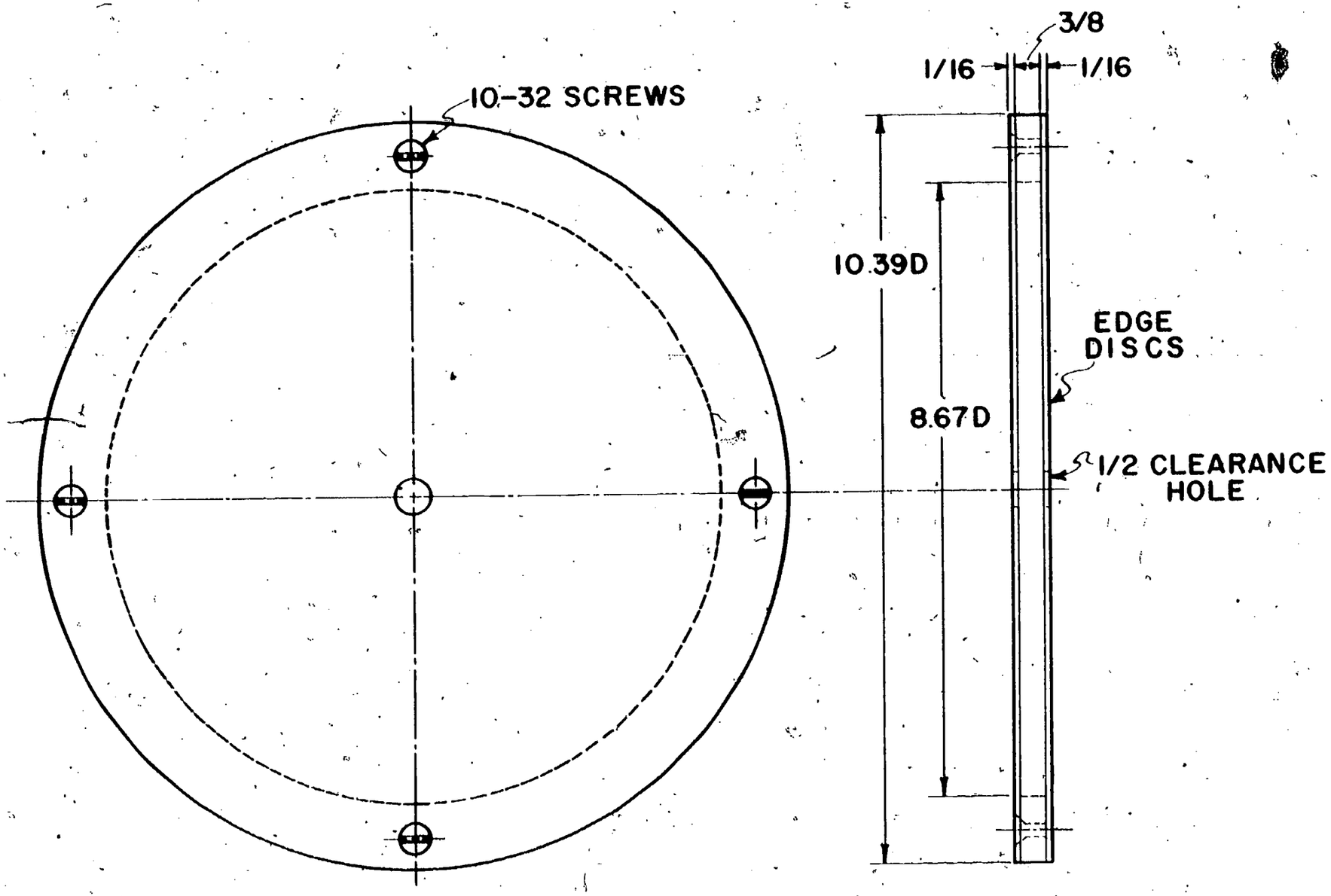

FIG. 6-4 ROTATING DISC - STEEL DISC - SCALE = 1/2

Variations of Experiment 6 can be introduced by altering the air resistance of the disc through the addition of vanes or spoilers to the disc, or adding roughness to the flat surface. Such changes would effect the air resistance which would reveal itself by changes in $c_1(\omega)$. Another variation is to construct a disc having the same mass and same moment of inertia but a different diameter. In this way the bearing resistance should remain the same as for the first disc, but because the surface area has changed, the air resistance will be changed. In this way the air resistance can be isolated from the bearing friction.

One means of changing the disc area without changing mass or inertia is to construct an annular disc as illustrated in Fig. 6-4. For example, suppose the material of the annular disc has a density 2.8 times that of the first (steel/aluminum) and the edge discs are 1/8 the thickness of the first disc, then for each value of outer diameter there is a certain inner diameter which will produce discs with mass and inertia equal to a solid disc. Values of the inner radius, r_1, are given for several choices of r_2 in the table below. The radii are made dimensionless by expressing them as the ratio of the radius to that of the plain disc.

Outer and inner radii for annular disc having mass and inertia of solid disc of radius R. Radii are given in terms of the ratio to the radius of the solid disc,

$r_1 = \frac{\text{inner radius}}{R}$ $\qquad$ $r_2 = \frac{\text{outer radius}}{R}$

r_2	r_1
0.9	.795
0.866 (3/4 area of solid disc)	.723
0.8	.514
0.773	0. (solid disc of dense material)

Notice that if r_2 is .773 times the radius of the first disc, the second disc is solid. An annular disc was constructed from steel, with an outside diameter of 10.390 inches and an inner diameter of 8.6 inches. For the solid disc having a diameter of 12 inches, this corresponds to an outer radius ratio, r_2, of .866. This results in the area of the annular disc being 3/4 that of the solid disc.

Values of $c_1(\omega)$ are again determined experimentally and compared graphically for the two discs. Coefficients can then be obtained for the second degree equation using a least squares criterion, then compared to those found for the solid disc. The question of which coefficient in the polynomial is most affected is of importance to evaluate how air resistance contributes to the total torque. The change in resistance can be related empirically to the face area of the discs.

References

1. Holman, J. P., Experimental Methods for Engineers, McGraw-Hill, New York (1966), pp. 108-129
2. Ibid, pp. 61-64.
3. Schlenk, H., Theories of Engineering Experimentation, McGraw-Hill, New York (1968), pp. 271-272.
4. Ibid, pp. 202-205.
5. Cook, N. H., and E. Rabinowicz, Physical Measurement and Analysis, Addison-Wesley, Reading, Mass. (1963), pp. 60-64.

Experiment No. 7

Fluid Friction in Pipe Flow

In this experiment the objective is to reproduce the well known curve of friction factors for fluid flow in circular tubes. The tubes will be made from sections of glass tubing or copper tubing with short connections for attaching a manometer.

The test facility

A sketch of the test set-up is shown in Fig. 7-1. For this text, 5/16 copper tubing was used having an inside diameter of 0.137 in. Pressure taps were located 60 7/16 in. apart, and there was a section 25 inches (79 diameters) upstream of the first tap to allow the flow to stabilize and develop. A section of tubing extended 10 inches beyond the downstream tap. The taps were connected to a U-tube manometer with an entrapped air bubble as shown, on which pressure drop was measured in centimeters of water. At the downstream end, the water was collected, and measured over a given time interval. From this the flow rate could be found. The tubing was clamped to a table and leveled.

Water was supplied from a constant head tank. This can be constructed easily, and proves to be a useful tool in the laboratory. A 5-gallon drum with an open top, such as a paint drum, serves for the tank. A 1-inch diameter overflow tube extends through the bottom. In the tank shown, the tube could be slid to any level by a collat arrangement. A threaded knurled ring was used to pull a rubber O-ring seal tight around the tube, which secured the tube in place. Also on the bottom of the tank a tube connection was fastened for the water outlet. Water was supplied by a hose having a perforated sleeve over the outlet to act as a baffle. A vertical plate with openings at the bottom acted as a second baffle to separate the disturbances set up by the inlet flow from the overflow, and outlet. Finally a gage glass was attached to permit observation of the water level in the tank. The tank was elevated on a stand to provide the elevation necessary for flow. Position of the tank on the stand could be altered for head changes with fine adjustments in head made by changing the height of the overflow pipe.

Test procedure

The level in the constant head tank was first established and the manometer reading and flow per unit time were measured. The level was changed to provide a new flow rate, and the new data recorded. About one minute was allowed to stablize flow before readings were made. Flow was collected for one minute using a stop watch, and the volume was determined by measuring in a graduate. Water temperature was recorded in order to establish the viscosity of water.

Calculation procedure

Velocity, v, was calculated as

$$v = \frac{Q}{A}, \text{ ft/sec.} \qquad 7\text{-}1$$

where Q = volume flow, $ft^3/sec.$

A = cross sectional area of tube, ft^2.

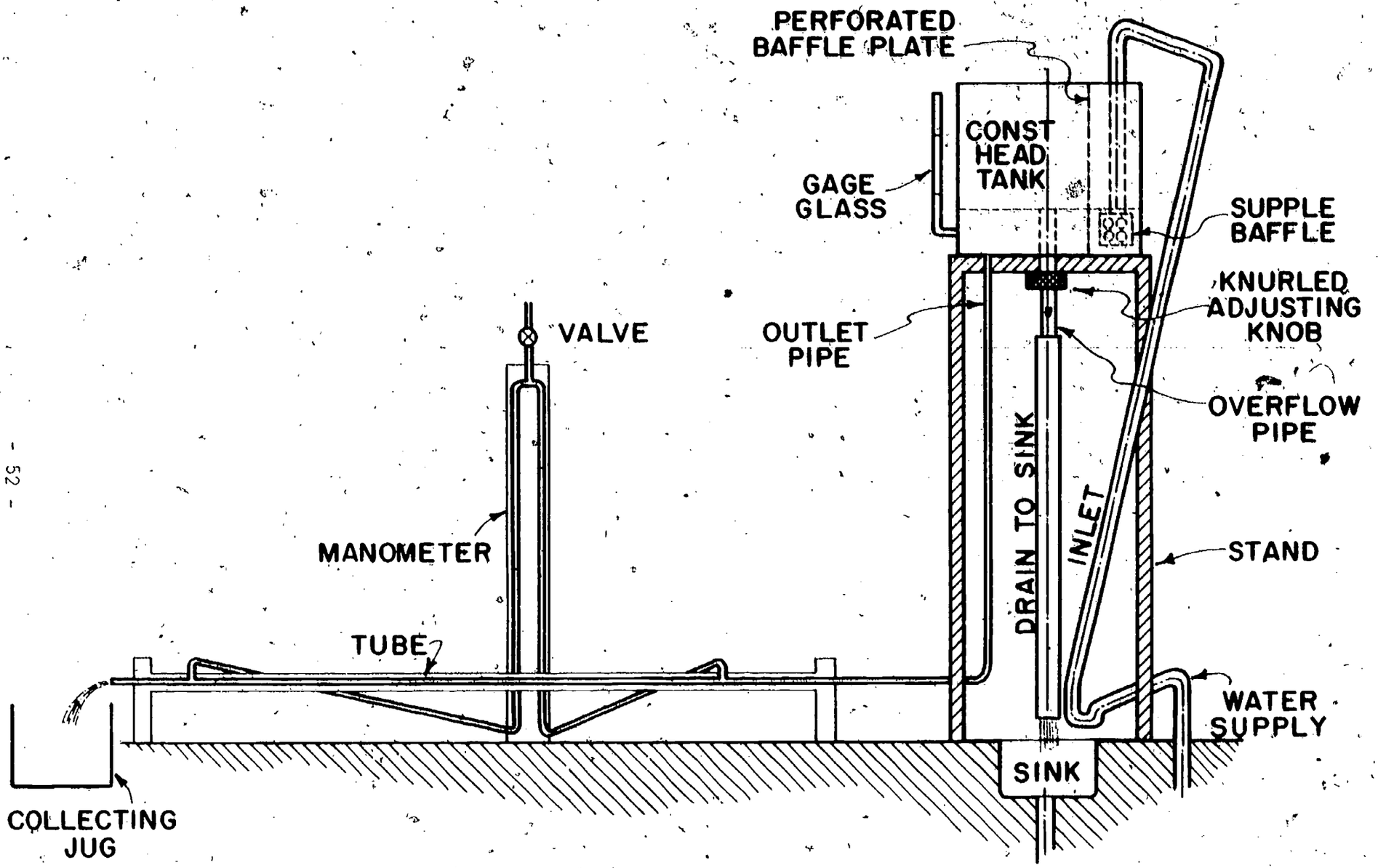

FIG. 7-1 TEST FACILITY FOR DETERMINATION OF FLUID FRICTION IN TUBES

Next the Reynolds number was found

$$Re = \frac{vD}{\nu} \qquad 7\text{-}2$$

where D = pipe diameter, ft.

ν = kinematic viscosity $ft^2/sec.$ at the water temperature

Finally the friction factor, f, was found from the definition

$$f = \frac{h_f}{(\frac{L}{D})\frac{v^2}{2g}} \qquad 7\text{-}3$$

where h_f = pressure drop due to friction, ft.

L = length of tube between pressure taps, ft.

g = acceleration due to gravity, $32.2 ft/sec^2$

v and D are as defined above.

Friction factor was then plotted against the Reynolds number on log-log graph paper, and the results compared to the Moody diagram found in any elementary text on fluid mechanics (for example ref. 1 or 2).

Some results

A word should be said about units and dimensionality, as it is an important educational aspect of this experiment. Both the Reynolds number and friction factor are dimensionless and their importance should be emphasized.

Furthermore the units must be consistent, and in this experiment some conversion has been necessary. As Q was taken as cc/min. it is necessary to convert it to $ft^3/sec.$ Hence, for the 0.137 in. diameter pipe,

$$v = \frac{Q}{A} = \frac{[\frac{cc}{min}][0.061023\frac{in^3}{cc}][\frac{1}{1728}\frac{ft^3}{in^3}][\frac{1}{60}\frac{min}{sec}]}{[3.1416][(0.317)^2\ in^2][\frac{1}{4}][\frac{1}{144}\frac{ft^2}{in^2}]}$$

$$= (0.0010739)\ Q,\ ft/sec.$$

where Q has the units $(\frac{cc}{min})$

$$Re = \frac{vD}{\nu} \quad \frac{[Q(.0010739)\frac{ft}{sec}][0.317\ in][\frac{1}{12}\frac{in}{ft}]}{[\nu\ \frac{ft^2}{sec}]}.$$

For the water temperature which ranged from 44F to 46F ν was taken as $1.58 \cdot 10^{-5}$ $ft^2/sec.$

Hence

$$Re = 1.79545\ Q\ [Dimensionless]$$

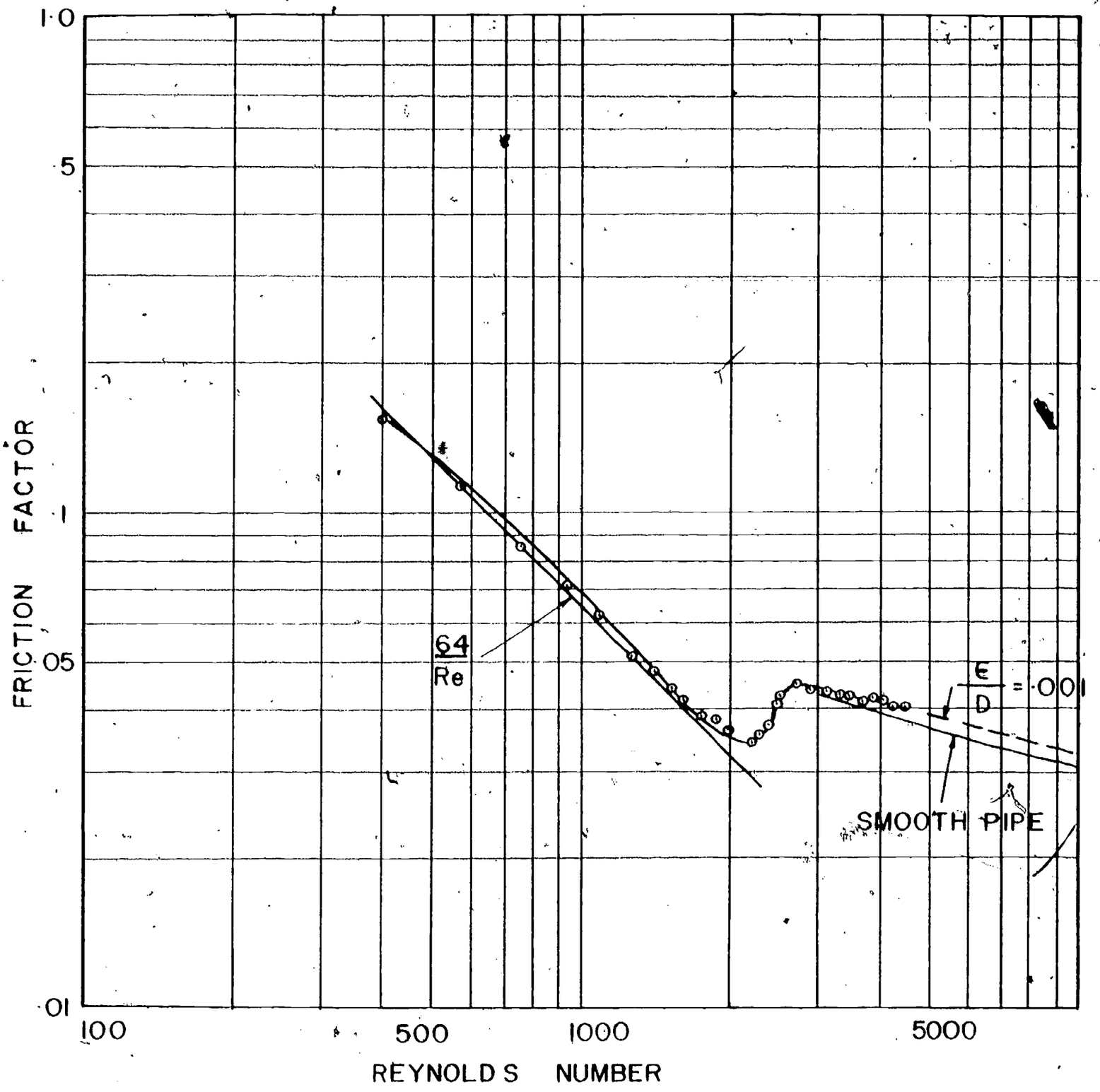

FIG. 7-2 RESULTS OF EXPERIMENTAL DETERMINATION OF FRICTION FACTOR

Finally the friction factor is

$$f = \frac{h_f}{(\frac{L}{D})\frac{v^2}{2g}} = \frac{[h_f \text{ cm}][2][32.2\frac{\text{ft}}{\text{sec}^2}]}{[\frac{60.4375 \text{ in}}{0.317 \text{ in}}][v^2\frac{\text{ft}^2}{\text{sec}^2}][30.48\frac{\text{cm}}{\text{ft}}]}$$

$$= [0.01108]\frac{h_f}{v^2} \text{ (Dimensionless)}$$

Calculations were tabulated with the data as illustrated in the table below. Two examples are given.

Trial No.	Data: Pressure drop (cm)	Data: Flow Rate (cc/min)	Velocity (ft/sec)	Reynolds No.	Friction Factor
5	2.3	596	0.6400	1070	0.0622
10	3.8	967	1.0384	1736	0.0390

A graph of friction factor versus Reynolds number was constructed from the results. This is Fig. 7-2. Comparison are very good both for the laminar flow range where $f = \frac{64}{Re}$ and in the turbulent range. The data compare best to the results for a pipe having a dimensionless roughness of $\frac{\epsilon}{D} = 0.001$.

Some modifications

Experiment 8 can be modified by adding elbows, or valves to the system and determining pressure drop as a function of the pipe Reynolds number. These can be compared to existing data.

References

1. Streeter, V. L., Fluid Mechanics, McGraw-Hill, New York, New York (1971), pp 288-289.
2. Hansen, A. G., Fluid Mechanics, John Wiley and Sons, New York, New York (1967), p. 421.

Experiment No. 8

Unsteady Flow of a Fluid

The object of this experiment is to predict the time required to empty a tank of liquid and to evaluate the prediction experimentally.

(Note: This can be performed as an experiment without the analysis if it is felt that the analysis is too difficult.)

Introduction

Designing systems in engineering requires application of theories to predict the behavior of the system before the system is actually constructed. It goes without saying that reliable predictions are essential for successful designs. Furthermore, it is much less expensive to modify the design on paper than to alter the system after its construction. The objective of this experiment is to predict the behavior of a system with a simple theory, then construct the system and evaluate its behavior experimentally. The system selected is the emptying of a tank of water through a simple piping system. There are many real situations where tanks of liquid (or gases) are emptied or filled, for which this experiment might serve as a model. For example, a rural water supply system, operating from a single standpipe might be required to supply water for emergencies at a prescribed rate and for a set time. How should this standpipe be elevated? If a hole were accidently made in the pressurized cabin of an aircraft at high altitude, how long would it take for the pressure to reach dangerously low levels? This involves flow of a compressible gas which is beyond the scope of this experiment.

Description of apparatus

The apparatus for the experiment is illustrated in Fig. 8-1. It consists of a 5-gallon tank with an opening in the bottom, to which is brazed a short tube, 3/8 inch outside diameter. Using Tygon tubing, copper tubing and piping, a simple plumbing system is added. This can be varied but, in the experiment shown in Fig. 8-1, it consists of a 90° turn in the tubing, a 1/4 inch (gate-type) valve, and a 1/4 inch pipe elbow.

Development of the theory

The tank is set at a prescribed elevation above the piping. It is filled with water to some level and allowed to drain through the plumbing system. The objective of the analysis is to predict the elevation of the surface of the water h, as a function of time. From this information, it is simple to compute flow rate or the velocity of discharge.

Bernoulli's equation relates the elevation (head), velocity and pressure in the steady flow of an incompressible fluid without losses due to friction. Between two stations, 1 and 2 (designated by subscript), the expression can be written

$$h_1 + \frac{v_1^2}{2g} + \gamma p_1 = h_2 + \frac{v_2^2}{2g} + \gamma p_2 = h_T \qquad 8\text{-}1$$

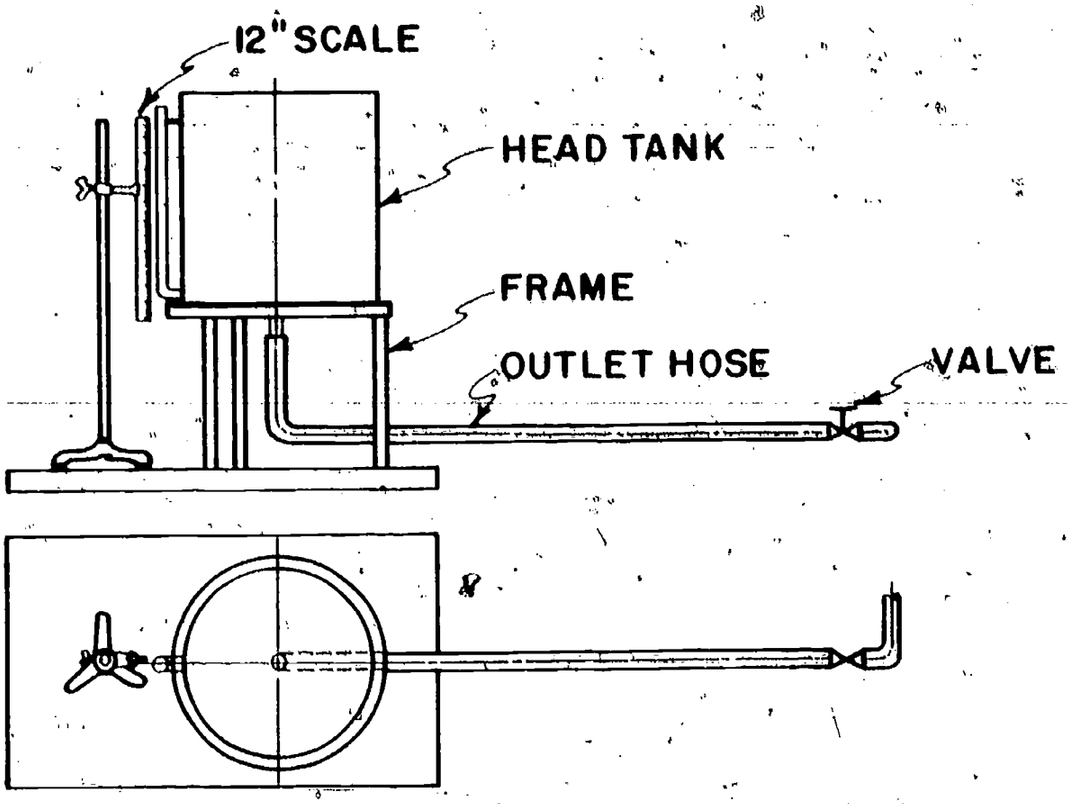

FIG. 8-1 TEST FACILITY

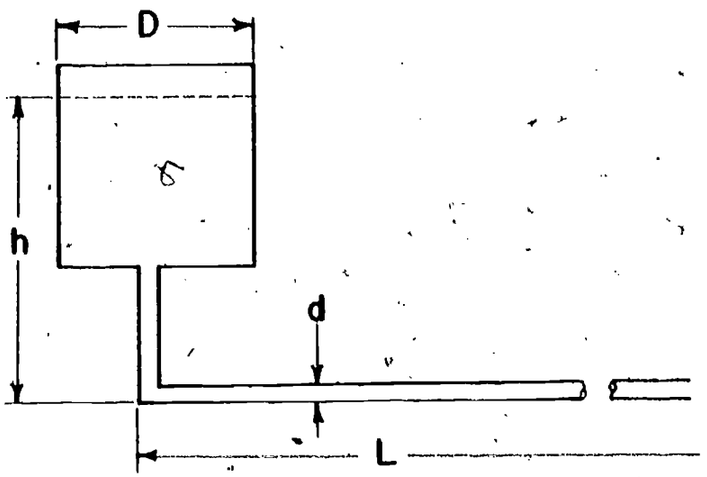

FIG. 8-2 IDENTIFICATION OF IMPORTANT DIMENSIONS

where h = elevation, ft

v = velocity, ft/sec

g = acceleration due to gravity, 32.2 ft/sec^2

p = static pressure, lbf/ft^2

γ = weight of fluid per cubic foot

h_T = a constant in the flow, called "total head", ft.

The specific weight of the fluid is related to the density by Newton's second law. Symbolically,

$$\gamma = \frac{\rho g}{g_o}$$

here ρ = density, lbm/ft^3

g_o = dimensionless conversion factor
32.2 lbm-ft/lbf-sec^2.

Notice that the specific weight is given in lbf/ft^3 and has the same magnitude as the density ρ. For water at room temperature, we can take $\rho = 62.4$ lbm/ft^3.

A practical modification to the Bernoulli equation is to recognize that there will be lossed in a real flow causing the right hand side of eq. (8-1) to be deficient by an amount, h_ℓ, the loss is the flow. Then

$$h_1 + \frac{v_1^2}{2g} + \gamma p_1 = h_2 + \frac{v_2^2}{2g} + \gamma p_2 + h_\ell \qquad 8\text{-}2$$

For the emptying tank, take station 1 as the free surface of water in the tank, and station 2 at the point of discharge as shown in Fig. 8-2. Let $h_1 = h$, the distance from the point of discharge to the surface of the water in the tank. From the same reference, $h_2 = 0$. The pressures on the free surface (p_1) and at the point of discharge (p_2) are both equal to atmospheric pressure and can be set to zero. Finally, the tank diameter is so much larger than the diameter of the jet at discharge that the velocity on the tank surface, v_1, can be neglected when compared to the discharge velocity, v_2. Then the modified Bernoulli eq. (8-2) can be written

$$v_2^2 = 2g\,(h - h_\ell) \qquad 8\text{-}3$$

To bring in the time dependence of h, write the equation for conservation of mass (continuity), equating the flow rate from the tank, Q_T, to the flow rate from the pipe Q_p,

$$Q_p = Q_T \qquad 8\text{-}4$$

For the tank, the flow rate can be expressed as the rate of change of level with time, t,

$$Q_T = -\frac{dh}{dt} A_T = -\frac{\pi D^2}{4} \frac{dh}{dt} \qquad 8\text{-}5$$

where A_T = the cross sectional area of tank, ft^2

D = the diameter of the tank, ft.

From the pipe, the flow rate can be related to the velocity of discharge, v_2, and the area of the pipe, A_p, which, with eq. (8-3), is

$$Q_p = A_p v_2 = \frac{\pi d^2}{4} \sqrt{2g\,(h-h_\ell)} \qquad 8\text{-}6$$

where d = the inside diameter of the pipe, ft.

Equations (8-5) and (8-6) can be substitued into eq. (8-4) to express the time dependence of h as

$$\frac{dh}{dt} = -\frac{d^2}{D^2} \sqrt{2g\,(h-h_\ell)} \qquad 8\text{-}7$$

We now seek an expression for h_ℓ. For this, we will use the loss coefficients found in elementary texts in fluid mechanics for the plumbing system. There are: a sharp-edged entrance, a straight pipe, a gate valve, and an elbow. Using a reference such as Streeter (1) or Brenkert (2), these are

sharp-edged entrance: $h_{\ell_E} = 0.5\, v_2^2/2g$ 8-8a

a pipe of length L: $h_{\ell_p} = f\,(v_2^2/2g)\,(L/d)$ 8-8b

gate valve wide open: $h_{\ell_v} = 0.19\, v_2^2/2g$ 8-8c

90° elbow: $h_{\ell_e} = 0.9\, v_2^2/2g$ 8-8d

The value of the friction factor f in eq. (8-8b) is a function of the velocity of the flow, the viscosity and density of the fluid and the diameter of the pipe. For laminar flow it can be written as

$$f = \frac{64\mu}{\rho v d} \qquad 8\text{-}9$$

where
ρ = density of the fluid, lbm/ft^3
v = velocity, ft/sec
μ = viscosity, lbm/sec-ft
d = pipe diameter, ft.

Note: f is dimensionless, and the expression $\rho v d/\mu$ is the flow Reynolds number, and is dimensionless. A value of Reynolds number larger than 2000 in pipe flow indicates that the flow is probably turbulent and eq. (8-9) should not be used. Instead, graphical value of f as a function of the Reynolds number $g(Re)$ should be obtained (see ref. 1 or 2).

When these expressions for head losses are substituted into eq. (8), the result is

$$\frac{dh}{dt} = -\frac{d^2}{D^2} \left(h - \frac{v_2^2}{2g}\right) (0.5 + 0.19 + 0.9 + \frac{L}{d}\, g\,(Re)) \qquad 8\text{-}10$$

For the case of laminar flow, the friction factor is an easily expressible function of Re, eq. (8-9), making eq. (8-10)

$$\frac{dh}{dt} = -\frac{d^2}{D^2} \left(h - \frac{v_2^2}{2g}\right) \left(1.59 + \frac{L}{d} \frac{64\mu}{\rho v_2 d}\right) \qquad 8\text{-}11$$

Equation (8-11) is difficult to solve because v_2 is a function of h and appears in non-linear form. Consequently, the solution must be a numerical one. A trial value is found for v_2 with h_ℓ set to zero in eq. (8-6).

$$v_2 = \frac{d^2}{D^2}\sqrt{2g\,h}$$

Then a value of h_ℓ is found using equations (8-8a) through (8-8d) and an evaluation of the Reynolds number. The equation is

$$h_\ell = \frac{v^2}{2g}\left(1.59 + L/d\ g\ (Re)\right) \qquad 8\text{-}12$$

An improved estimate of the velocity can now be made by using eq. (8-6) with the newly computed value of h_ℓ,

$$v_2^{(1)} = \frac{d^2}{D^2}\sqrt{2\ g\ (h-h_\ell)}$$

At this point, the improved velocity $v_2^{(1)}$ should be compared to v_2. One way is to ask if

$$|v_2^{(1)} - v_2| \leq \varepsilon$$

where ε is some small value assigned to test the accuracy of the iteration. If this is not true, the new value of v_2, $v_2^{(1)}$, is used in eq. (8-12) to find a new h_ℓ, which in turn is used in eq. (8-6) to find an improved value of v_2. When the iteration has converged, that is $|v_2^{(1)} - v_2| \leq \varepsilon$, then eq. (8-10) is solved for $\frac{dh}{dt}$. Integration of this expression can be carried out from the initial state by any of several methods including a simple technique called Euler's method (see ref. 3). In this method a new value of h is found from the expression

$$h^{(1)} = h^{(0)} + \left(\frac{dh}{dt}\right)^{(0)} \delta t$$

In this case $h^{(0)}$ is the initial value of h; $\left(\frac{dh}{dt}\right)^{(0)}$ is the value found above; and δt is some small interval of time for the next step. Having found $h^{(1)}$, the process can be repeated. That is, a new trial value of v_2 found; h_ℓ calculated; an improved value of v_2 calculated; the test made for conversion; iteration until the best values are found for v_2 and h_ℓ; and then Euler's method applied to find $h^{(2)}$. Gradually the integration goes forward until h has reached some prescribed value at which point the computation is terminated. For each step in time, the velocity and head, h, are known.

It is evident that this is a tedious calculation. If a digital computer is available, a program can be written to handle this. In the discussion of an actual experiment, a program written by students performing this experiment is presented.

Experimental procedure

When the calculations have been made, a curve of head versus time can be constructed. Now, using the apparatus, the tank can be filled with water and measurements of head versus

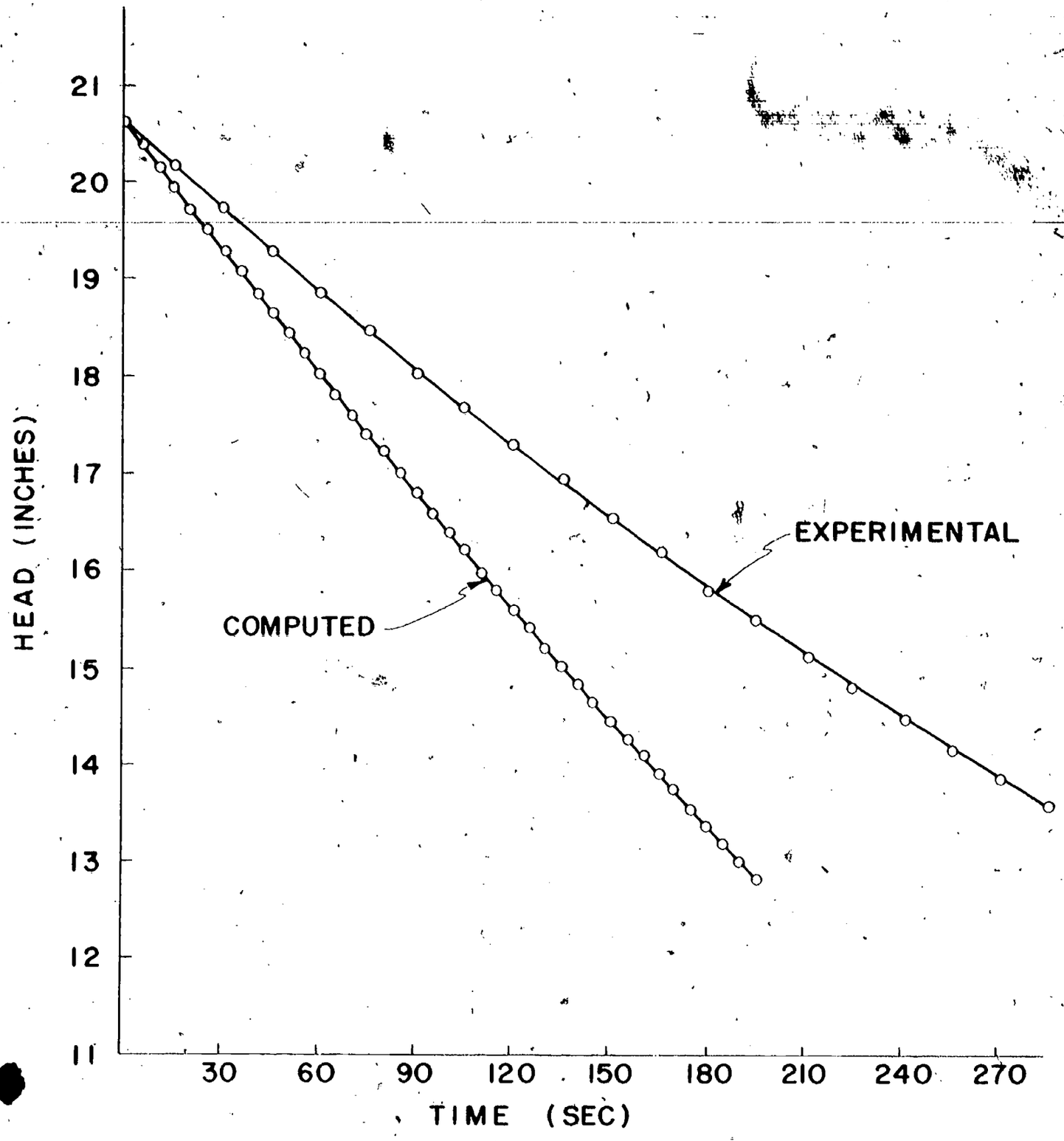

FIG. 8-3 HEAD OF LIQUID IN TANK AS A FUNCTION OF TIME

```
C  C      UNSTEADY FLOW ANALYSIS  BARLOW, JONES, YNGVE
       PUNCH 10
   10  FORMAT (10X,4HTIME,10X,4HHEAD,10X,10HDIFFERENCE)
   20  READ 30,G,HO,HL,DT,DP,DELT,CI,CII,CIII,F,DIST,TIME,V
   30  FORMAT(7F10.5)
   32  HL=V**2/(24.*G)*(CI+CII+CIII+F*DIST/DP)
       VP=SQRTF(24.*G*(HO-HL))
       IF ((SQRTF((V-VP)**2))-1.00)38,38,35
   35  V=V+0.25
       GO TO 32
   38  DHDT=-((DP**2)/(DT**2))*SQRTF(24.*G*(HO-HL))
       TIME=TIME+DELT
       V=V-2.
       HOI=HO+DHDT*DELT
       DIFF=HO-HOI
       HO=HOI
       PUNCH 40,TIME,HO,DIFF
   40  FORMAT (7X,F7.2,9X,F6.3,10X,F8.4)
       IF(HO-13.)50,50,32
   50  STOP
       END
    32.174      20.625      0.          12.         0.375       5.          0.5
    0.9         0.19        0.032       62.         0.          40.
```

Fig. 8-4 A Computer Program to Predict the Time History of Head in a Draining Tank.

time recorded as the tank is allowed to drain. This can be done using a stop watch and recording the time when the surface of the water crosses pre-selected points on a meter stick; or, collecting the water in a graduate and measuring the time necessary to collect a certain amount of water, then converting this to change in head. For a small diameter piping system, and large tank diameter, the readings with the watch can be made with reasonably good accuracy.

Sample results

In the model used by the students, the water level was read in a gage glass which was attached to the tank as shown in Fig. 8-1. The tank was filled with a clamp on the hose. At time zero, the clamp was removed and the tank began to drain while readings were recorded. Two sets of readings were made, and first differences were evaluated to determine whether the results were linear. (First divided differences are found as the difference between two successive values of head divided by the time difference between them.) As expected, the first differences were smaller for higher times than they were initially. That is to say, the change in elevation for a given time change is less for the smaller head because the velocity is less. This curve of the experimental data, Fig. 8-3, looks very close to a straight line.

In the computer program, the students entered an average value of friction factor, 0.032. This simplified the calculation as it was necessary neither to calculate Reynolds numbers nor to use a table look-up for evaluating f. This could have introduced error in that the value of f L/d for this case, with a 62 inch long section of 3/8 inch tubing was

$$(.032)\ \frac{(62)}{(.375)} = 5.29$$

which was the dominant term in the expression for h_ℓ. Values of loss factors, diameters; and a trial value of velocity were read into the program. The program, Fig. 8-4, is self-explanatory.

The predicted curve shown in Fig. 8-3 shows a slower rate of draining than the measured curve. Possible sources of errors are the use of an average value for f and the rather large value of ϵ used in the program. In this case, $\epsilon = 1$. However, the students' approach to the problem, the qualitative agreement between analysis and experiment, and the recognition of sources of error made this a worthwhile exercise. It provides an opportunity for theory-testing and gives the student a chance to relate analysis, digital computation and experiment in a single exercise.

Modifications of the experiment

Several modifications of this experiment are possible. For one thing, the piping can be altered in many ways. A system of piping can be employed, and a single element added or removed, and the results compared. Particularly interesting is the addition of a globe valve to the system. Comparison can be made between the losses with a globe valve and a gate valve.

Fluids can be changed. Using a glycarine of known viscosity will provide results

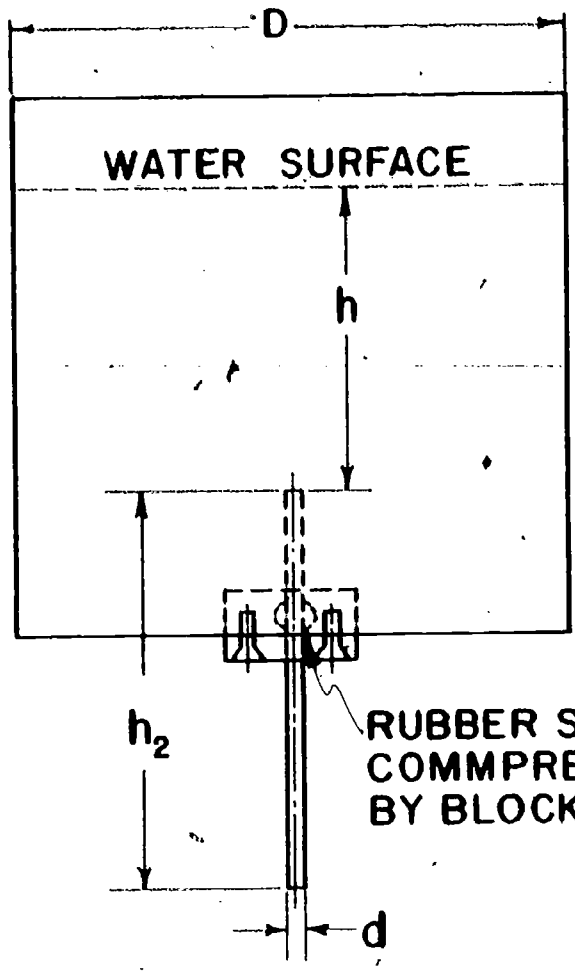

FIG. 8-5 a.
BUCKET SHOWING
PRINCIPAL
DIMENSIONS

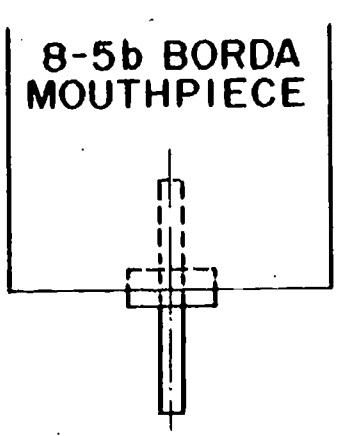

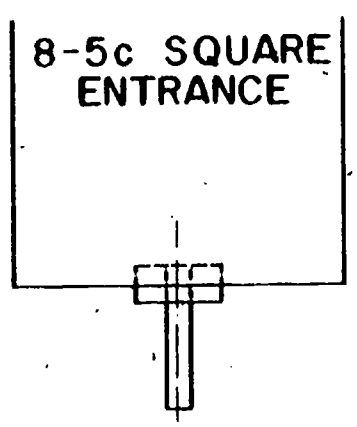

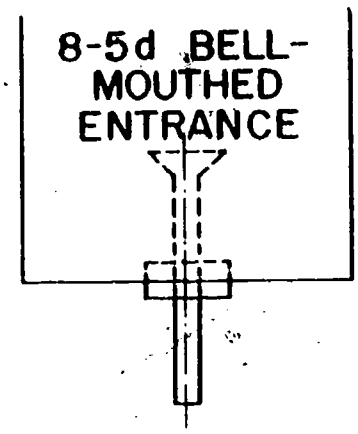

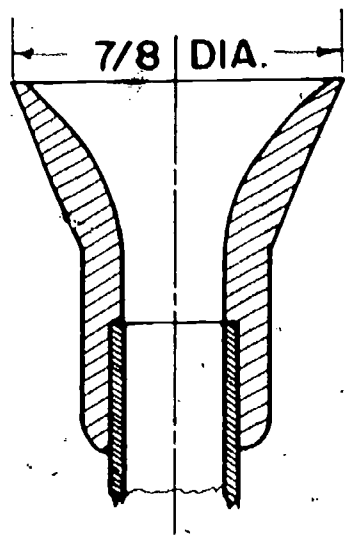

8-5e SECTION OF
BELL-MOUTHED
ENTRANCE

which are quite different from experiments with water.

The height of the tank can be changed as can the diameter of the piping to insure turbulent flow.

Using a pressurized tank equipped with a pressure gage, the time for a gas to leave the tank can be measured. Here, the important term is the tank pressure expressed as a function of time. This experiment should include an assumption of compressible flow.

Any of these can be done as an experiment without introduction of the analysis which may be too advanced for some first and second-year students.

Experiment 8A

The Effect of Entrance Geometry

In this experiment several entrance conditions will be employed and head losses determined for the draining of liquid from a tank.

Introduction

The previous experiment was modified to investigate the effect on the emptying rate of the tank for several inlet geometries. Three were used. Each is illustrated in Fig. 8-5. The first is a Borda mouthpiece, Fig. 8-5b. In the second, the tube has been lowered to form a sharp-edge entrance Fig. 8-5c. The third was a bell-mouthed entrance, Fig. 8-5d..

A five-gallon drum was used for the tank with a 1/4 in. diameter brass tubing. The tubing entered through a rubber seal fastened to the base of the tank. This is shown in Fig. 8-5a. The tubing could be pushed through the rubber seal so that the tubing end was set at any selected distance above the bottom, or flush with the bottom. A small bell-mouthed entrance was made of aluminum. It had a 7/8 inch diameter opening at the entrance. The bottom was recessed to fit snugly over the end of the brass tubing as shown in Fig. 8-5e.

Referring back to eq. (8-2) and the analysis that follows, it is apparent that the only difference between the previous case and the present one is that h_2 is not zero, but is equal to the length of the tube. Consequently eq. (8-7) becomes

$$\frac{dh}{dt} = -\frac{d^2}{D^2}\sqrt{2g((h-h_2) - h_\ell)} \qquad 8\text{-}13$$

As the tube length is fixed, h_2 is a constant for all of the experiments.

The experiment

The tank was filled to a pre-determined level with water. A scale was fastened inside the tank to provide a measure of the level of the water surface while the lower end of the tube was closed with a stopper. One of the inlet conditions was established. Several minutes were allowed to pass for the fluid to come to a quiescent state. At a signal, the stopper was removed and a stop watch started. At a succession of closely spaced intervals, the time was recorded and, simultaneously, the scale was read to indicate the height of the water surface.

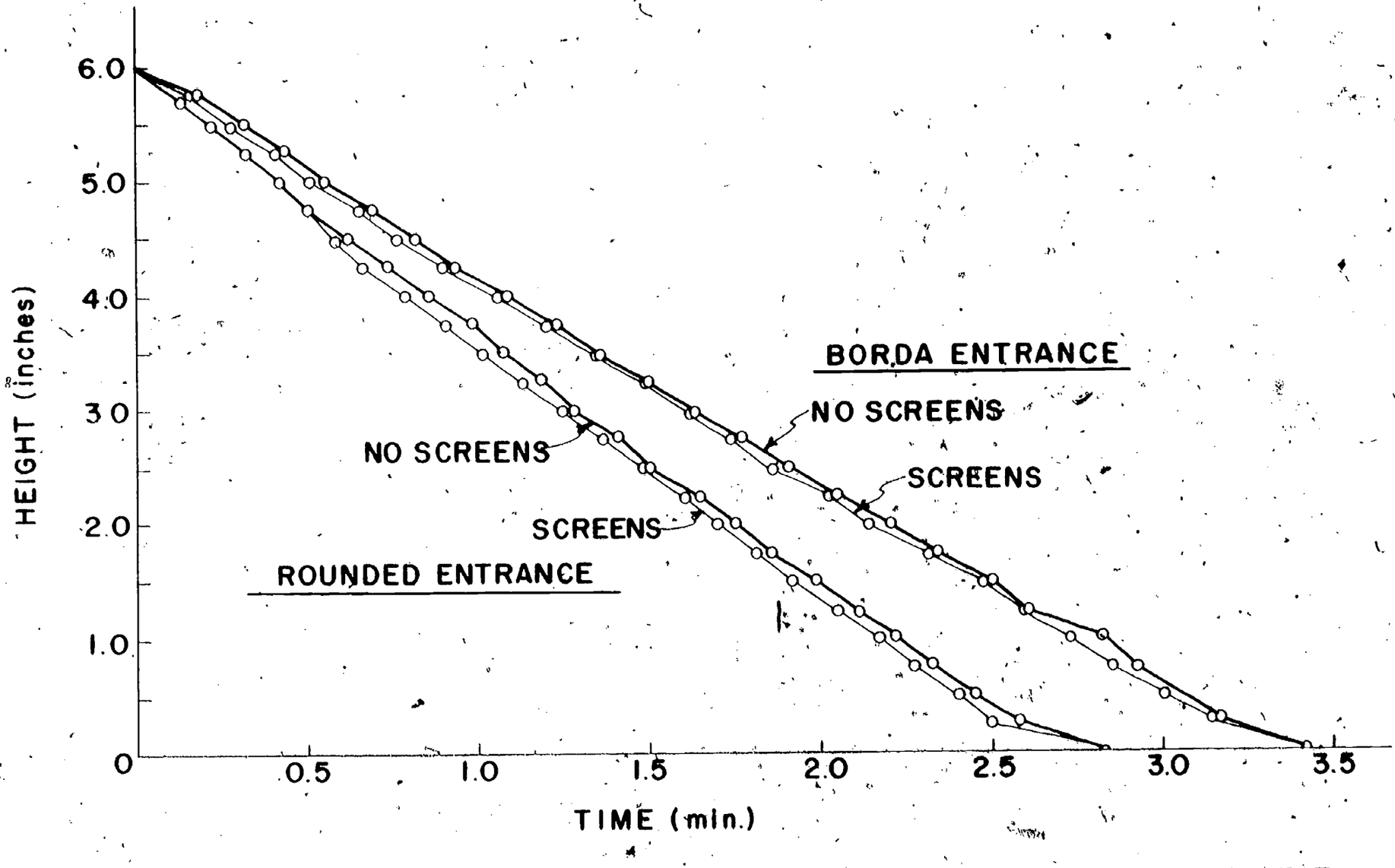

FIG. 8-6 HEAD - TIME CURVES FOR A DRAINING TANK SHOWING THE EFFECT OF THE VORTEX FOR TWO ENTRANCES.

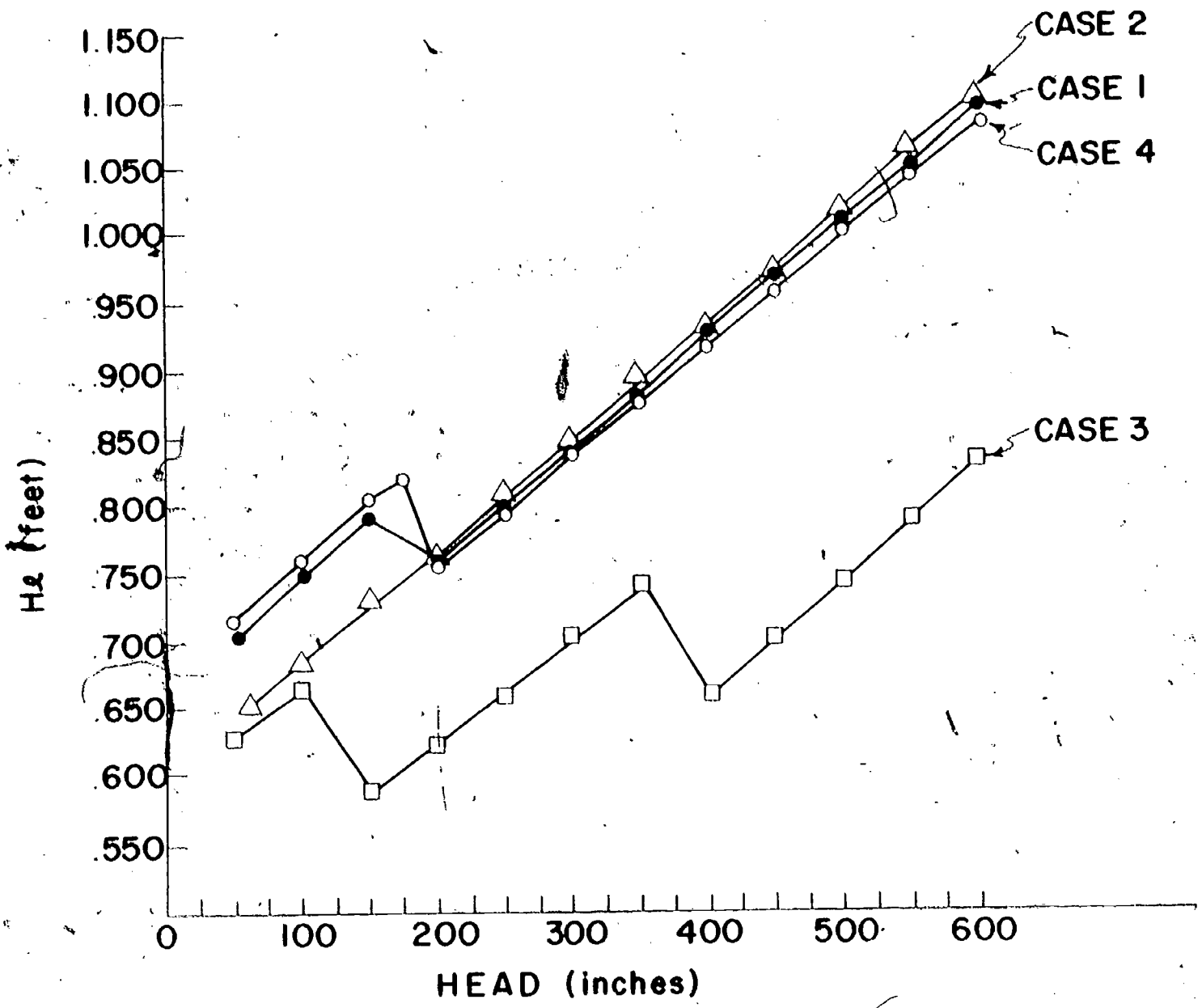

FIG. 8-7 HEAD LOSS FOR FOUR INLET CONDITIONS AND WITH SCREENS.

Plotting h vs. time, the values of $\frac{dh}{dt}$ could be determined for a set of values of h. This can be done graphically or by approximating the derivative in finite difference form

$$\frac{dh}{dt} \approx \frac{h^{(2)}-h^{(1)}}{\delta t}$$

Here $h^{(1)}$ and $h^{(2)}$ are values of h at two times, separated by a small interval δt.

With d, and D, measured from the experiment, h_1, h_2 and $\frac{dh}{dt}$ were known; a calculation for h_ℓ was made from eq. (8-13).

Graphs can be prepared for the several cases of h vs. t and for h_ℓ vs. h, to compare the effect of each entrance on losses. When the experiment is run, it will be noted that a single vortex is formed which is quite spectacular. It becomes apparent that its presence affects the results, and better evaluation of the entrance conditions can be made if the vortex is destroyed. This is possible if several pieces of window screening are put in the tank dividing the tank into pie-shaped sections. The screening should go from the tank bottom to above the water surface. A modification of the experiment, which is concerned only with this vortex, is presented as Experiment 8-B.

Sample results

Measurements were made during emptying for a tank having a diameter, D, of 11.13 inches, and a tube having an inside diameters, d, of 0.25 inch. Four entrance conditions were used:

Condition 1. Borda entrance, 6 inches above base

Condition 2. Borda entrance, 3 inches above base

Condition 3. Bell-mouthed entrance, 3 inches above base

Condition 4. Sharp-edged entrance -- tube moved to a position flush with the bottom of the tank.

Tests were made without screening (vortex present) and with screens (vortex absent). Graphs of the head, h, versus time were constructed for each case. Shown in Fig. 8-6 are conditions 2 and 3 with and without screens. From these data $\frac{dh}{dt}$ was approximated and the head loss determined. Head loss, h_ℓ, is shown for conditions 1, 2, 3 and 4 with screens in Fig. 8-7.

These results indicate that the emptying times are not appreciably reduced by the elimination of the vortex. Also indicated is the conclusion that the losses are measurably less for the rounded entrance than for any of the other entrance conditions. There is not a large difference among cases 1, 2 and 4. Erratic behavior in the values of h_ℓ is due to difficulty in evaluating the derivative accurately from the loss-time curves.

It is probably more useful to plot the head loss in a dimensionless form, one which compensates for the change in velocity with head. Using an expression like the friction factor or f has this characteristic,

$$f = \frac{\frac{h_\ell}{2}}{\frac{v^2}{2g}}$$

8-14

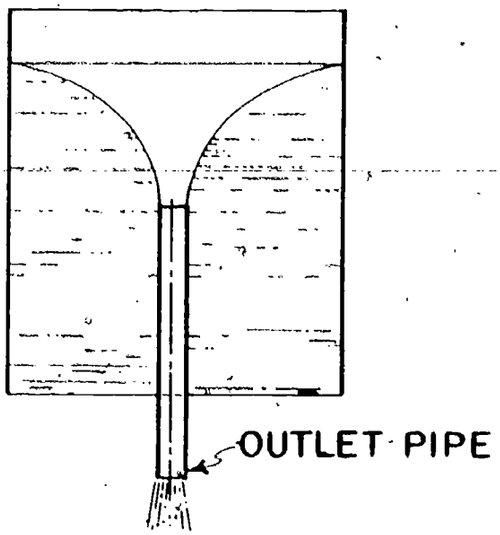

FIG. 8-8a SECTION SHOWING WATER SURFACE IN A VORTEX

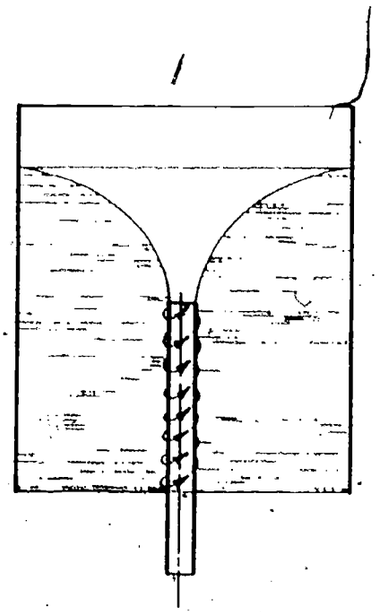

FIG. 8-8b SECTION SHOWING DIE TRACES IN THE VORTEX

Here the velocity can be defined as an ideal velocity if losses were zero,

$$v = \sqrt{2g\ (h-h_2)} \qquad 8\text{-}15$$

or, as the measured velocity,

$$v_2 = \frac{Q}{\frac{\pi d^2}{4}} = \frac{D^2}{d^2}\left(\frac{dh}{dt}\right) \qquad 8\text{-}16$$

Examination of eq. (8-16) shows a source of error in this experiment that might be excessive. When the pipe diameter, d, is small compared to the tank diameter, D, the head is easily measured in the transient as it is changing slowly. However, the ratio D^2/d^2 is a very large number and must be multiplied by a small number, dh/dt, which is difficult to obtain. It is always difficult to determine derivatives from data. For a curve of a given function, the curve of the derivative is less smooth than the curve of the function, and the integral produces a curve that is smoother than that of the function. Errors in data are magnified in differentiation and suppressed in integration. Consequently, for this test, more accurate results might be obtained by measuring Q directly. this can be done by collecting flow in a graduate for a short period; finding q as the amount collected per second; and computing v_2 from the expression

$$v_2 = \frac{Q}{\frac{\pi d^2}{4}}$$

This will be the average velocity over the interval taken to measure tho flow.

Equations can then be left in terms of v_2 and the losses computed as before.

Experiment 8B

Study of a Vortex

The objective is to examine a vortex in a tank being drained.

As indicated in the previous experiment, when flow was established in the draining tank, a vortex was formed. The profile of the water surface is shown in Fig. 8-8a. An experiment can be devised to study the behavior of this vortex under different flow conditions, and to trace the flow in the vortex system.

The tank is filled with water, and allowed to settle for ten minutes. Flow is begun by removing the plug at the bottom of the pipe. It may be found that the vortex will not develop soon enough if the water is too still, and the tank could empty before the vortex is established. A small swirl can be encouraged before draining to induce the vortex.

Food coloring can be injected through a long hypodermic tube at different points in the flow, to observe the direction of flow at different levels. Surface movement can be detected by "vortex meters". These can be constructed from small bits of paper, with a cross on each, which float on the surface.

Sample results

The vortex meters will show the surface velocity in the vortex and indicate whether the surface flow is "irrotational" or not. It is found that the velocity decreases as one moves away from the center of the vortex. The meters rotate less in the regions away from the wall and not too close to the center. If there is no rotation of the meters, the flow is behaving as an ideal free vortex. Viscous effects cause rotation in the vortex which will cause the meters to revolve on their own axes.

Observation of the dye traces shows the entire mass to be swirling. The dye will be seen to move in along the bottom of the tank and then spiral upwards along the outlet pipe as shown in Fig. 8-8b. When it reaches the inlet, it is drawn into the tube.

References

1. Streeter, V. L., Fluid Mechanics, McGraw-Hill, New York, New York (1971), p. 297.
2. Brenkert, K., Elementary Theoretical Fluid Mechanics, John Wiley and Sons, New York, New York (1960), p. 224.
3. Arden, B. and K. N. Astill, Numerical Algorithms, Addison-Wesley, Reading, Mass. (1970), p. 221.

Experiment No. 9

Convection Heat Transfer

When an object at one temperature is immersed in a fluid at another temperature, heat is transferred from or to the object. The mode of heat transfer is called convection. One measure of the rate of convective heat transfer is the coefficient of heat transfer, h. It is defined from Newton's law of cooling as

$$\frac{q}{A} = -h\,(t-t_o) \qquad 9\text{-}1$$

where

q = rate of heat transfer per unit of time

A = surface area of the object

t = surface temperature of the object

t_o = bulk temperature of the fluid.

Typical units of h are Btu/hr-ft^2-^{o}F. Sometimes h is grouped with a length dimension, L, and the conductivity of the fluid medium, k, to form a dimensionless number called the Nusselt number,

$$Nu = \frac{hL}{k} \qquad 9\text{-}2$$

If the object is in a gravitational field, and the fluid moves over it due to gravitational effects, the heat transfer is described as natural or free convection. For the same fluid, the rate of heat transfer can be increased by blowing or pumping the fluid past the object. This is forced convection. One soon learns that the magnitude of h depends on the fluid velocity, the geometry of the object and fluid properties such as conductivity, k; viscosity, μ; density, ρ; and specific heat, c_p.

In this series of experiments we shall determine the coefficient of heat transfer between a small object and a fluid for several situations by means of a transient temperature measurement. The objects will be small enough with high conductivity (copper or aluminum) so that we can assume the temperature of the object to be uniform. Let that temperature of the object be t. From eq. (9-1), the heat transfer between the fluid and the surroundings is

$$q = -h\,A\,(t-t_o)$$

This will be reflected as a change in temperature of the object. For a mass, m, with specific heat, c_p, the rate of heat transfer is related to the time rate of change of temperature by the equation

$$q = m\,c_p\,\frac{dt}{d\tau} \qquad 9\text{-}3$$

where τ is time.

We can now record the temperature history of the object as it is heated or cooled. At any point in time we can obtain t and $\frac{dt}{d\tau}$.

We can obtain values of m, c_p and A for the object and then solve for the coefficient of heat transfer by equating the two expressions for q,

$$h = \frac{-m\,c_p\left(\frac{dt}{d\tau}\right)}{A\,(t-t_o)} \qquad 9\text{-}4$$

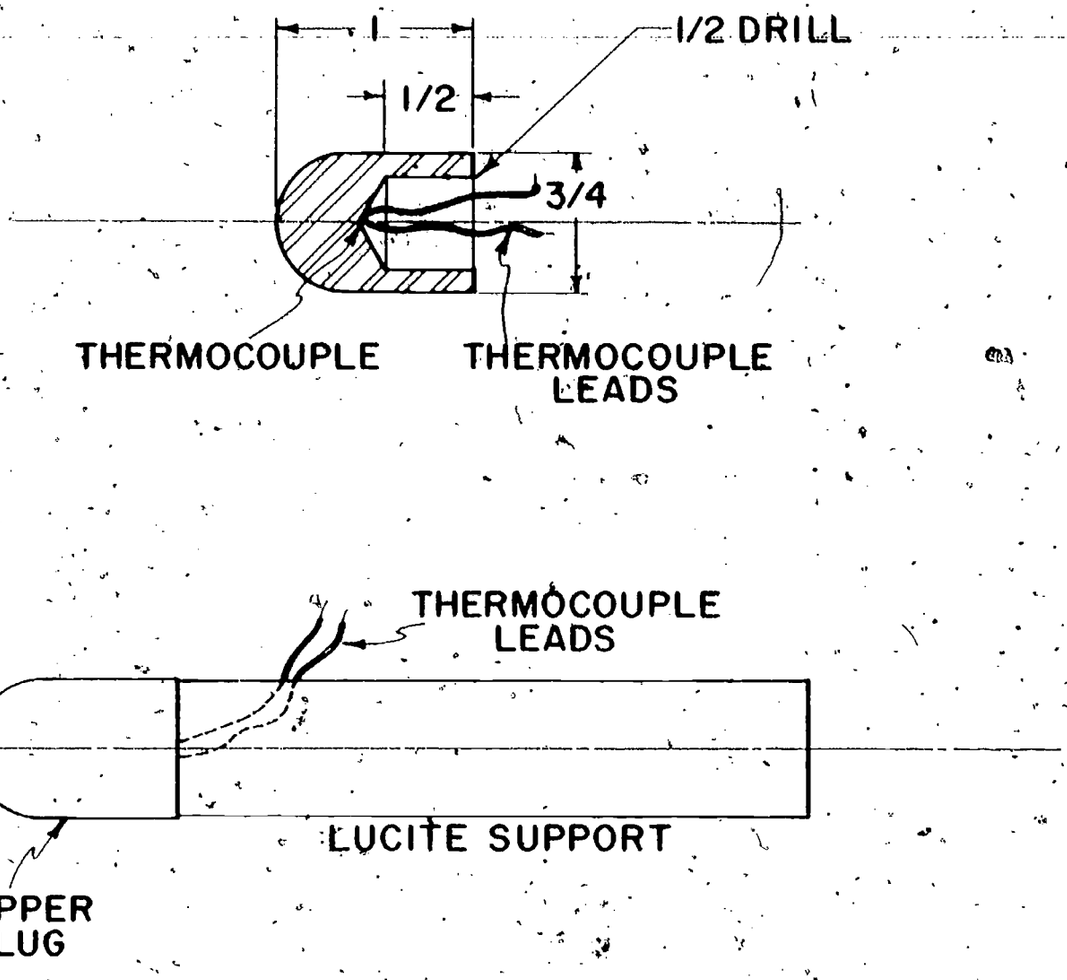

FIG. 9-1 COPPER SLUG FOR HEAT TRANSFER TEST

Experiment 9A

Determine the Coefficient of Heat Transfer for Natural Convection

The object is to determine the coefficient of heat transfer in natural convection from a small copper object by making a transient measurement of the temperature.

The object to be tested is a small cylindrical copper slug with a rounded end. This is hollowed out and mounted on a plastic support as shown in Fig. 9-1. Some dimensions are given on the figure. Embedded near the center of the object is a copper constantin thermocouple with the leads carried out through the plastic rod. For information on thermocouples, see ref. 1 or 2. A diagram of the test set-up is given in Fig. 9-2. (For natural convection eliminate the air supply and hot-wire anemometer.)

The copper slug is first heated by putting it in a blast of hot air, or immersing it in boiling water. If water is used, dry the slug before beginning the test. Using the plastic support and a ring stand, the slug is placed in still air with its axis horizontal. The temperature is then measured at specific intervals. A better approach is to use a millivolt recorder such as a Leeds and Northrup Speedomax recorder. The chart record gives a curve of millivolt output of the thermocouple versus time which can be easily converted to temperature versus time. A chart record is shown in Fig. 9-3. Air temperature is read from a second thermocouple suspended in the free air.

Derivatives of temperature with time can be obtained from the chart record and the coefficient of heat transfer computed at various temperatures along the cooling curve.

Sample results

For the copper probe illustrated with $c_p = 0.092$ Btu/lbm-°F, the product

$$\frac{mc_p}{A} = 0.434 \text{ Btu/ft}^2\text{-°F}.$$

At a temperature of 177.5F, the change in temperature was measured as 5°F in 37 seconds from the chart. From this,

$$\frac{dt}{d\tau} \approx -\frac{5}{37}(3600) = -486.5\text{°F/hr}.$$

With the air temperature measured as 78F, the coefficient of heat transfer from eq. (9-4) is

$$h = \frac{(0.434)(486.5)}{(177.5 - 78)} = 2.12 \text{ Btu/hr-ft}^2\text{-°F}.$$

Converting this to a Nusselt number using as the characteristic length the diameter of the copper slug, 0.75 in, and $k = 0.015$ But/hr-ft-°F for air,

$$Nu = \frac{(2.12)}{(.015)}\frac{(.75)}{(12)} = 8.84$$

Curves of Nusselt number versus air temperature can be developed and the results compared to those given in ref. 3 or 4.

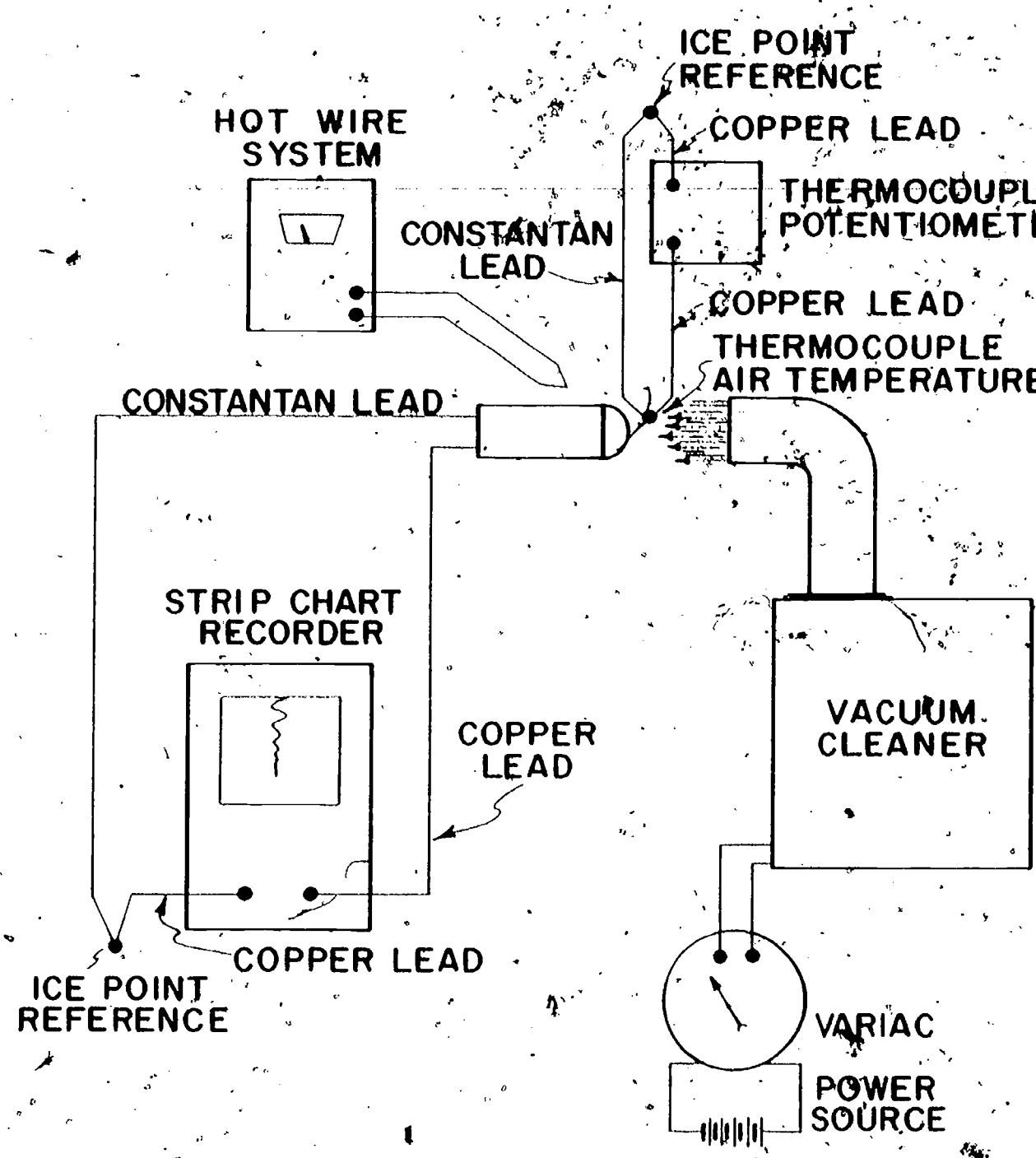

FIG. 9-2 TEST SET-UP FOR FORCED CONVECTION TEST. FOR FREE CONVECTION NO AIR SOURCE IS NEEDED.

Modifications

In natural convection the geometry is an important factor. The experiment can be modified by making the measurements with the axis vertical, and the blunt nose pointing downward. A second slug made of copper but with a diameter of 1/2 inch was used to evaluate the effect of diameter on the convective heat transfer. Results for h were about 10 percent higher for the small probe which is about what would be expected for free convection from horizontal cylinders (ref. 3). To evaluate the effect of properties of the slug on the experimental results, an aluminum slug can be made having the same dimensions as the large probe. Differences between heat transfer for an aluminum and for the copper slug were less than the observed errors in any given test run.

Instead of air, the response in an ice bath or hot water can be measured. This requires a recorder to obtain the temperature history as the temperature response is too rapid to follow by manually balancing a potentiometer.

Experiment 9B

Determination of the Coefficient of Heat Transfer in Forced Convection

The object is to determine the heat transfer coefficient in forced convection by making transient measurement of the temperature in a copper object.

This experiment differs from the former in that the object is placed in a stream of moving air. Air can be supplied by a commercial vacuum cleaner, a woman's hair drier or a heat gun. The object can be heated or cooled and put in a stream of unheated air, or it can be at room temperature and placed in a stream of heated air. In any case, it will be necessary to measure the temperature of the air being blown past the object, using a thermocouple suspended in the free air stream. It is also important to be able to change the approach velocity of the air and to measure its speed just ahead of the object. This should be done with the object in place, but not necessarily during the time that the temperature record is made. A simple hot-wire apparatus capable of indicating the magnitude of the air velocity works best.

The slug is brought to some temperature different from that of the air stream. It is then placed in the stream and the thermocouple record made on a strip chart recorder. Using these results to evaluate t and dt/dτ, eq. (9-4) is solved for h, and the Nusselt number calculated. Graphs of h versus slug temperature and h versus flow velocity can be made. Most useful are graphs of Nusselt number versus the flow Reynolds number. Here the Reynolds number is defined as

$$Re = \frac{\rho v d}{\mu}$$

where ρ = density of the air, lbm/ft^3

μ = viscosity of the air, lbm/sec-ft

v = velocity of the air, ft/sec

d = diameter of the copper slug, ft

Dimensionless correlations can then be made, having the form

$$Nu = A\,(Re)^m$$

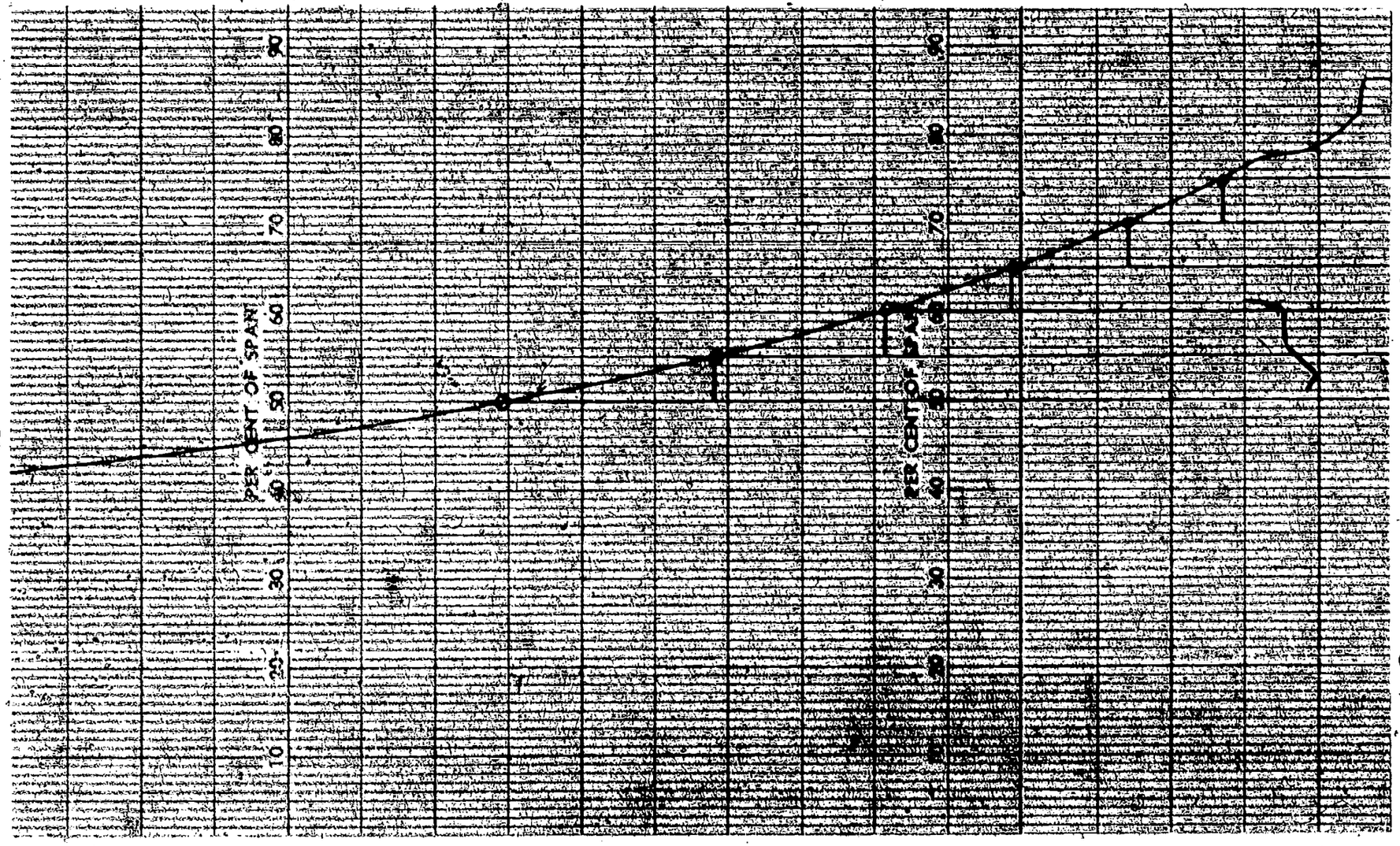

Fig. 9-3 Strip Chart Record for Temperature History

where A and m are constants found from the plot.

Sample results

The test set-up is shown in Fig. 9-2. Air was supplied from a vacuum cleaner exhaust, with the speed of the motor controlled with a Variac. The speed of the blower was set and the air velocity and temperature measured at the point where the slug was to be placed. The slug was heated in boiling water, withdrawn, dried and set in place with a ring-stand support. It was positioned with its axis parallel to the air stream as shown in Fig. 9-2. The time temperature record was made as done in Experiment 6A.

Results were computed from the records and graphs made of h vs. temperature and h vs. velocity for velocities ranging from 1000 ft/min to 2500 ft/min. Nusselt numbers were plotted against Reynolds numbers on log-log graph paper for several temperatures, as shown in Fig. 9-4. It is apparent that the effect of velocity is more important than the effect of slug temperature on the heat transfer. Tests were run for the large and small copper (3/4 inch diameter) (1/2 inch diameter) slugs, and the results correlated for a range of Reynolds numbers from 3000 to 10000, as follows:

$$\text{For the small probe, } Nu = 0.144\ Re^{0.681}$$

$$\text{For the large probes, } Nu = 0.151\ Re^{0.669}$$

Modifications

One obvious change is to place the probe so its axis is normal to the air velocity. Another modification is to induce turbulence ahead of the object by placing a wire crosswise to the flow. In a series of experiments using the large copper slug, an increase of five to ten percent was measured in the heat transfer coefficient with the tripping wire creating turbulence.

Both Experiments 9A and 9B offer an opportunity to consider and, whenever possible, evaluate sources of experimental error.

References

1. Schenck, H., Theories of Engineering Experimentation, McGraw-Hill, New York, New York (1968), pp. 99-100.
2. Beckwith, T. G. and N. L. Buck, Mechanical Measurements, Addison-Wesley, Reading, Mass. (1969), pp. 463-470.
3. McAdams, W., Heat Transmission, 3rd Ed., McGraw-Hill, New York, New York (1954), pp. 176-177.
4. Rohsenow, W. M. and H. Y. Choi, Heat, Mass and Momentum Transfer, Prentice Hall, Englewood Cliffs, New Jersey (1961), p. 206.

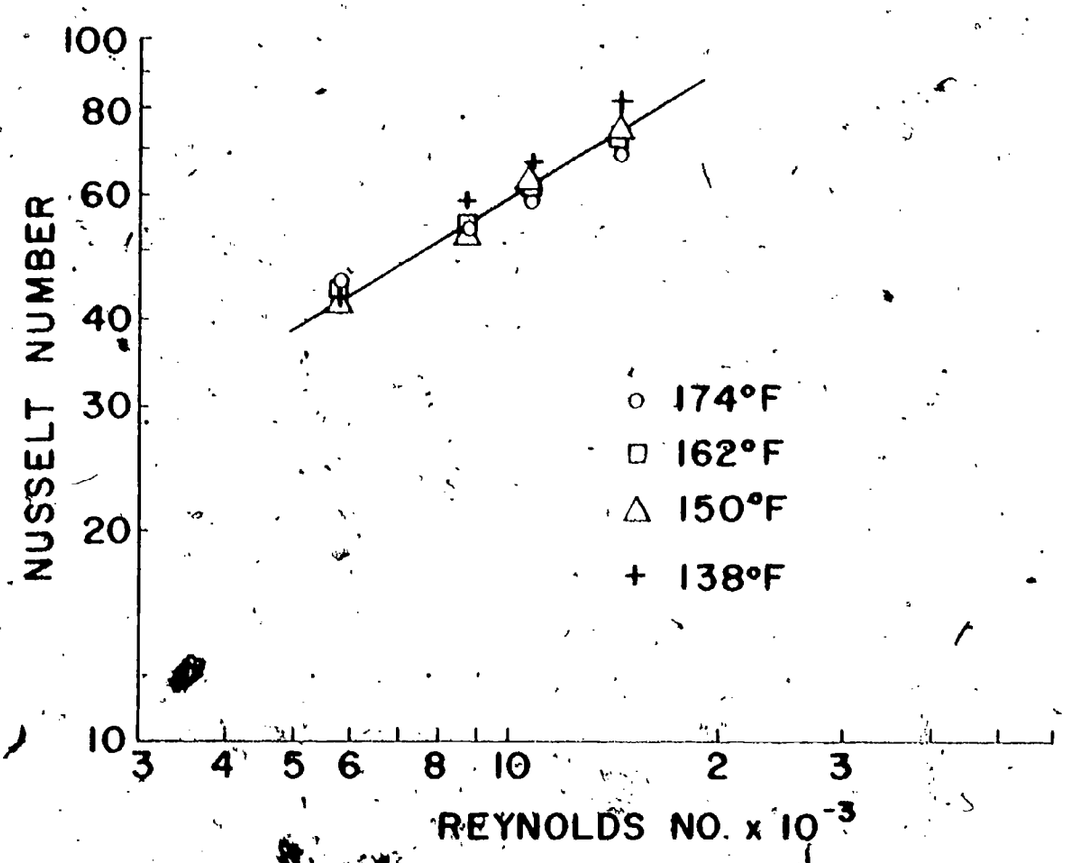

FIG. 9-4 NUSSELT NO. AS A FUNCTION OF REYNOLDS NO. AT FOUR TEMPERATURES

Experiment No. 10

The Magnus Effect*

The objective is to determine the effect of rotation on the trajectory of a cylindrical body moving through air.

It is well known that the trajectory of a spinning ball or cylindrical rotor is curved. A curve thrown by a baseball pitcher is one example. The spin of the object sets up pressure forces normal to the flight of the object. These forces cause the path to curve. This is called the Magnus effect. The Flettner rotor ship was designed to utilize this principle as a means of propulsion (ref. 1). A simple experiment can be performed to illustrate this phenomenon and evaluate its influence.

Experimental model

The model was a simple cardboard tube such as used for a paper towel or toilet paper roll. In this case, the roll was 1½ inches in diameter and 4 inches long. A circular disc was cemented to each end. These were cardboard, 3 inches in diameter and 0.025 inch thick. They were used to mark the flight. The assembly is shown in Fig. 10-1.

Propulsion of the tube was accomplished by using nine rubber bands tied together. These were attached to a string 58 inches long. The tube was wrapped with the string and placed horizontally on the table. The string was connected to the rubber bands which were stretched as shown in Fig. 10-2. When the tube was released, the bands pulled the string forward giving the tube spin and forward velocity. A little practice is necessary to control the flight.

Experimental procedure

It was necessary to be able to measure the position of the object as a function of time, to determine the trajectory, velocity and rate of spin. A Strobotac might be used. The technique used in this experiment was to ignite a corner of one of the circular discs before starting the flight. By photographing the flight on a single exposure, the trajectory as well as the spin can be recorded. Photographs made in this way are shown in Fig. 10-3. These were made on Polaroid 3000 film using a Speed Graphic camera with a lens opening of 4.5. The shutter was held open from 1 second before flight until after the flight was completed. Photographs were made in a darkened room with the camera 15 feet from the flight path. To record time, a vibrating reed was used, formed by fastening a cardboard flag on the end of a steel bar which passed in front of the lens. Shown in Fig. 10-4, this caused the dark regions on the photograph of the trajectory. The flag was placed two inches from the lens, and vibrated at the rate of 3.8 times per second. A scale in the flight plane was photographed to give a scale of length to the photographs. It is important that the flight be confined to a plane parallel to the film surface. This is accomplished better in Fig. 10-3b than in 10-3a.

*Suggested by Professor Lloyd Trefethen, Dept. of Mechanical Engineering, Tufts University, Medford, Massachusetts.

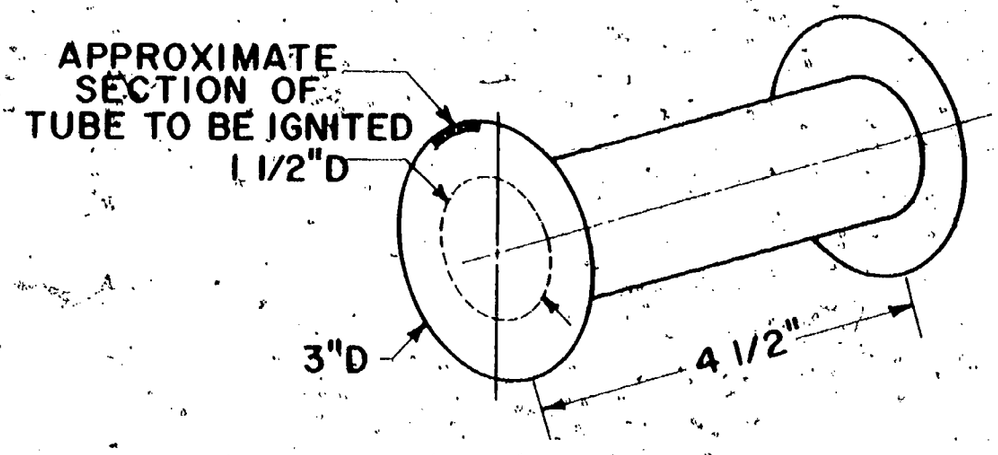

FIG. 10-1 CARDBOARD TUBE WITH DISKS

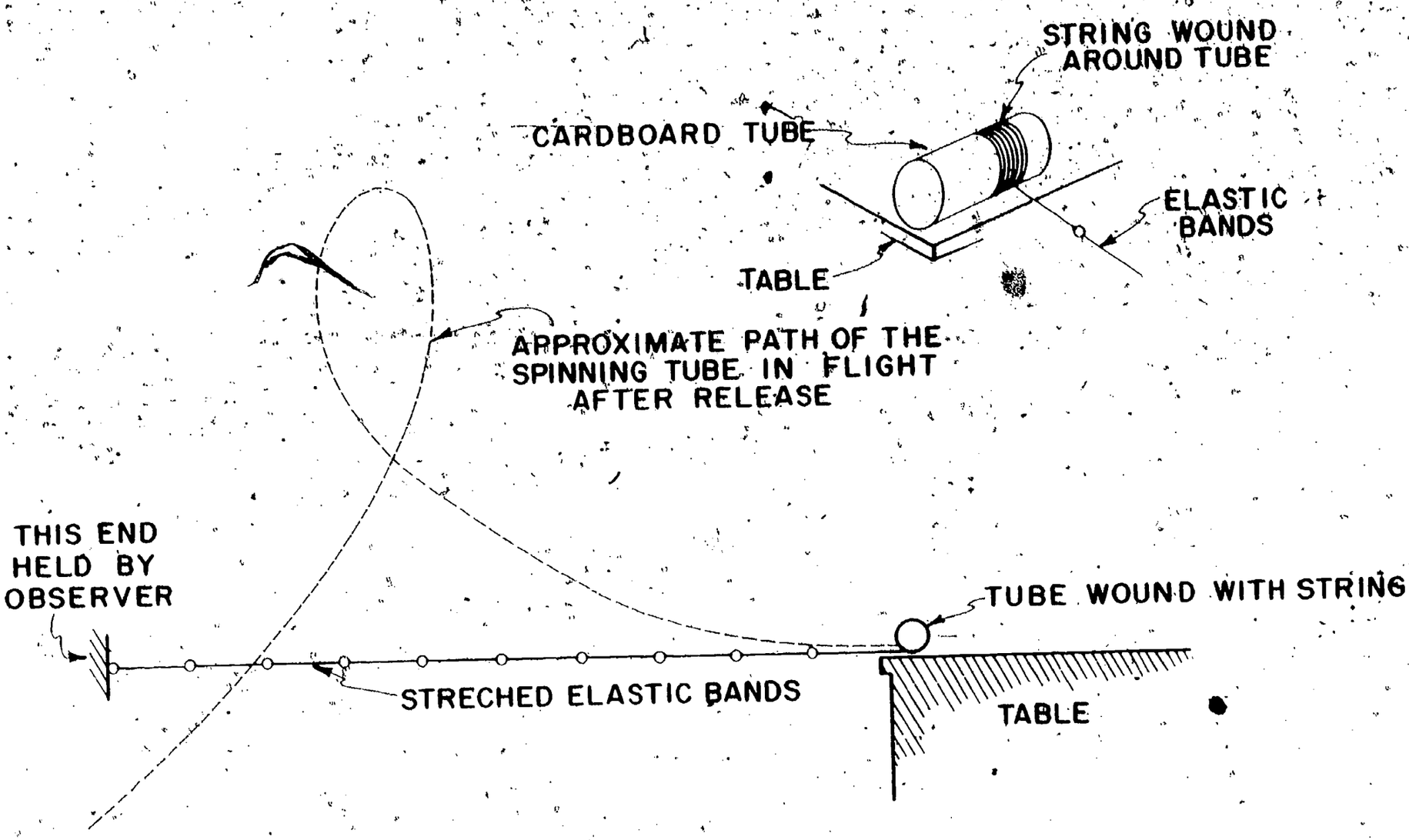

FIG. 10-2 VIEW SHOWING POSITION OF COMPONENTS IN EXPERIMENTAL SET-UP JUST BEFORE RELEASE OF TUBE

(a)

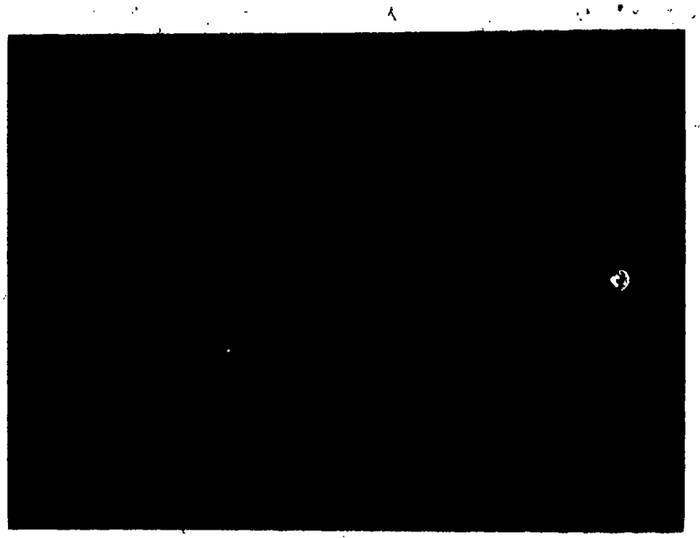

(b)

Fig. 10-3. Photographs of flight path of Spinning Tube

Analysis of data and sample results

From the photographs, the velocity, angle of trajectory and rate of spin could be measured. This was done for each of the time segments, which were of 5/19 seconds duration. It was noted that while velocity was slowed during flight, the rate of spin did not change appreciably. The variables are the spin rate, N; the velocity along the path, v; the distance along the path, S; the angular velocity of spin, ω; the angular direction of the trajectory, θ; and the time, T. Several interesting graphs and cross-plots can be made for combinations of these. Of most interest is the lift coefficient, C_L. This is defined as the ratio of the force normal to the trajectory, (the lift) L, divided by the force equivalent to the dynamic pressure, $\rho v^2/2g_o$. Using the projected area of the cylinder to relate pressure and force,

$$C_L = \frac{L}{\frac{\rho v^2}{2g_o}(2\,r\ell)} \qquad 10\text{-}1$$

where

ℓ = tube length, ft

r = tube radius, ft

ρ = air density, lbm/ft^3

v = velocity determined from photographs, ft/sec

g_o = conversion factor, 32.2 lbm-ft/lbf-sec^2

It is necessary to compute the lift force from the photographs. Consider the sketch, Fig. 10-5. The lift force is normal to the trajectory. Acting on the body are the forces causing centrifugal and tangential acceleration and the weight force, (mg/g_o). The tangential force is drag and does not contribute to the lift. Hence, lift is equal to the "centrifugal force" term plus the component of weight in the direction of lift; or

$$L = \frac{mv^2}{g_o R} + \frac{mg}{g_o}\cos\theta \qquad 10\text{-}2$$

where

m = the mass of the roll, lbm

θ = defined in Fig. 10-5

g = the acceleration due to gravity, ft/sec^2

g_o = mass conversion factor, 32.2 lbm-ft/lbf-sec^2

R = the radius of curvature defined in Fig. 10-5, ft.

The angle θ can be measured from the photograph using a drafting machine or equivalent. To find the radius of curvature, recall

$$R\delta\theta = \delta S$$

or

$$R = \frac{\delta S}{\delta\theta} \qquad 10\text{-}3$$

The approximation to the derivative $\frac{\delta S}{\delta\theta}$ can be found by taking tangents to a curve of S versus θ, or using a finite difference approximation from measurements of S and θ. With R, θ and v determined from the photographs as described, and the mass of the paper roller determined, lift can be computed from eq. (10-2). Measuring ℓ and r, and

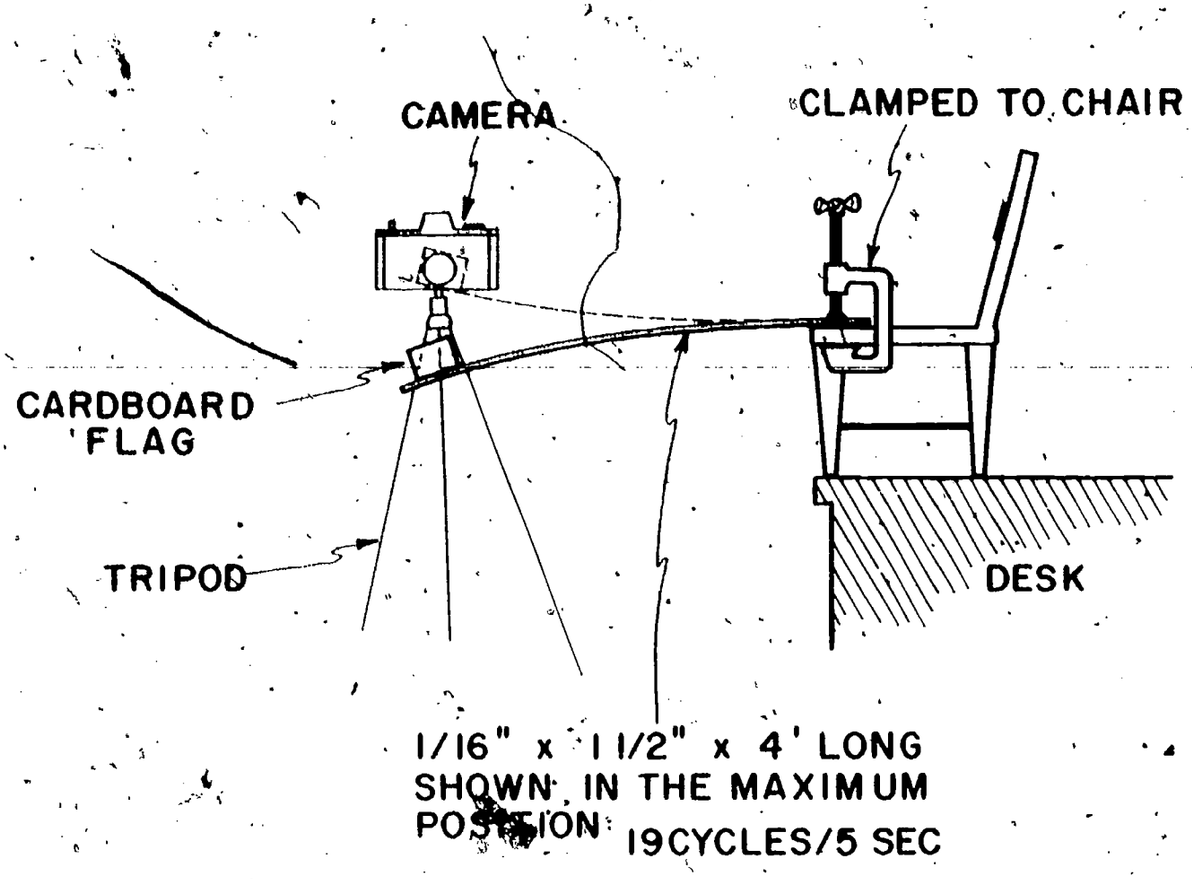

FIG. 10-4 VIEW OF VIBRATING APPARATUS LOOKING FROM OBJECT TOWARD CAMERA

NOTE: AT TOP POSITION THE FLAG BLOCKS THE CAMERA LENS

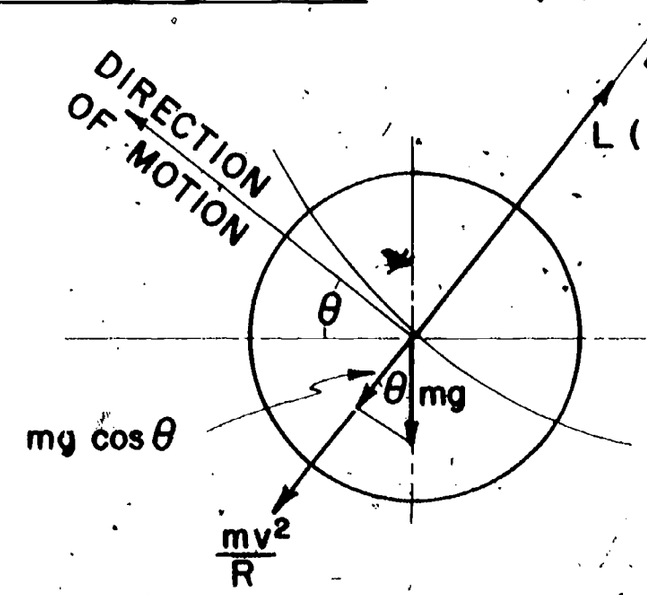

$$L = \frac{mv^2}{R} + w\cos\theta$$

FIG. 10-5 DIAGRAM OF FORCES ON TUBE

obtaining the proper value for ρ, the lift coefficient can be found from eq. (10-1).

Relation can be investigated between lift coefficient and a tangential velocity Reynolds number, or a spin velocity Reynolds number by graphing the results. Since the lift is related to the circulation, it can be demonstrated that a relationship exists between the lift and the ratio of spin velocity, ωr, to tangential velocity, v. Here ω is the spin rate of the tube, radians per second, and r is the tube radius. This result is given by Prandtl, ref. 2.

The lift coefficient was plotted against $\omega r/v$ and compared to the result in reference 2 for tubes with discs on the ends. These curves appear in Fig. 10-6. The results of the experiment are in very good agreement with the curves from Prandtl.

References

1. Streeter, V. L., Fluid Mechanics, McGraw-Hill, New York, New York (1971), p. 426.
2. Prandtl, L. and O. G. Tietjens, Applied Hydro and Aeromechanics, Dover Publications, New York, New York (1934), pp. 84-85.

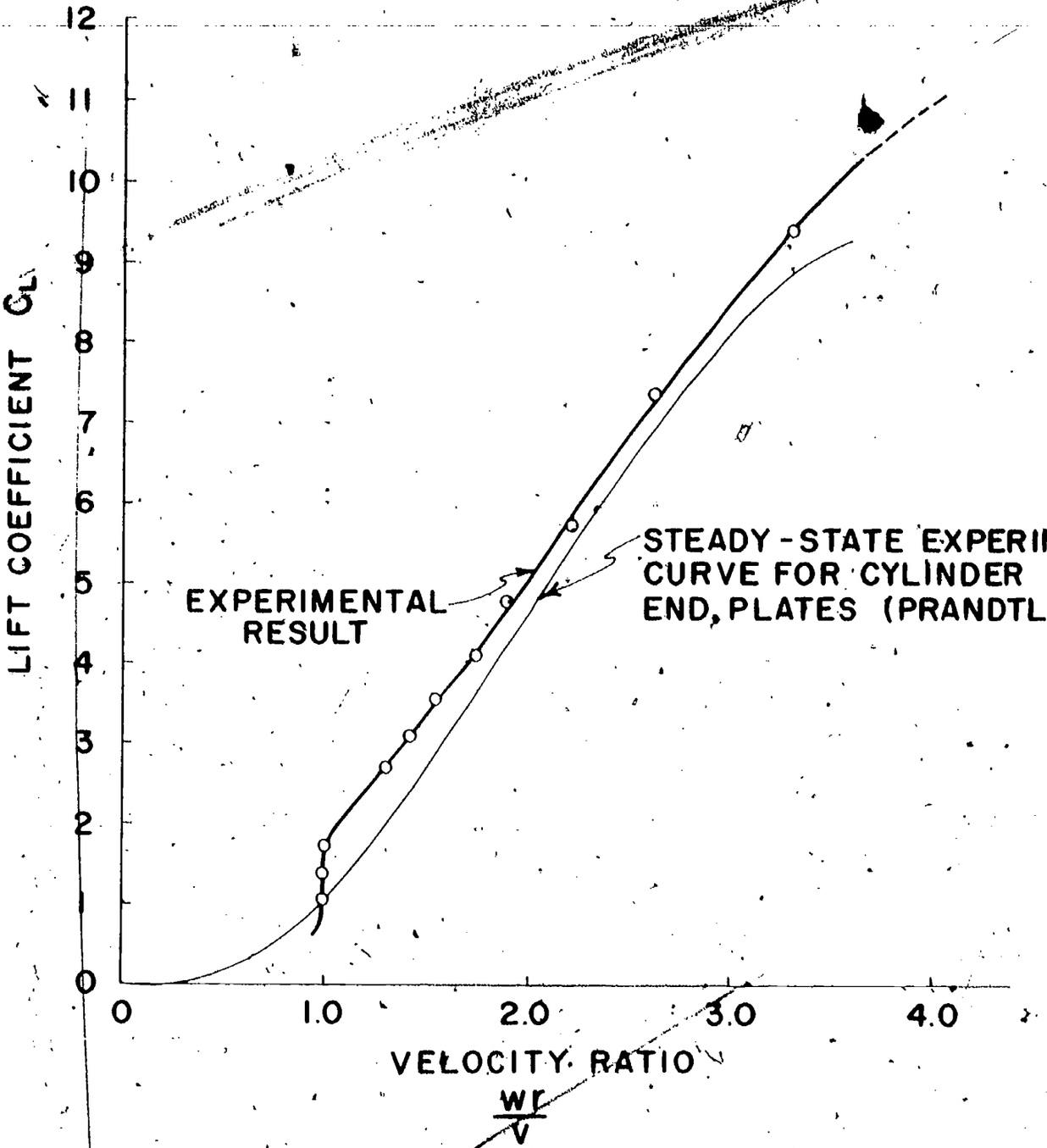

FIG. 10-6 LIFT VS VELOCITY RATIO FOR A SPINNING TUBE WITH END PLATES

Experiment No. 11

The Archimedes Screw Pump

The objective is to investigate the principle of the Archimedes Screw and to evaluate its performance as a pump.

Archimedes (287-212 B.C.) is usually credited with inventing the water screw pump which bears his name (ref. 1). A relatively simple model can be constructed by wrapping transparent, flexible plastic tubing in a spiral around a cylinder as shown in Fig. 11-1. The tubing is open at both ends, with one end in a tank of water. Water is carried up the tubing as the cylinder is rotated. In each coil, the water is trapped at the bottom, and moves up the spiral because gravitation keeps it from being carried over the loop.

Performance variables

It is evident that, if the angle of the shaft, α, is made too large, depending upon the angle of the spiral, β, the water in the spiral would run out and the flow rate would be zero. This would occur when one leg of the spiral became horizontal, or $\alpha = 90 - \beta$.

Design variables include: angle of elevation, α; helix angle β; tubing diameter; diameter of the helix (shaft diameter); and length of spiral. Operating variables are: depth of liquid in the tank, shaft speed, properties of liquid such as viscosity. Experiments can be developed around any of these variables. As one normally builds a single system, the tube diameter, shaft diameter and length are fixed, but it is simple to change elevation angle or helix angle.

Performance parameters include the volumetric pumping rate, Q; the volumetric efficiency, η_v; and the pumping efficiency η_p. Pumping rate is easily measured by collecting liquid over a given time span. Volumetric efficiency is the ratio of volume actually pumped, divided by a maximum displacement. Maximum displacement differs depending upon the velocity of the pump. If the velocity were very slow, the tube would fill to the level of the water in the tank; that is, everything in the angle $2\pi-\theta$ illustrated in Fig. 11-2. This is called static flow volume. When the tube is rotated, the maximum volume is equal to the volume swept out by the mouth of the tube. If the last turn of the helix were at 90° to the axis of rotation, these two would be the same. As it usually isn't the swept-out volume Q_{max} is related to θ and the helix angle, β, as

$$Q_{max} = A_o[(R + r)(2\pi-\theta)]\ \omega \cos\beta \qquad 11\text{-}1$$

where r = tube radius

R = shaft radius

A_o = open area of tube, πr^2

ω = angular velocity of shaft

β and θ are defined above.

Then the volumetric efficiency is

$$\eta_v = Q/Q_{max} \qquad 11\text{-}2$$

The pumping efficiency, η_p, is the ratio of the work done to raise the water to the work required to drive the screw, or

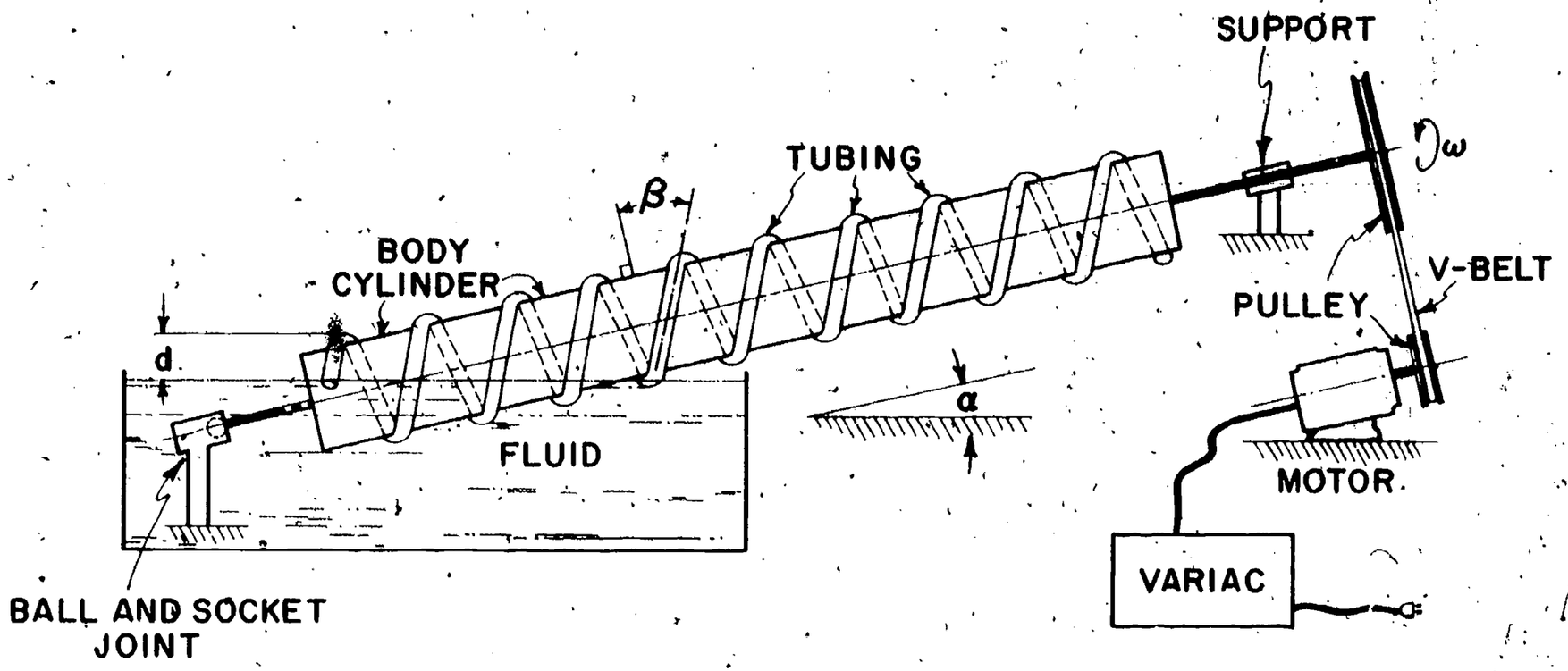

FIG. II-1 TEST MODEL OF ARCHIMEDES SCREW PUMP

$$\eta_p = \frac{Qh}{W}\left(\frac{\rho g}{g_o}\right) \qquad 11\text{-}3$$

where

ρ = density of liquid, lbm/ft^3

g = gravitational acceleration, ft/sec^2

g_o = conversion factor, 32.2 lbm-ft/lbf-sec^2

Q = flow rate, ft^3/min

h = total lift or vertical distance from water surface to shaft centerline at point of delivery, ft

W = work, lbf-ft/min.

In order to compute η_p, it is necessary to measure the work in addition to Q. One method would require converting the motor to a dynamometer. To do this, the motor is supported in bearings so the casing is free to revolve, as shown in Fig. 11-3 (see also ref. 2). It is constrained by a spring scale fastened to an arm on the casing. The torque required to drive the motor pulley is the product of the net force on the spring scale, F, and the arm length, ℓ. For the scale to indicate net force, it is necessary to counterbalance the static torque due to the weight of the arm. The net work, W, is then

$$W = 2\pi \ell N F \qquad 11\text{-}4$$

where N is the motor speed in rpm. With units of ℓ in feet and F in lbf, units of W are ft-lbf/min as required in eq. (11-3). Losses due to the drive system will be included in W measured this way. Other methods of obtaining W might include using a transmission dynamometer (ref. 3). This requires using a pulley with "elastic beams" for the spokes. Using strain gages fastened to the spokes, the output of the strain gages can be calibrated against torque. Measuring pulley speed, the work can be found using eq. (11-4). A crude estimate of work might be obtained by driving the system through lowering weights. Speed control is lost this way and results may be inaccurate unless kinetic energy of weights and system is accounted for.

The experiment

A test set-up was built like that shown in Fig. 11-1. The shaft was 42 inches long and 3½ inches in diameter with ½ inch diameter plastic tubing. Ball and socket joints were used to support the bearings. The bottom bearing was able to carry the thrust load. Because of the flexible joints, the angle α could be changed. Drive was through a V-belt, using an A.C. motor controlled with a Variac. Water was used and collected to determine flow rate. Water was supplied to the tank at a rate to keep the level constant. Tests were run changing variables of shaft angle, α; depth of water in the supply tank; and shaft speed. Analyses were developed to determine volumetric efficiency and pumping efficiency. Numerous interesting questions can be developed concerning the operation of this device. Does it work if the end of the tubing is completely submerged? How does viscosity affect performance? What causes the work losses?

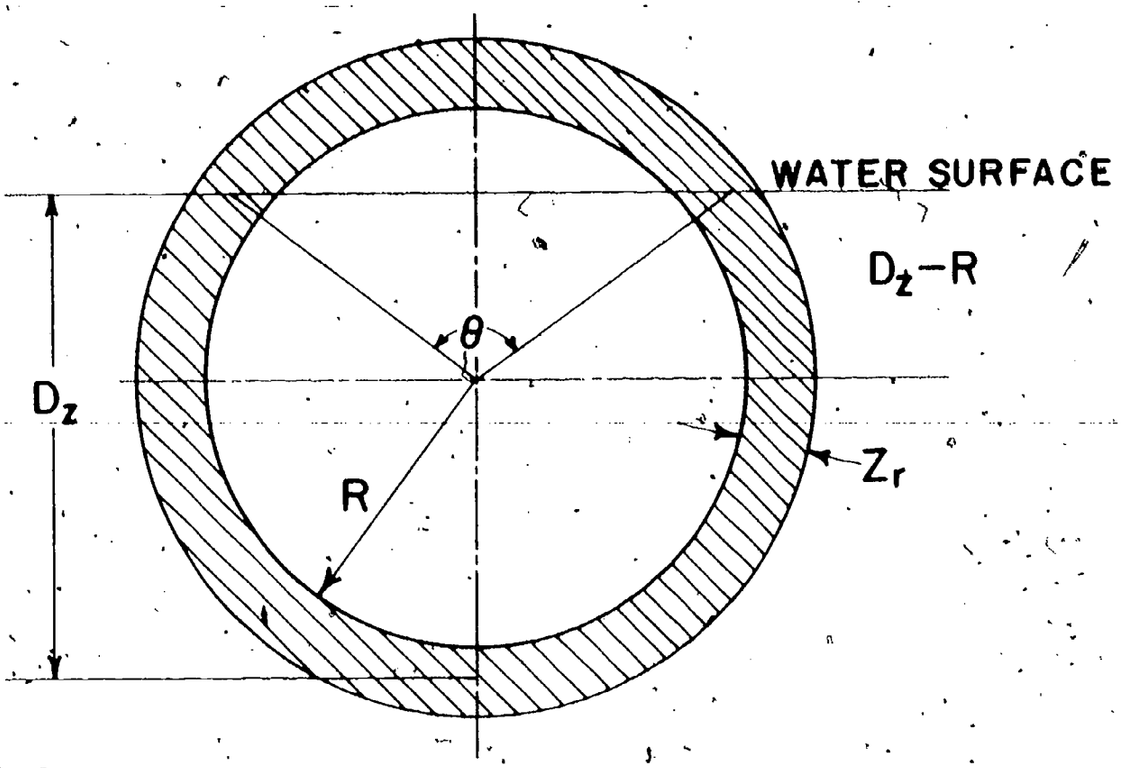

$$\frac{\theta}{2} = \cos^{-1}\frac{R}{D_z - R} = \cos^{-1}\frac{1}{\frac{D_z}{R} - 1}$$

FIG. II-2 SECTION THROUGH SPIRAL SHOWING ANGLE SWEPT OUT BY OPEN END OF TUBING

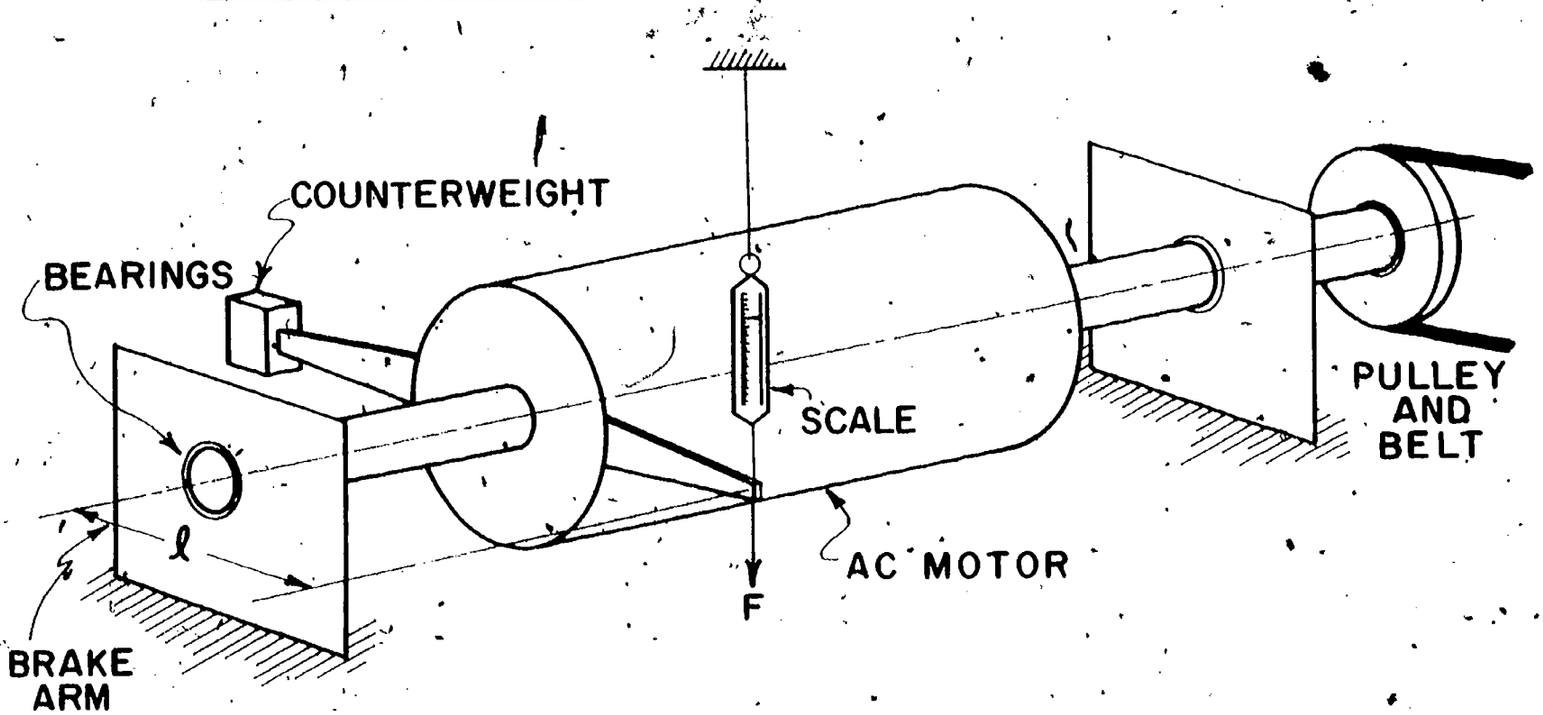

FIG. II-3 SIMPLE DYNOMOMETER

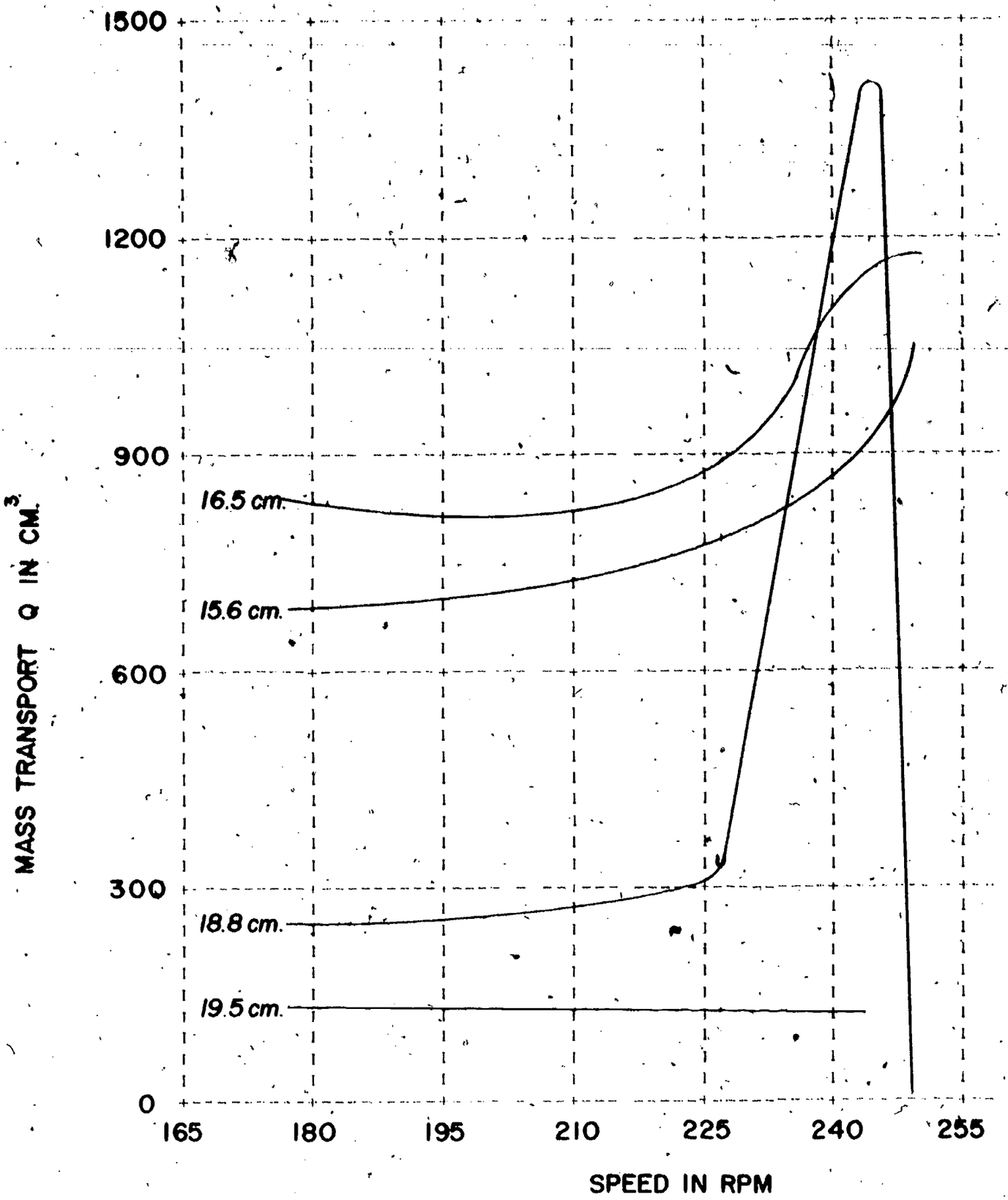

MASS TRANSPORT Q vs. RPM

FIG. 11-4

Sample results

In Fig. 11-4, a graph is shown of the flow rate versus speed for a number of operating depths in the supply tank. Tests were made at various speeds for a fixed tank depth. The water level was changed and the tests repeated. Results can be graphed for η_v and η_p against speed, tank depth or inclination, α. From the results given here, the students concluded that for an inclination of $\alpha = 40^{\circ}$, optimum shaft speed was 245 rpm with enough water to cover one-half of the first coil of the helix.

References

1. Rouse, H. and S. Ince, History of Hydraulics, Dover Publications, New York, New York (1957), pp. 15-17.
2. Holman, J. P., Experimental Methods for Engineers, McGraw-Hill, New York, New York (1966), pp. 319-322.
3. Beckwith, T. G. and N. L. Buck, Mechanical Measurements, Addison-Wesley, Reading, Massachusetts (1969), p. 371.

Experiment No. 12

A Solar Water Pump

The objective is to design, build and evaluate the performance of a model solar water pump.

Operating principle

In regions where power sources are not available but there is much sunlight, one seeks to utilize solar energy to accomplish useful tasks. One proposal is a water pump using solar energy. Its principle is to use the expansion and contraction of a confined volume of air to pump water, energy for the process coming from solar radiation.

The system is shown in Fig. 12-1. A sealed volume is connected to a water source, and a water delivery line. Air is trapped between the water surface and a sealed cover plate. The plate is the radiation receiver. It must have a surface which absorbs solar radiation efficiently and it must conduct this energy into the air bubble. Heating or cooling the air will cause the pressure to rise or fall.

The operation can be described by a cycle. Solar radiation raises the air temperature at constant volume. This is shown as process 1-2 on the pressure volume diagram for the air (Fig. 12-2). At some pressure, p_2, a one-way check valve in the delivery line is forced open and the air expands, forcing the water through the delivery line to the storage tank. A second check valve in the suction line prevents water flowing back through that line. As the delivery head, h_2, is essentially constant, this process, 2-3 in the cycle, is ideally at con stant pressure, p_2. At point 3, the air is cooled. This could be done naturally by waiting until night, or shading the surface. It could be done more frequently if some of the water from the tank were allowed to flow over the plate. At any rate, the pressure will drop during cooling, and with both valves closed, the process, 3-4, will be at constant volume. When the pressure, p_1, is reached, the suction-line valve will be opened and water will be drawn into the pump chamber. As suction head, h_1, is constant, the process, 4-1, will ideally be at constant pressure. Atmospheric pressure would normally lie between p_1 and p_2 as shown in Fig. 12-2.

There are several performance quantities of interest. In the actual device, the volumetric flow rate, Q, the total head developed, $h_1 + h_2$, and the working efficiency η_p are important. A thermodynamic cycle analysis can be developed to evaluate the thermodynamic efficiency for an ideal machine. This we call η_i and it can be shown to be a function of the pressure ratio, p_2/p_1 and the temperature ratio, T_3/T_1. These temperature are the maximum and minimum attained in the cycle and are expressed as absolute temperatures.

Cycle analysis

To develop the cycle efficiency, we require the following concepts:

1. Assume the trapped air obeys the gas law

$$\frac{pV}{T} = \text{constant} \qquad 12\text{-}1$$

where p, V and T are pressure, volume and temperature respectively.

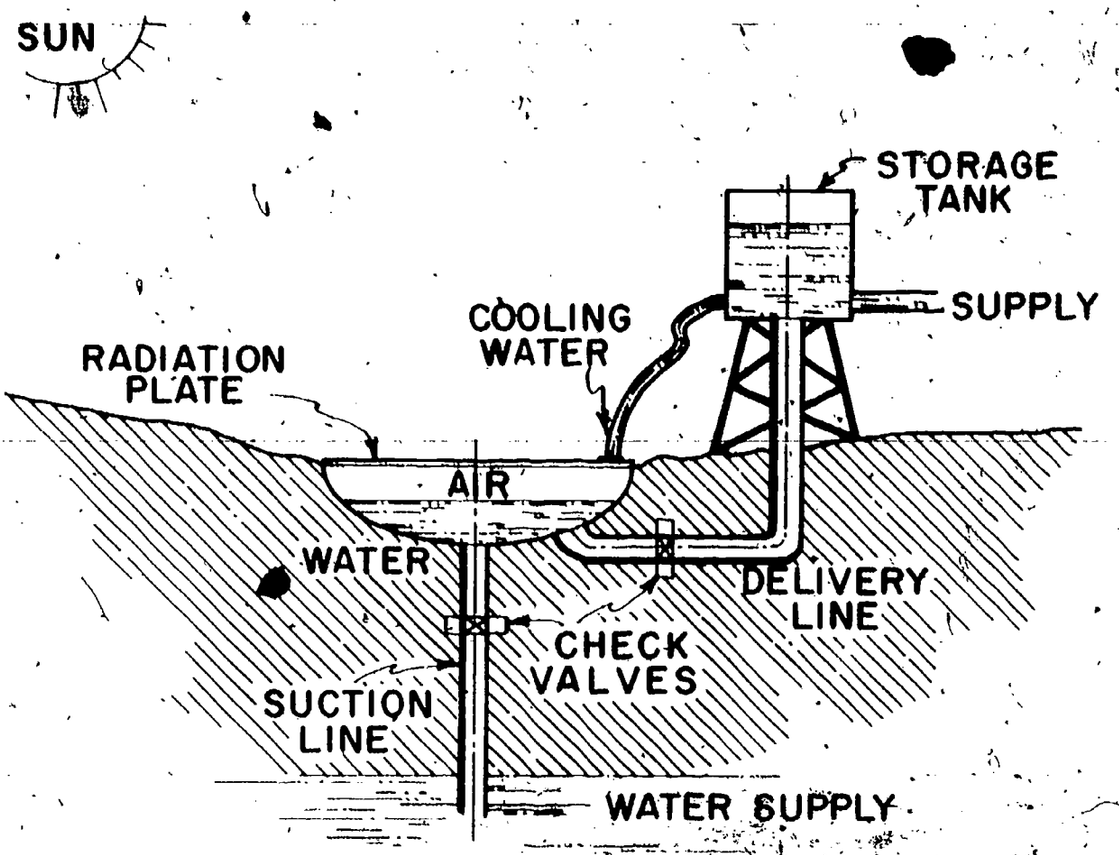

FIG. 12-1 DIAGRAM OF A SOLAR PUMP

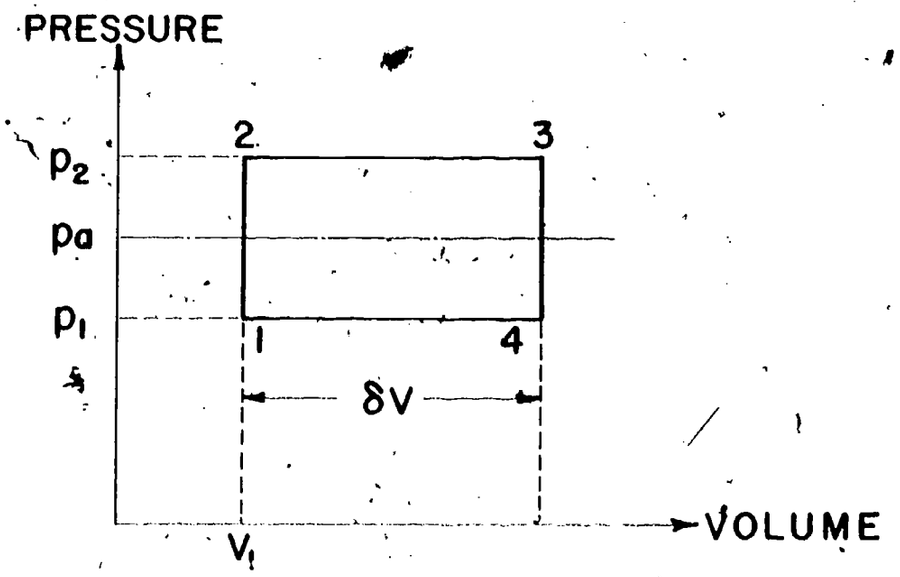

FIG. 12-2 PRESSURE-VOLUME DIAGRAM OF SOLAR PUMP CYCLE

2. Work done by a gas during a constant pressure process between states A and B is

$$p\,(V_B - V_A) \qquad 12\text{-}2$$

3. Work done by a gas during the constant volume process is zero.

4. Heat transferred to the gas in a constant pressure change, from A to B, is H_p

$$H_p = c_p\,(T_B - T_A) \qquad 12\text{-}3$$

where c_p is specific heat at constant pressure.

5. Heat transferred in a constant volume change, H_v is

$$H_v = c_v\,(T_B - T_A) \qquad 12\text{-}4$$

where c_v is specific heat at constant volume.

6. For a thermodynamic cycle, the summation of the work equals the summation of the heat transfer.

7. The cycle efficiency is the ratio of the work done divided by the heat transferred into the gas, H_I, or

$$\eta_i = \frac{\text{Work}}{H_I} \qquad 12\text{-}5$$

As the net work can be expressed as the heat transferred into the gas minus the heat transfer from the gas, H_o, the efficiency can be written as

$$\eta_i = 1 - \frac{H_o}{H_I} \qquad 12\text{-}6$$

The net work of the cycle can be expressed with eq. (12-2). Defining this quantity as W_i, the net work is done along paths 2-3 and 4-1 in Fig. 12-2. Hence,

$$W_i = p_2\,(V_3 - V_2) + p_I\,(V_1 - V_4)$$

noting $V_3 - V_2 = V_4 - V_1 = \delta V$, this becomes

$$W_i = (p_2 - p_1)\,\delta V \qquad 12\text{-}7$$

In terms of the pump head,

$$p_2 = p_a + \frac{\rho g}{g_o}\,h_2$$

$$p_1 = p_a - \frac{\rho g}{g_o}\,h_1 \qquad 12\text{-}8$$

where

p_a = atmospheric pressure, lbf/ft^2

ρ = density of liquid pumped, lbm/ft^3

g = acceleration due to gravity, ft/sec^2

g_o = mass conversion factor, 32.2 lbm-ft/lbf-sec^2

and h_1 and h_2 are suction and pumping head, ft.

To express efficiency we can evaluate H_I and H_o. Heat is transferred into the cycle along paths 1-2 (constant volume) and 2-3 (constant pressure).

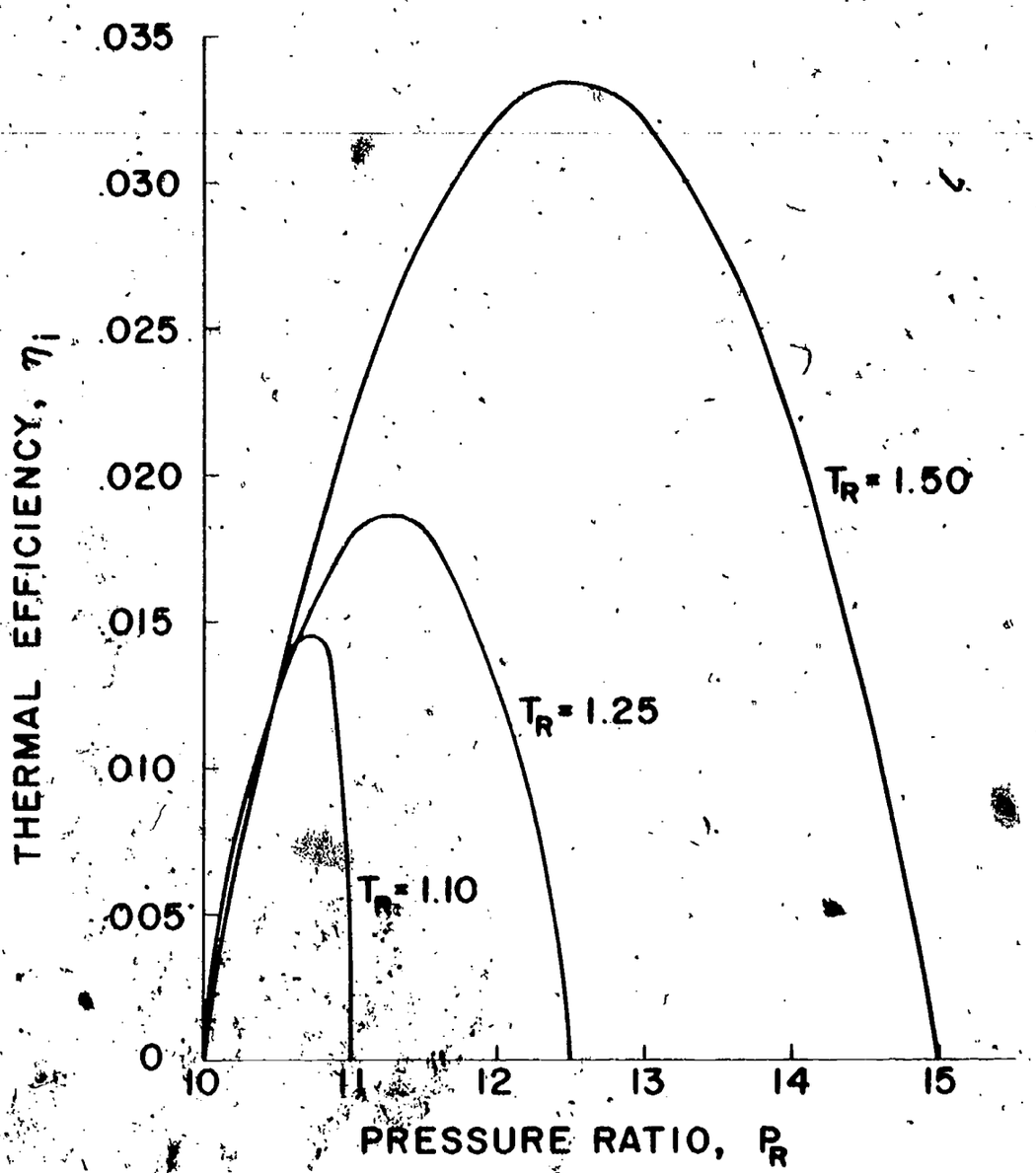

FIG. 12-3 THERMAL EFFICIENCY OF SOLAR PUMP

Then $$H_I = c_p (T_2 - T_1) + c_v (T_3 - T_2) \qquad 12\text{-}9$$

Heat is rejected (transferred from the air) along paths 3-4 and 4-1. The absolute value of H_o is

$$H_o = c_v (T_3 - T_4) + c_p (T_4 - T_1) \qquad 12\text{-}10$$

Putting these expressions in the efficiency eq. (12-6)

$$\eta_i = 1 - \frac{c_v (T_3 - T_4) + c_p (T_4 - T_1)}{c_v (T_2 - T_1) + c_p (T_3 - T_4)} \qquad 12\text{-}11$$

After some algebraic manipulation and expressing $c_p/c_v = k$, this equation becomes

$$\eta_i = 1 - \frac{T_3 \left[1 - \frac{T_1}{T_2} + k \frac{T_1}{T_3} \left(\frac{T_3}{T_2} - 1\right)\right]}{T_1 \left[\frac{T_2}{T_1} - 1 + k \frac{T_3}{T_1} \left(1 - \frac{T_2}{T_3}\right)\right]} \qquad 12\text{-}12$$

Now we can define two cycle parameters which are important. These are the pressure ratio,

$$P_R = P_2/P_1 \qquad 12\text{-}13$$

and the temperature ratio,

$$T_R = T_3/T_1$$

In addition, noting that

$$\frac{T_3}{T_2} = \frac{T_3}{T_1} \cdot \frac{T_1}{T_2} = \frac{T_R}{P_R} \qquad 12\text{-}15$$

equation (12-12) becomes

$$\eta_i = 1 - \frac{\frac{T_R}{P_R} \left[P_R - 1 + k \frac{P_R}{T_R} \left(\frac{T_R}{P_R} - 1\right)\right]}{\left[P_R - 1 + k P_R \left(\frac{T_R}{P_R} - 1\right)\right]} \qquad 12\text{-}16$$

Pump capacity is important and related to the volume change δV. Applying the gas law, eq. (12-1) to the constant pressure change, 2-3, we can write

$$\frac{T_3}{T_2} = \frac{V_3}{V_2} = 1 + \frac{\delta V}{V_1} \qquad 12\text{-}17$$

Using the expression, eq. (12-15) for T_3/T_2, we can write

$$\frac{\delta V}{V_1} = \frac{T_R}{P_R} - 1 \qquad 12\text{-}18$$

An expression for efficiency can be developed in terms of $\delta V/V_1$ and P_R by substituting eq. (12-18) into eq. (12-16). So we have expressed the important performance parameters for the thermodynamic cycle, η_i and flow ($\delta V/V_1$) in terms of two dimensionless ratios T_R and P_R.

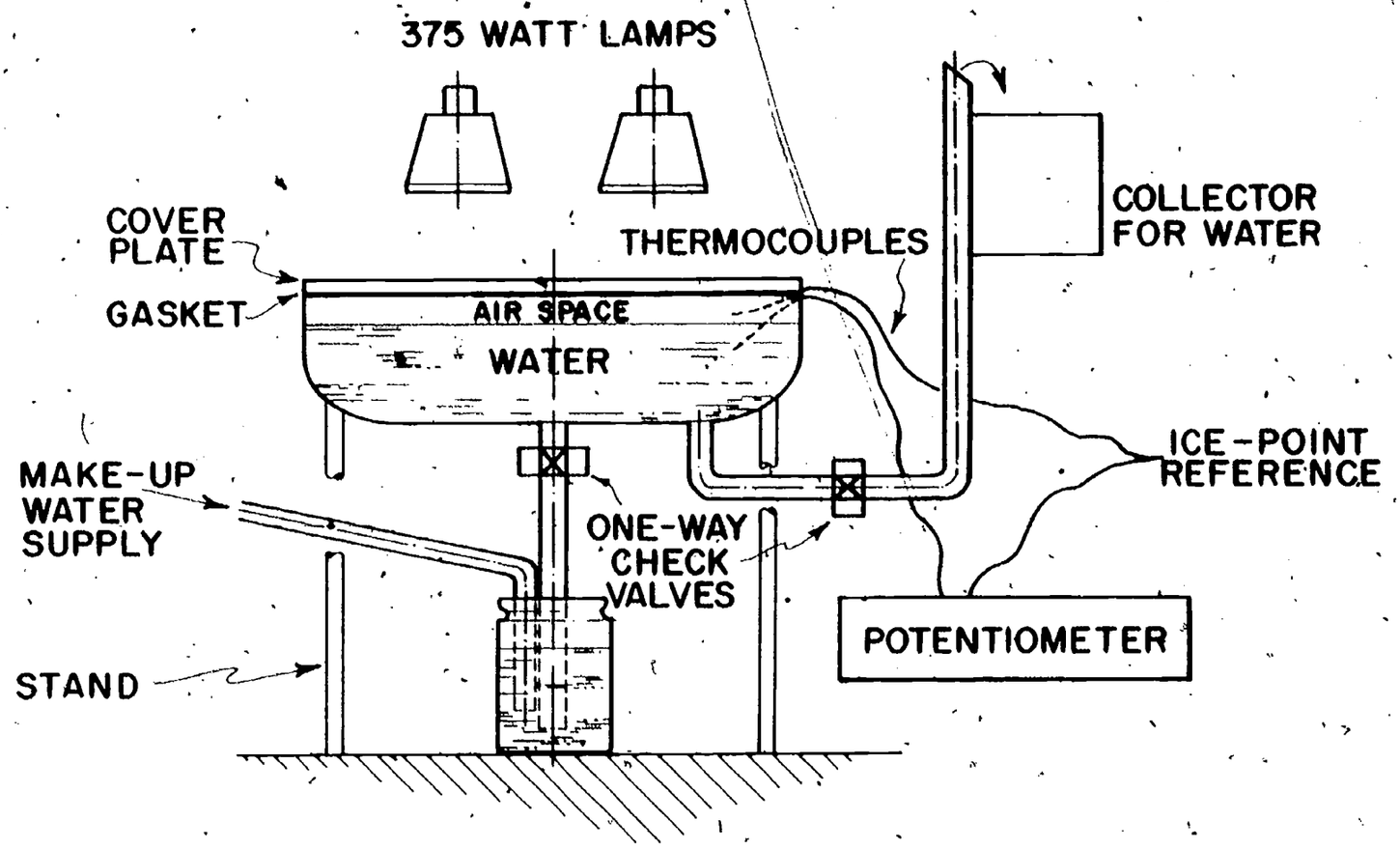

FIG. 12-4 TEST MODEL OF SUGAR - WATER PUMP

A series of calculations was made to evaluate the cycle efficiency in terms of T_R and P_R using eq. (12-16). Calculations were made for three temperature ratios, 1.1, 1.25 and 1.50. It is doubtful that temperature ratios larger than 1.5 are attainable. Curves are shown in Fig. 12-3. It is apparent that the efficiency is zero for a zero pressure ratio. Efficiency is also zero when the pressure ratio equals the temperature ratio. At this time, the temperature at 2 has reached the value at 3 so no constant pressure process is possible. The cycle is completed by returning to point 1 along path 2-1 with no work being accomplished. Consequently, there is a pressure ratio which gives a well defined maximum for cycle efficiency for any given ratio of temperatures. It would be well to design for that condition.

The test model

A model system can be built and tested. One is shown in Fig. 12-4. It consisted of a steel tank 18 inches in diameter having a capacity of 3 gallons. A delivery tube and suction tube were brazed into the bottom. These were 1/4 inch diameter copper. One-way check valves were installed in each line. The top plate was of 1/8 inch thick aluminum, held in place with 39 bolts. A rubber ring gasket was used to seal the plate and tank. Gasket cement was applied to insure a good seal. The tank was checked for leaks by blowing air into it while it was submerged in water. The suction pipe was put in a one-gallon jug of water and the system was primed.

As a heat source, two 375-watt "heat" lamps were used, placed a few inches from the top surface of the plate. The plate surface was given a dull black coating. Thermocouples were located in the air space and in the water below.

Cycling was accomplished by turning the lights off for cooling. The delivery head was adjusted so that the system pumped water, and the cycling begun. The two lights made possible a maximum temperature of over 200F for the air, which was reached in 35 minutes. Although a higher temperature might have been reached, the temperature had begun to level off, and this point was selected as point 3 (lights off). This can be seen in Fig. 12-5.

The test

It required at least one cycle to have repeatable results. During each cycle, the water was collected and measured at the delivery, and the amount taken in during suction was noted. Temperatures of the air were recorded every minute, and for the water every five minutes. Cycle time was 70 minutes, with 35 minutes for heating. Times were marked at valve openings and closings. Results for two cycles are shown in Fig. 12-5. Here temperature histories are given for the air and water. Along the bottom are noted the events taking place. "H" stands for heating and "C" for cooling. Numbers correspond to states in the ideal cycle.

Sample results

For the test described above, some measurements were:

tank volume	3 gal. or 11,353 ml.
water volume	4216 ml.
air volume	7137 ml.

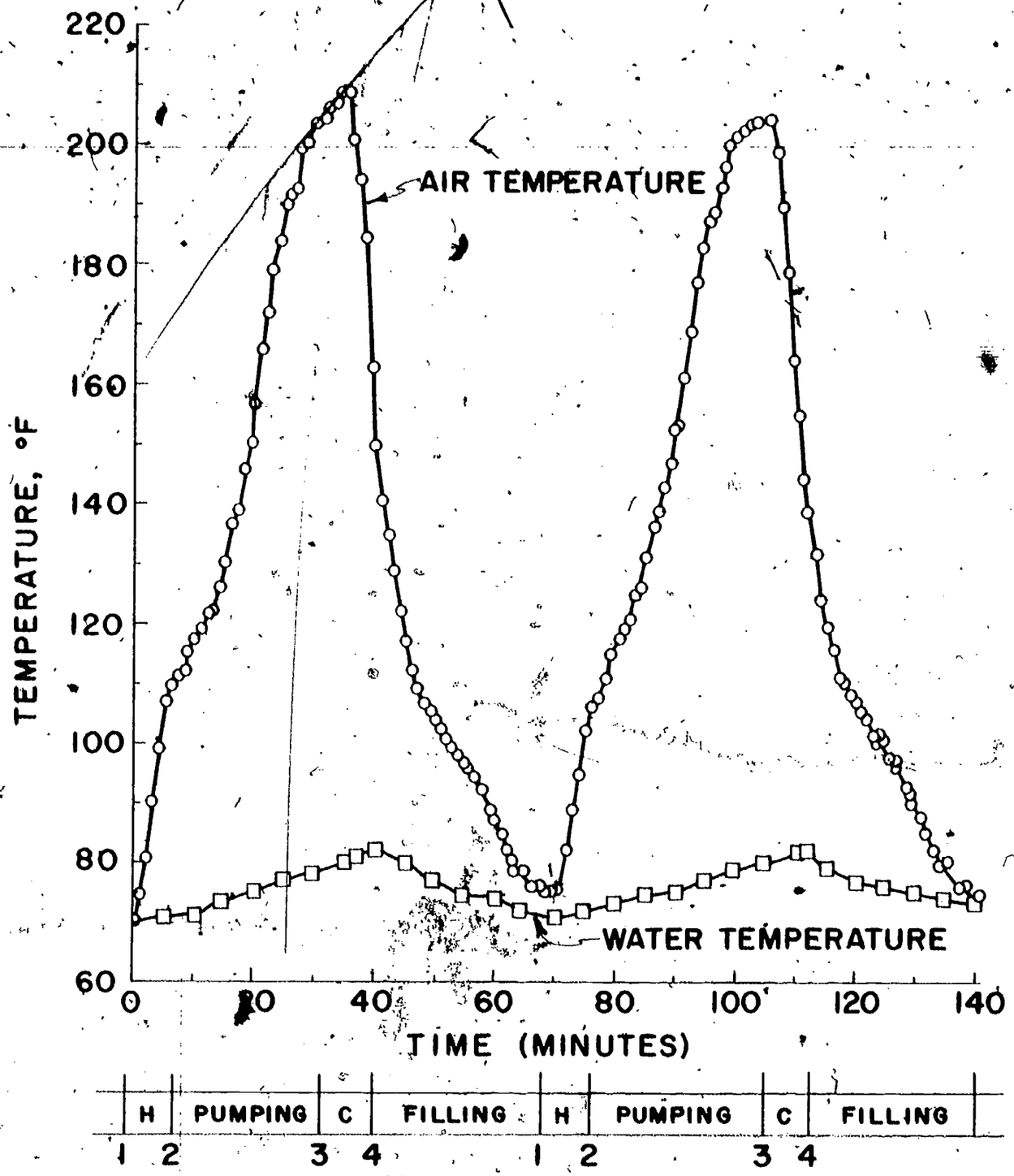

FIG. 12-5 TEMPERATURE HISTORY OF AIR & WATER FOR TWO CYCLES OF A SOLAR WATER PUMP

room air temperature	73 F
Volume pumped per cycle (average)	1040 ml.
Head, h_2	6 in.
Head, h_1	10 in.
Atmospheric pressure	29.85 in Hg

From these data we can determine pressures (ρ=62.4 lbm/ft^3) from eq. (12-8):

$$p_2 = 29.85\ (.491) + 62.4\ (\frac{32.2}{32.2})\ \frac{0.5}{144}$$

$$= 14.66 + 0.22 = 14.88 \text{ psia}$$

$$p_1 = 14.66 - 62.4\ (\frac{32.2}{32.2})\ \frac{10}{12(144)} = 14.30 \text{ psia}$$

Therefore $P_R = \frac{14.88}{14.30} = 1.041$

From the test (Fig. 12-5), T_3 207 + 460 = 667 R and

T_1 73 + 460 = 533R

T_R $\frac{667}{533} = 1.251$

From the curve (Fig. 12-3), the ideal cycle would be expected to have an efficiency of 1.2%. In this test, the heat flux to the plate was not measured, so no comparison could be made.

Using eq. (12-18), the flow per cycle for the ideal case can be determined as

$$\frac{\delta V}{V_1} = \frac{1.251}{1.041} - 1 = 0.202.$$

In the actual cycle, the volume of water pumped (which equals the volume change of air) was 1040 ml. For an original air volume of 7137 ml.,

$$(\frac{\delta V}{V})_{\text{Test}} = \frac{1040}{7137} = 0.146.$$

This is somewhat less than the predicted value.

Work and efficiency

For the model, or prototype pump, the actual useful work, W, can be expressed in terms of the flow per cycle, and the head, or

$$W = Q\ \frac{\rho g}{g_o}\ (h_1 + h_2), \text{ ft-lbf/cycle} \qquad 12\text{-}19$$

For a measured initial air volume, V_A, Q is related to the volumetric ratio as

$$\frac{Q}{V_A} = \frac{\delta V}{V_1}$$

The energy supplied to the device per cycle, E, must be measured from the incident radiation on the surface. For a lamp source this might be difficult to get. For a solar source, tabular values are available for radiation from the sun normal to the sun's rays for various latitudes and seasons. An average value of 425 Btu/hr can be used. Knowing

the angle of inclination between a normal to the plate and the sun (α) the radiation received per cycle is

$$H_R = \text{(Area of plate) (Solar radiation) } \cos\alpha\ (\delta t) \qquad 12\text{-}20$$

where δt is the hour fraction for heating.

While it is doubtful that solar radiation on the plate could be as intense as that from the lamp, let's make an estimate of pump efficiency assuming that the sun's radiation supplied the energy in the test described. Pump efficiency will be defined as

$$\eta_p = \frac{W}{H_R} \qquad 12\text{-}21$$

The volume pumped per cycle was

$$Q = 1040 \text{ m}\ell / 28316 \text{ m}\ell/\text{ft}^3 = 0.037 \text{ ft}^3$$

From eq. (12-19)

$$W = 0.037 \left(\frac{62.4 \cdot 32.2}{32.2}\right) (.5 + .833)$$

$$= 3.08 \text{ ft-lfb/cycle or}$$

$$\frac{3.08 \text{ ft-lbf}}{778(\text{ft-lbf/Btu})} = 0.0039 \text{ Btu/cycle}$$

Assuming the sun's inclination as 45°, and noting the heating cycle took 35 minutes, then from eq. (12-20)

$$H_R = 425 (\cos 45)\left(\frac{\pi(1.5)^2}{4}\right)\left(\frac{35}{60}\right)$$

$$= 310 \text{ Btu/cycle.}$$

Finally, from eq. (12-21), the actual efficiency is

$$\eta_p = \frac{.0039}{310} = 0.001\%$$

This is considerably less than predicted by the thermodynamic analysis. There are losses due to heat transfer to the environment from the plate and from the air to the water. While the temperature rise of the water was small, it must be remembered that the heat capacity is very large compared to the air. A flexible partition with thermal insulating properties could be used to separate the air and water thereby reducing this loss. In spite of the low ideal efficiency and the even lower actual efficiency, these are not critical when you consider that the energy is "free".

Modifications

Tests can be made to evaluate design variables such as:

a. changing surface characteristics of the plate,
b. varying the initial air/water volume,
c. varying the delivery head h_2 or the suction head h_1,
d. evaluating the effect of water cooling on the surface,
e. testing under actual conditions (solar radiations).

Experiment No. 13

Ultrasonic Determination of Material Properties

prepared by Robert Greif
Associate Professor of Mechanical Engineering
Tufts University

The object of this experiment is to use ultrasonic waves to determine properties of engineering materials in an efficient and accurate manner.

Introduction

In this work, some elementary concepts in wave propagation and elasticity theory are combined so that common material properties can be found experimentally. Tests are performed by transmitting short bursts of high frequency vibrations (ultrasonic wave trains) into material specimens and making calculations based on the measured times between reflections. Since the specimen length is known, these time intervals may be easily converted to wave speed; the relations between wave speed and material properties are then used to find results. Typical material properties determined in this manner by students are Young's modulus, shear modulus, and Poisson's ratio and their respective variation with temperature.

Nomenclature

E	Young's modulus
G	shear modulus ($= E/2(1+\nu)$ for isotropic materials)
ν	Poisson's ratio
ρ	mass density
ℓ	length of specimen
t_o	round trip transit time for extensional wave
t_s	round trip transit time for torsional wave
C_o	velocity of extensional waves

Basic principles

The basic principles of ultrasonics involve using an ultrasonic transducer to convert electrical energy to acoustical or vibrational energy (ref. 1-3). In the experiments to be described, the reverse process is also used, i.e. conversion of vibrational energy to electrical energy. Ultrasonic waves are usually defined as high frequency waves above the limit of human hearing, i.e. above 16,000 Hertz (cycles per second). The frequency range generally used in practical ultrasonic equipment ranges from 20 kHz (kilohertz) to 25 MHz (megahertz). Two typical methods used to generate ultrasonic waves involve the piezoelectric effect and the magnetostrictive effect.

Piezoelectric transducers make use of the fact that a varying electric field can expand and contract certain crystalline materials. Some typical materials that exhibit this peizoelectric effect are quartz, barium titanate, lead zirconate titanate, lead metaniobate, and

lithium sulphate. Applying a voltage across a piezoelectric material will lead to a thickness variation proportional to the voltage variation. Conversely, applying a force of a certain frequency to this piece will generate a voltage of the same frequency.

Magnetostrictive transducers make use of the fact that a varying magnetic field can expand and contract certain ferromagnetic and ferrimagnetic materials. Some typical materials that exhibit this magnetostrictive effect are nickel, remendur, and permendur. This effect can be reversed; a mechanical stress applied to a magnetostrictive material causes a change in intensity of magnetization.

In a typical ultrasonic application utilizing the pulse echo technique, waves of a certain frequency are usually produced in either of two ways; in the first method, the frequency of the applied electrical current is set at the desired level while in the second method a shock pulse is used, with the frequency then determined by the resonant characteristics of the transducer. Typically, the transducer is driven for a short period of time resulting in a short burst of ultrasonic waves. The pulse travels through the material to the opposite boundary and is reflected back to the source as an echo (Fig. 13-1). After the transducer has transmitted the short burst of waves, it then acts as a receiver for the returning echoes. The echo signals are then amplified and displayed on an oscilloscope so that the time interval between two successive echoes can be measured accurately.*

Experiment

The object of the experiment is to obtain material properties for engineering materials using low cost ultrasonic accessories. A typical experiment that will satisfy these requirements involves the pulse echo method for thin wire specimens (ref. 4), as shown in Fig.(13-2). The ultrasonic equipment that a typical laboratory would require are a pulse generator and an ultrasonic transducer; the total cost of these items can be purchased for less than $600. For example, this equipment can be purchased from Panametrics (Waltham, Mass.) as follows: $395 for the pulse generator ("Panapulser") and $195 for the ultrasonic transducer ("Modulus Transducer"). General purpose pulse generators are also available from manufacturers such as Hewlett-Packard (model 214B, approx. $800) or from General Radio (model 1217C pulse generator and model 1397A power amplifier, total cost approx. $950). All of these pulse generators are used by just plugging into a regular 60 cycle AC wall outlet without the need for any additional power supply.

As shown in Fig. (13-2), the pulse generator energizes a magnetostrictive transducer, launching ultrasonic waves down the lead-in wire. The specimen** is joined to the lead-in wire by using bonding, brazing or welding. The waves are reflected from the front and from the back of the specimen. These reflected waves (echoes) travel through the lead-in wire to the transducer which now acts as a receiver. Because of the magnetostrictive effect these waves generate a voltage which is shown on the oscilloscope. The time interval, t_o, between

---

* Enough time must be allowed between transmitted pulses to permit the return of the desired echo signals and the decay of any subsequent reverberations.

** The specimen should be thin compared to wavelength; the largest cross-sectional dimension should be less than 5mm for a wavelength of 25mm.

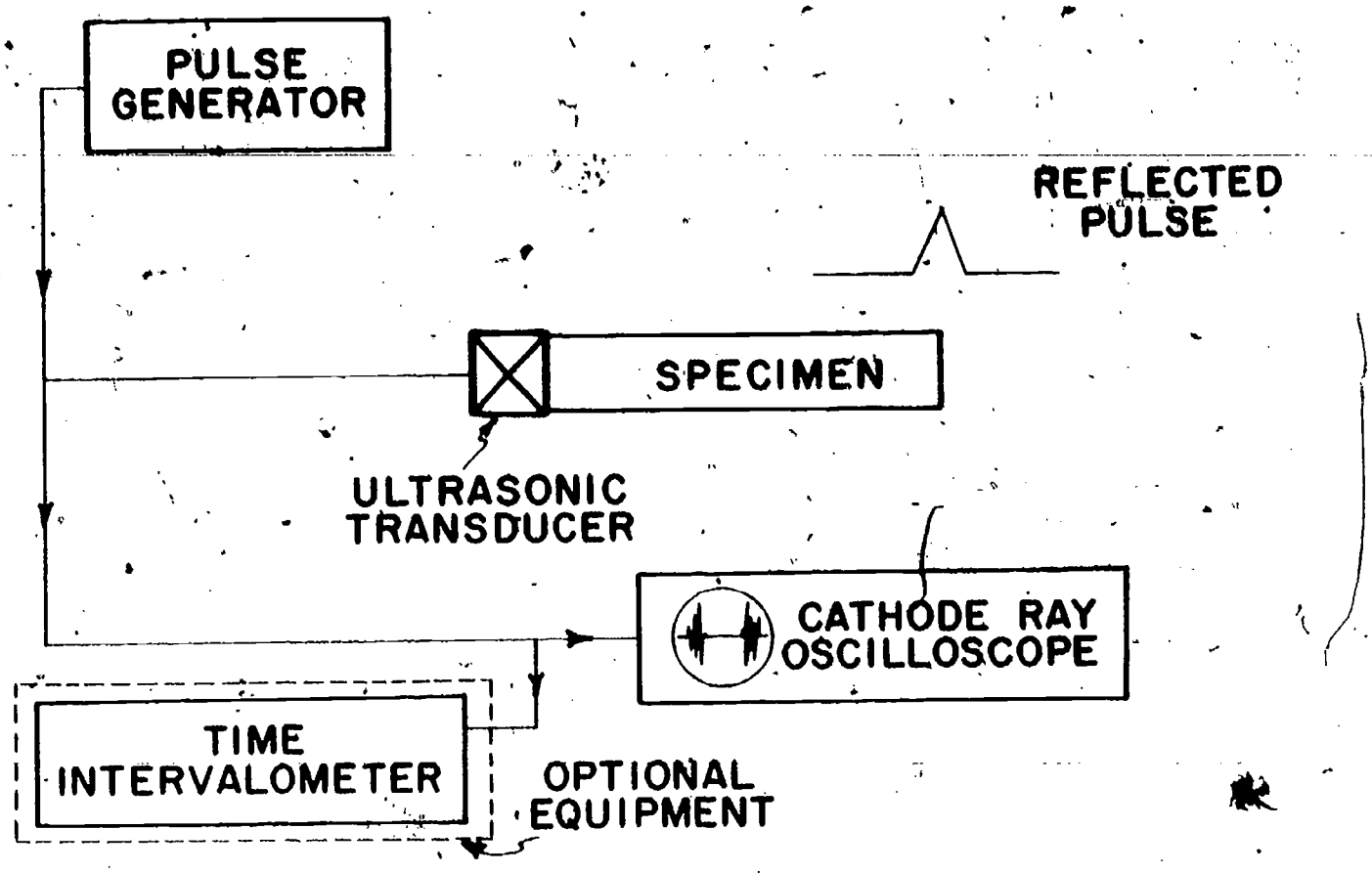

FIG. 13-1 SCHEMATIC FOR PULSE-ECHO METHOD

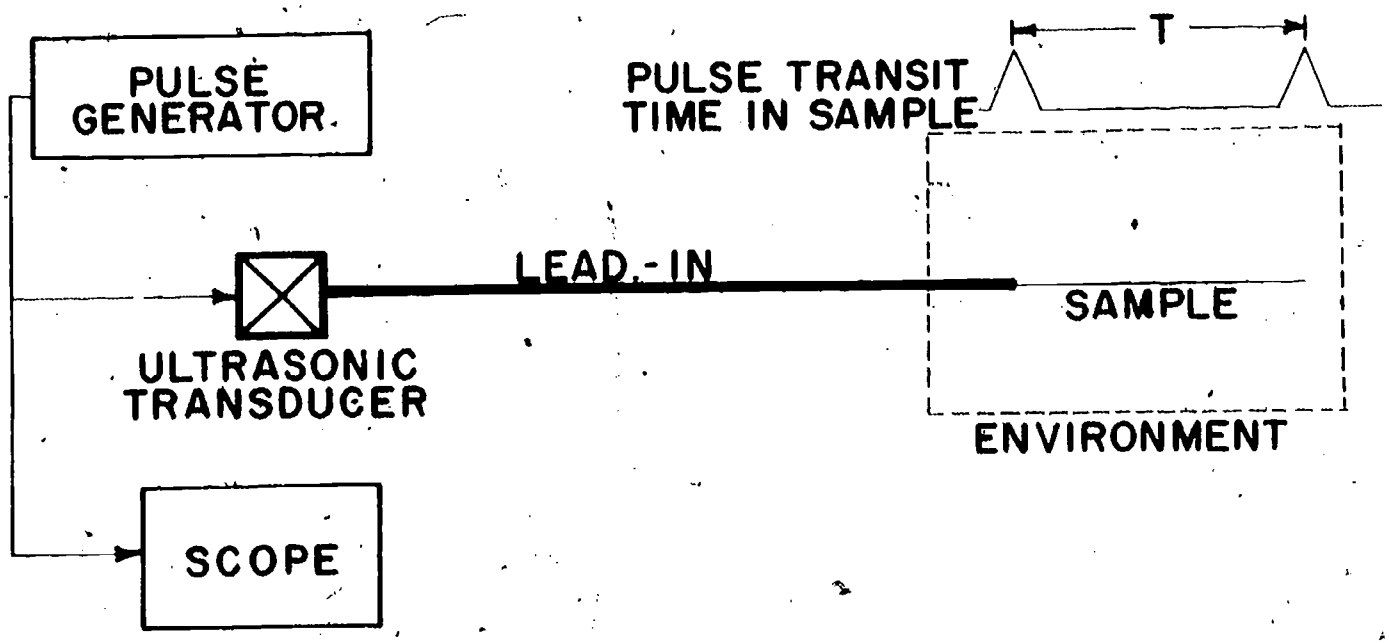

FIG. 13-2 SCHEMATIC FOR THIN-WIRE EXPERIMENT

these voltage signals is equal to twice the time for the waves to travel through the specimen. (Typical pulses may be read off a calibrated oscilloscope to an accuracy approaching 0.1 μsec). This time interval leads to the determination of the modulus.

To determine the modulus, we may use some results from elasticity theory (ref. 5). For an elastic solid which is thin compared to the wavelength of the propagating waves, it may be proven that Young's modulus, E, is

$$E = \rho C_o^2 \qquad 13\text{-}1$$

where ρ is the mass density and C_o is the velocity of propagation of extensional waves. If the length of the specimen is ℓ, then the time interval t_o is

$$t_o = \frac{2\ell}{C_o} \qquad 13\text{-}2$$

so that from (13-1)

$$E = 4\rho (\ell/t_o)^2 \qquad 13\text{-}3$$

Equation (13-3) is used to find numerical values of modulus. It should be noted that the length of the specimen is relatively unimportant. Lengths from 10mm to 10 meters can be employed with a typical length being 50mm.

Shown in Fig. 13-3 is an actual photograph of the oscilloscope trace for a test of work hardened stainless steel 304 wire. The diameter of the lead-in wire (which is also SS304) is 1.5mm while the specimen diameter is 0.75mm. The lead-in length is 33" (84cm) and the specimen length is 2" (5.08cm). In Fig. 3 we see a double exposure in which the top picture has a (horizontal) time scale of 50μs/cm while the lower trace has been expanded to 10μs/cm and is therefore much easier to read. The echo pattern shows the time between the interface echo (i.e. the interface between the lead-in and the specimen at which there is an abrupt impedance change associated with the diameter change) and the end echo (i.e. the echo from the end of the specimen). This time is $t_o = 19\mu s$, and from eq. (13-2) the wave velocity C_o is

$$\begin{aligned} C_o &= 2\ell/t_o \\ &= 10.16/19 \\ &= 0.53 \text{ cm/}\mu\text{sec} \end{aligned} \qquad 13\text{-}4$$

which may be written as $C_o = .53 \times 10^6$ cm/sec. Then from eq. (13-1) it follows that

$$\begin{aligned} E &= \rho C_o^2 \\ &= (7.8)(.53 \times 10^6)^2 \\ &= 2.2 \times 10^{12} \text{ dyne/cm}^2 \\ &= 32 \times 10^6 \text{ lb/in}^2 \end{aligned} \qquad 13\text{-}5$$

In this manner, material property data can be obtained for a great variety of materials including metals, ceramics and plastics. Some typical results obtained by using this pulse echo method are listed below.

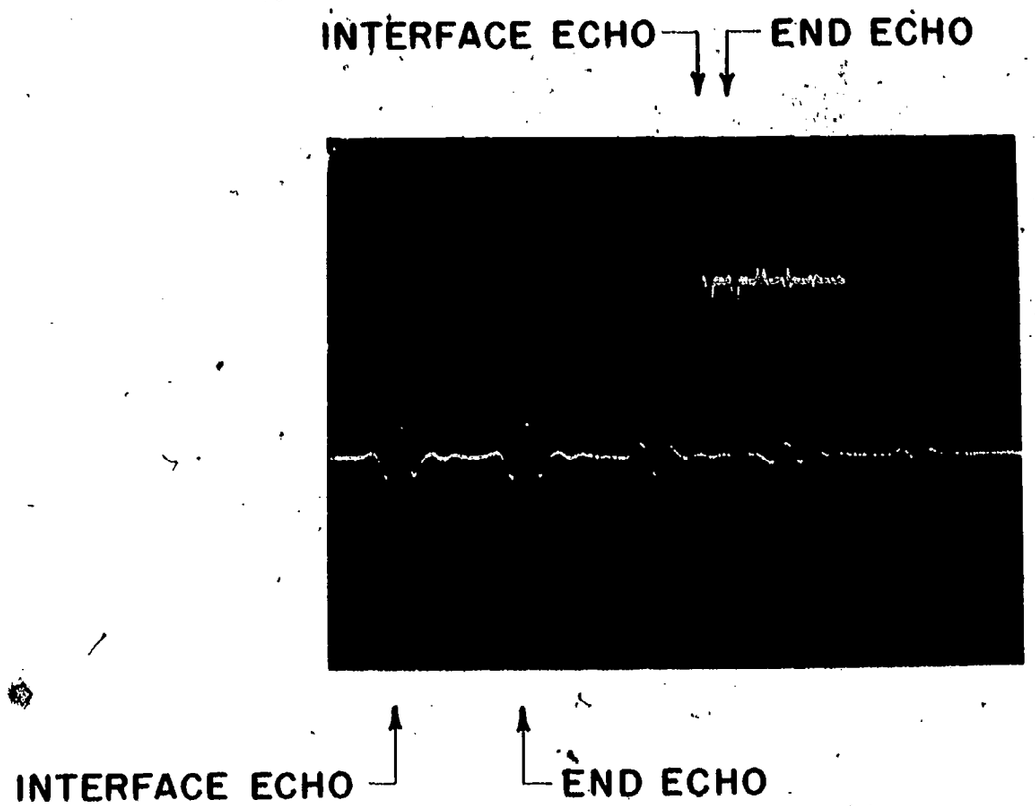

FIG. 13-3 PULSE ECHO TEST FOR STAINLESS STEEL 304

Table of Young's Moduli ($lb/in^2 \times 10^6$)

Aluminum	10.4
Beryllium	43.0
Copper	17.0
Nickel	30.0
Lucite	0.48

There are several modifications that can be made in the preceding experiment to obtain additional property data. Shear modulus G and Poisson's ratio ν may be obtained by using a transducer that generates both extensional and torsional waves simultaneously (ref. 6). Since torsional wave speed is about .6 of extensional wave speed for many materials, the time separation between the two types of waves may be controlled by varying the length of the lead-in wire. It is possible, by proper impedance matching between the lead-in wire and the specimen, to have the extensional wave echoes damp out before the torsional wave echoes appear on the scope. The resulting trace on the scope will then show both these wave patterns clearly and the appropriate time intervals can be picked off accurately. The shear modulus G may be determined in terms of the time intervall t_s between shear echo peaks using

$$G = 4\rho(\ell/t_s)^2 \qquad 13\text{-}6$$

Poisson's ratio may be calculated from the relationship between E and G for an isotropic material

$$G = \frac{E}{2(1+\nu)} \qquad 13\text{-}7$$

Using eqs. (13-3) and (13-7) ν may be solved in terms of t_o and t_s,

$$\nu = \frac{E}{2G} - 1 \qquad 13\text{-}8a$$

$$\nu = \frac{t_s^2}{2t_o^2} - 1 \qquad 13\text{-}8b$$

It is interesting to note that the specimen length ℓ does not appear explicitly in this relationship for ν.

The variation with temperature of the foregoing material properties may also be determined by modifying the basic experiment. The additional experimental apparatus needed to include thermal effects is sketched in Fig. 13-2 in the form of dashed lines enclosing the specimen. Essentially one can build a small oven facility to enclose the specimen and subject it to various environmental conditions. The experiment is run in the same fashion as before with time differences between peaks being read off the scope*; consequently, the variation of modulus with temperature can be determined. It should be noted that in most solids the sound velocity decreases as the temperature increases which leads to an increasing value of transit time.

*Enclosing part of the lead-in wire has no effect on the transit time since only time differences are found.

Acknowledgement

The author acknowledges several helpful discussion with L. C. Lynnworth, Department Head, Nondestructive Testing and Measurement, Panametrics, Inc., Waltham, Mass.

References

1. McGonnagle, W. J., Nondestructive Testing, (2nd Edition), Gordon & Breach Publishers, Chapter 8, (1961).
2. Glickstein, C., Basic Ultrasonics, John F. Rider Pub., (1960).
3. Blitz, J., Fundamentals of Ultrasonics, (2nd Edition), Plenum Press, (1967).
4. Fowler, K., "A New Way to Measure Elastic Moduli", Metal Progress, Vol. 95, (No. 6), (June 21, 1969).
5. Kolsky, H., Stress Waves in Solids, Dover Publications, (1963).
6. Fowler, K. A. and L. C. Lynnworth, "Ultrasonic Measurements of Temperature Using Extensional and Torsional Waves", in Proc. 6th Temperature Measurement Society Conference, Hawthorne, California (April 1969).

Experiment No. 14

Flow of Air Through a Nozzle

The objective is to evaluate the performance of a nozzle in compressible flow by measuring the reaction force in a nozzle.

Note: Experiments 14 and 14A involve compressible fluid mechanics, which may be too advanced for students below the junior or senior level.

We have a small converging nozzle approximately 0.1 inch in diameter which we intend to use for a small air turbine. It will be used to expand air from a high pressure to a pressure near that of the atmosphere in order to produce a high velocity jet. Turbine blades will convert the momentum in the jets to work in a small turbine wheel. For the turbine to be efficient we want an efficient nozzle. To aid in the design we would like to have some quantitative expression of the efficiency of the nozzle.

A nozzle velocity coefficient will be determined as the ratio between the measured velocity of the jet to the ideal velocity.

$$k_n = \frac{v_j}{iv_j} \qquad 14\text{-}1$$

By ideal velocity we mean the velocity which should have been attained by an ideal gas flowing from the high pressure to the exhaust back pressure in an idealized way; i.e. reversibly without heat transfer. This is also isentropic, or at constant entropy. If we consider the flow of air through a control volume consisting of a large diameter chamber and the nozzle, we can write, for steady flow,

$$\frac{Q}{\dot{m}} = \frac{W}{\dot{m}} + h_2 - h_1 + \frac{v_2^2 - v_1^2}{2} + g(z_2 - z_1) \qquad 14\text{-}2$$

Q = heat transfer

W = shaft work

h = enthalpy, $u + pV$

v = velocity (hence $\frac{v^2}{2}$ is kinetic energy)

gz = potential energy; product of elevation and acceleration due to gravity

$\dot{m}$ = mass flow into or out of control volume

u = internal energy

pV = product of pressure times specific volume, or flow work

For the present case, there is no shaft work done; heat transfer is small enough to neglect; change in potential energy is zero; and the entering kinetic energy $\frac{v_1^2}{2}$ is small compared to that leaving $\frac{v_2^2}{2}$. This last assumption is validated by the large

area ratio at the two cross sections. Consequently

$$v_2 = \sqrt{2g_o J}\ (h_1 - h_2)^{1/2} \qquad 14\text{-}3$$

Here g_o and J are conversion factors. To convert Btu to ft-lbf, J is used, $J = 778\ \frac{\text{ft-lbf}}{\text{Btu}}$; and to provide proper units for mass we introduce $g_o = 32.2\ \frac{\text{lbm-ft}}{\text{lbf-sec}^2}$. Then with h in Btu/lbm, the units are correct. In terms of units the right hand side of the velocity equation is $(\frac{\text{lbm-ft}}{\text{lbf-sec}^2} \cdot \frac{\text{ft-lbf}}{\text{Btu}} \cdot \frac{\text{Btu}}{\text{lbm}})^{1/2} = (\frac{\text{ft}^2}{\text{sec}^2})^{1/2} = \frac{\text{ft}}{\text{sec}}$ which are proper units for velocity. For an ideal gas (assuming constant specific heat) $h = c_p T$. With this the velocity can be expressed in terms of temperatures

$$v_2 = \sqrt{2g_o J c_p}\ (T_1 - T_2)^{1/2} \qquad 14\text{-}4$$
$$= 223.8 \sqrt{c_p\ (T_1 - T_2)}$$

This does not require that the process be ideal. It is not practical to measure T_2 in the high speed flow, so we seek another way of determining the actual velocity. However, if the ideal T_2 is available, then with this in the velocity equation wa can find iv_2. In terms of inlet states and exit pressure, for an ideal adiabatic (no heat transfer) expansion of an ideal gas having constant specific heat,

$$iT_2 = T_1 (\frac{p_2}{p_1})^{\frac{k-1}{k}} \qquad 14\text{-}5$$

where k is the ratio of specific heat c_p/c_v. It is simple to measure the temperature of the gas at the low velocity of state 1. From these equations, and the measured T_1, p_1 and p_2 it is possible to compute iv_2 under the assumption that p_2 = barametric pressure of surroundings.

The objective of this experiment is to devise a means of measuring v_2 and compare it to iv_2 as a function of pressure ratio p_1/p_2.

Experimental scheme

One approach to the determination of the actual value of v_2 is to use Newton's second law, and by measuring reaction of the nozzle, (or impulsive force of the jet) calculate v_2. A device is to be built like that of Fig. 14-1. The nozzle will be mounted into the end of a large (1-1/2 in. nominal dia.) pipe. In fact it is simple to form a converging nozzle in a pipe cap. Air will be supplied to the large pipe with a very flexible rubber tube. The pipe is then suspended by wires to form a long pendulum. Use wires 8-10 ft. in length for this. When air flows through the nozzle, a reaction force will be set up and the pendulum will swing to a stable position, causing the wire to traverse a measurable angle θ. The force of the reaction, F_R, will be related to the weight of the pipe and attachments, w. Using a force balance this relation is

$$F_R = w \tan\theta. \qquad 14\text{-}6$$

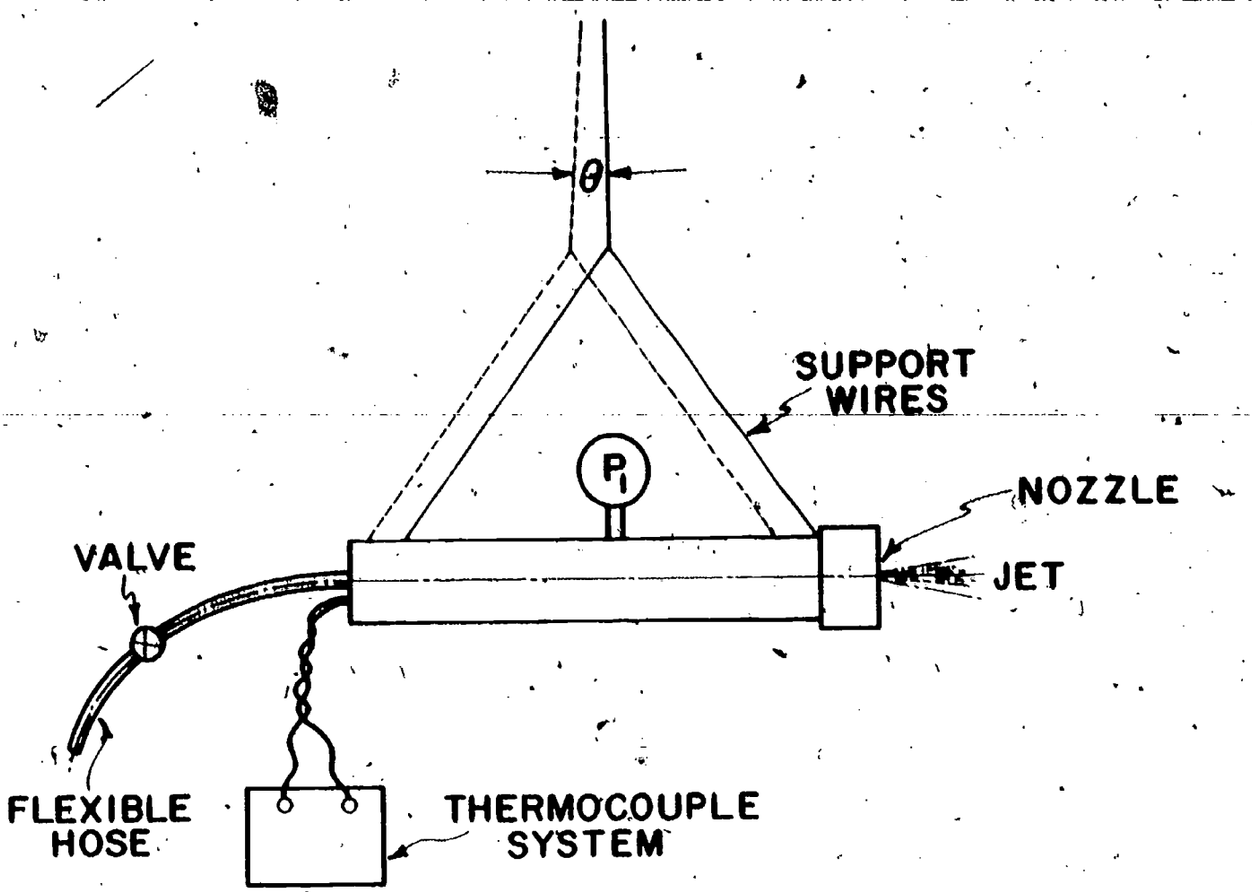

FIG. 14-1 NOZZLE SYSTEM

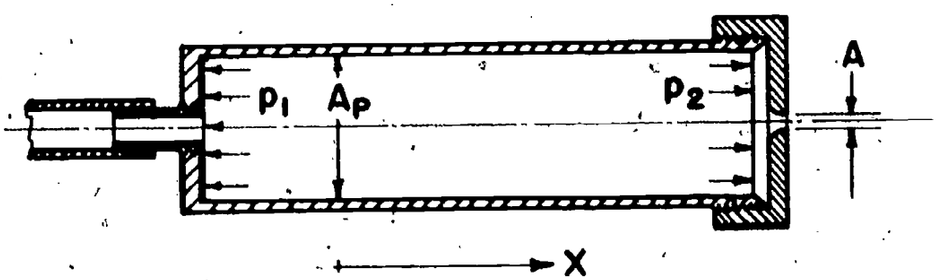

FIG. 14-2 NOZZLE AS A CONTROL VOLUME

Using the momentum equation, applied to the control volume (the pipe) the force can be related to velocity.

In the x-direction the momentum equation for steady flow is

$$\Sigma \text{ Forces on control volume} = \Sigma \text{ momentum flux out} - \Sigma \text{ momentum flux in.}$$

With + assigned to forces at the right, we see from Fig. 14-2.

$$\Sigma \text{ Forces} = F + p_1 (A_p - A) - p_{\text{surrounding}} A - p_1 A_p = F + A (p_1 - p_{\text{surr}})$$

Because the x-component of the entering velocity is zero, the momentum flux entering is zero, while the momentum flux out of the control volume is

$$\dot{m} v_2 = \rho_2 A v_2^2 \quad \text{(see note 1 below)} \qquad 14\text{-}7$$

where the mass has been found using continuity. A good approximation to ρ_2 is

$$\rho_2 = \rho_1 \left(\frac{p_2}{p_1}\right)^{1/k} \qquad 14\text{-}8$$

Although this assumes reversible flow, the error in calculating the density will be very small for a nozzle. Then the force of reaction on the walls of the control volume, which is equal and opposite to F, is

$$F_R = A (p_{\text{surr}} - p_1) - \frac{\rho_2 A v_2^2}{g_o}$$

(Notice that the force is to the left in Fig. 14-1 as F_R will have a negative value). We could write in terms of absolute values

$$|F_R| = \left|A (p_1 - p_{\text{surr}}) + \frac{\rho_2 A v_2^2}{g_o}\right| \quad \text{(see note below)} \qquad 14\text{-}9$$

By measuring $|F_R|$, p_1, p_{surr}, T_1 and A, we can now compute v_2. F_R is measured by determining the swing of the pendulum and the weight of the pipe. A pressure gage and thermocouple in the pipe allow p_1 and T_1 to be measured. Area A is simply measured

---

Note:

1. When the ratio of the nozzle exit pressure to the nozzle pressure, p_{surr}/p_1 is less than a certain critical value, the flow is restricted by the properties at the nozzle throat. These are called critical properties, which can be designated p^*, ρ^*, T^*, etc. For air, $p^*/p_1 = 0.53$. Consequently the reaction force must be written

$$|F_R| = \left|A (p_1 - p^*) + \frac{\dot{m}}{g_o} v_2\right|$$

and $\dot{m} = \rho^* A v^*$

But $v^* = k g_o R T^*$

hence for air, $k = 1.4$, $R = 53.8$ lbf-ft/lbm-$^\circ$R

$$\dot{m} = 0.532 \frac{p_1 A}{T_1} \text{ lbm/sec.}$$

for ideal flow to the nozzle exit. For a more complete discussion of this see, for example, Shapiro, A, "The Dynamics and Thermodynamics of Compressible Flow", vol. 1, The Ronald Press, New York, N. Y., 1953, p. 85.

as is environmental pressure p_{surr}. Now both v_2 and iv_2 can be found along with k_n. This can be repeated for various nozzle pressures, p_1, and a graph of k_n vs. iv_2 can be prepared. Pressure p_1 can be controlled by means of a valve on the air supply.

Sample results

An experiment was performed using the test facility illustrated in Fig. 14-1. Air was available from a tank supplied by a small compressor. The air system was capable of sustaining a pressure of 35 psig at the nozzle.

Results for two tests are given in the following table:

Deflection of pendulum, θ, degrees	Nozzle Conditions Temperature T_1, ^oF	Pressure p_1, psig
5	75	30.0
6	75	40.0

Atmospheric pressure 14.7 psi

Weight of nozzle, pipe and attachments = 8.5 lbm

Diameter of nozzle at exit = 0.125 in

Area of nozzle at exit = $\frac{\pi(.125)^2}{4}$ = 0.0123 in^2

c_p = 0.24 B/lbm - ^oF

First Test $iT_2 = T_1 \left(\frac{p_{surr}}{p_1}\right)^{\frac{k-1}{k}} = 535 \left(\frac{14.7}{44.7}\right)^{.286} = 389R$

$iv_2 = 223.8 \sqrt{.24\ (535-389)} = 1325$ ft/sec.

$F_R = 8.5 \sin 5 = 0.741$ lbf

As the pressure ratio is $\frac{14.7}{44.7} = .328 < .53$ the mass flow is (see foot note)

$\dot{m} = .532 \frac{(44.7)(.0123)}{535} = 0.0126 \frac{lbm}{sec}$

Then for the sub critical pressure ratio, with $p^* = p_1\ (.53) = 23.7$ psia the velocity found from eq. (14-9) is

$$v_2 = \frac{F-A(p_1-p^*)}{} = \frac{0.741-0.0123\ (44.7-23.7)}{\left(\frac{.0126}{32.2}\right)}$$

v_2 = 1234 ft/sec.

$k_n = v_2/iv_2 = 1234/1325 = .93$

Second Test $iT_2 = 535 \left(\frac{14.7}{54.7}\right)^{.286} = 367R$

$iv_2 = 223.8\ \ .24\ (535-367) = 1419$ ft/sec.

$F_R = 8.5\ (\sin 6) = 0.946$ lbf

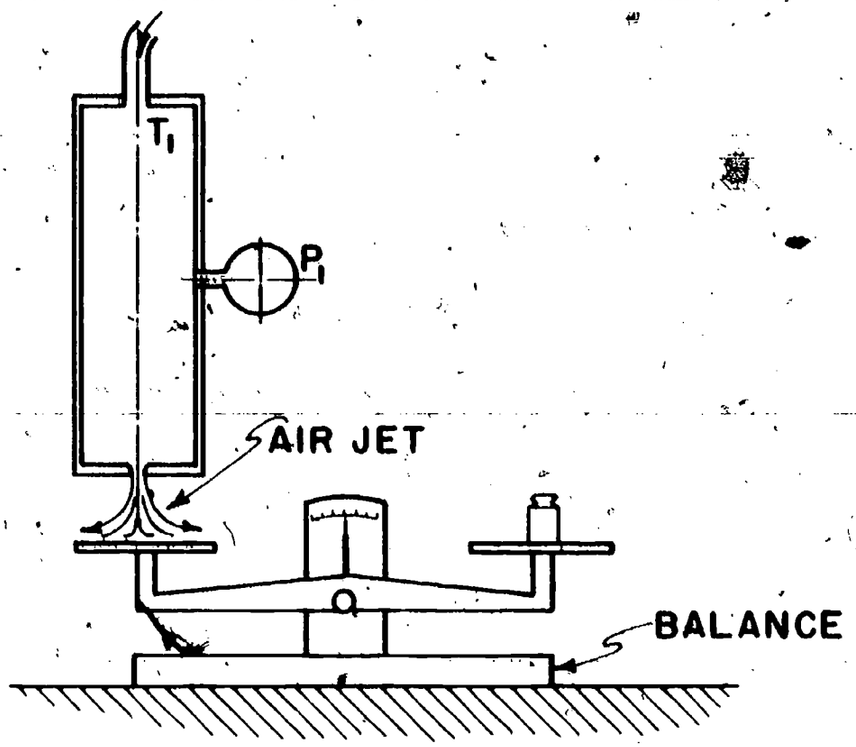

FIG. 14-3 IMPULSE EXPERIMENT

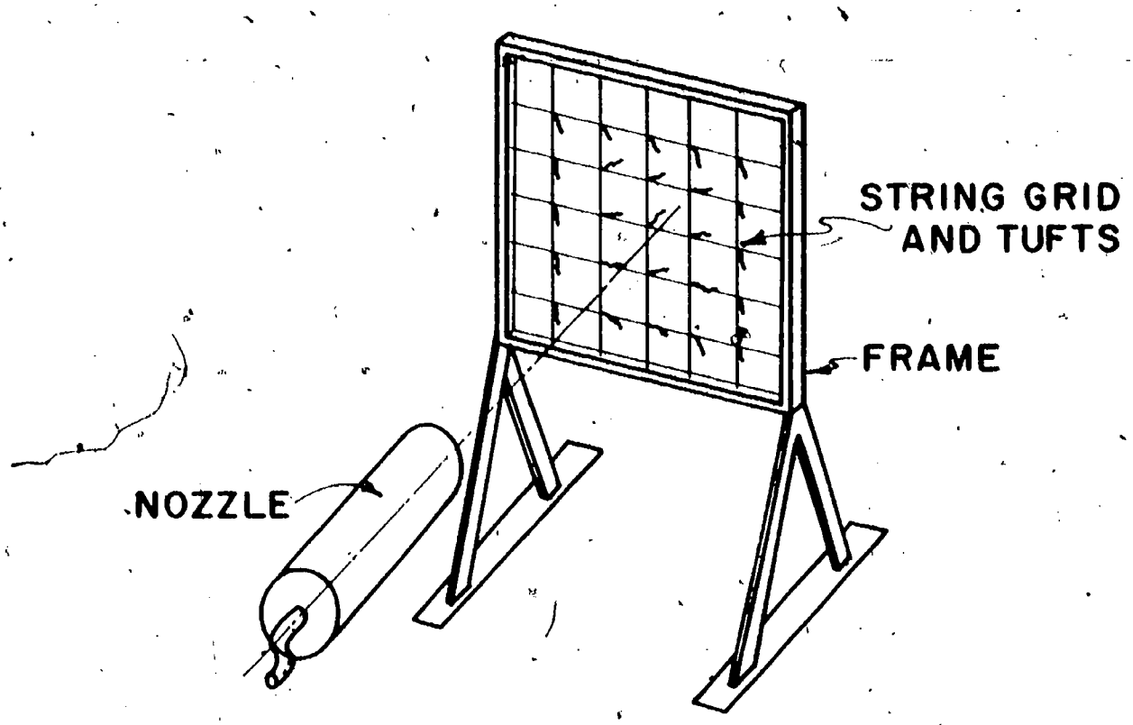

FIG. 14-7 TUFTS FOR JET VELOCITY DISTRIBUTION

Again, the pressure ratio is less than critical. It is

$$\frac{14.7}{54.7} = .269 < .53$$

The mass flow is (see foot note)

$$\dot{m} = \frac{\sqrt{532(54.7)(0.0123)}}{535} = 0.0155 \frac{\text{lbm}}{\text{sec}}$$

Then with $p^* = 54.7(.53) = 29.0$ psia

$$v_2 = \frac{0.946 - 0.0123(54.7-29.0)}{(\frac{.0155}{32.2})} = 1309 \text{ ft/sec.}$$

$$k_n = \frac{1309}{1419} = 0.92$$

With additional test data these results can be plotted as a function of the nozzle pressure, p_1, or the ideal exit velocity v_2.

One possible modification of this experiment can be done by constructing nozzles of different lengths or shapes. Then velocity coefficients can be compared for the different nozzle shapes

A simpler form of this experiment can be done using water as the fluid.

Experiment 14A

Measurement of Impulse in a Jet of Fluid

The object of this experiment is to measure the impulse force when a jet strikes surfaces of different geometry.

An extension of the previous experiment can be made by measuring the impulse in the jet from the nozzle of Experiment 14. A system was built, as shown in Fig. 14-3. The nozzle was fastened to a support, with the jet pointing vertically downward. Placed several inches below the nozzle was a balance at which the jet was directed. This permitted the impulsive force (reaction force in the jet) to be measured by means of the balance. The objective of the experiment was to measure the force with several shapes used to change the impulse. Based on measurements of T_1, p_1 and p_2 the mass and velocity (or momentum) in the jet could be determined. These are idealized values. Then the measured impulse force could be compared to the value computed from the pressure and temperature measurements. Five shapes were used. These are shown in Fig. 14-4. They vary from a simple flat plate to surfaces with two dimensional flow dividers.

Method of calculation

For each test, the pressure in the nozzle, p_1, was set, and readings of T_1, p_{surr} and the force on the balance were recorded.

To compute the theoretical force, the momentum of the jet at the nozzle exit was found as the product of mass, $\dot{m}$, times velocity.

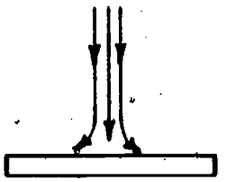

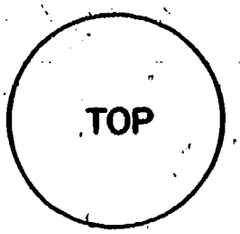

SHAPE A
FLAT PLATE

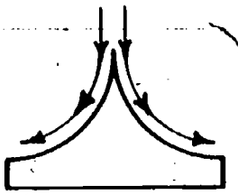

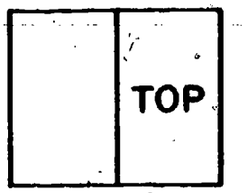

SHAPE B
TWO DIMENSIONAL CURVE

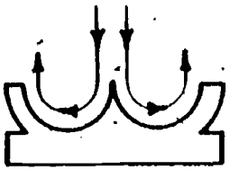

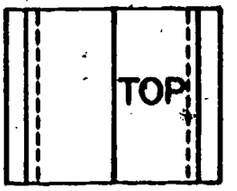

SHAPE C
TWO-DIMENSIONAL
REVERSE CURVE

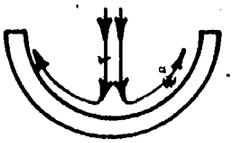

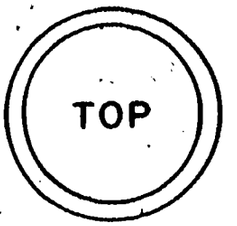

SHAPE D
HEMISPHERE

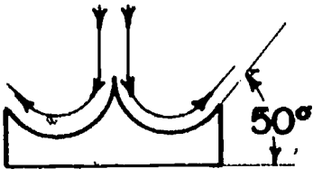

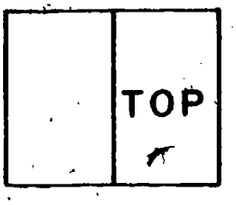

SHAPE E
TWO-DIMENSIONAL
50° EXIT ANGLE

FIG. 14-4 IMPULSE SHAPES

Here, referring to Experiment 14, eq. (14-4), (14-5), (14-7) and the gas law,

$$iv_2 = 223.8\sqrt{c_p\,(T_1 - iT_2)}$$

$$iT_2 = \left(\frac{p_1}{p_2}\right)^{\frac{k-1}{k}} T_1$$

$$\dot{m} = \frac{\rho \pi d^2}{4}\,(iv_2)$$

$$\rho = \frac{p_2}{RT_2}$$

For cases in which the pressure ratio is less than critical determine the mass flow as

$$\dot{m} = 0.532\,\frac{p_1 A}{T_1}$$

The force depends on the geometry of the object placed on the balance. For steady flow, the force can be found by applying the momentum equation to a control volume. As the jet is not confined the pressure forces are balanced, thus the force against the object is

F = momentum flux in vertical direciton flowing out
- momentum flux in vertical direction flowing in

For the flat plate, case A, the efflux of momentum is horizontal so $\dot{m}v_y = 0$ and

$$F = \dot{m}v_2 \qquad 14\text{-}10$$

where v_2 is the nozzle velocity or gas velocity in y-direction entering the control volume.

This is also true for configuration B. The sphere andsplit through, cases C and D have y- momentum flowing out of the control volume. It is

$$\text{momentum out} = -\dot{m}v_2$$

Consequently, as the in-flux of momentum is $\dot{m}v_2$, the total force is,

$$F = 2\dot{m}v_2 \qquad 14\text{-}11$$

With the exit reduced to 50°, configuration E, the efflux was

$$\dot{m}v_2 \sin 50^\circ = \dot{m}v_2(.7660)$$

and the force on the balance

$$F = \dot{m}v_2 + \dot{m}v_2\,(.7660) = 1.7660\,\dot{m}v_2 \qquad 14\text{-}12$$

With the several impulse surfaces mounted on the balance, the actual impulse force F_R can be measured as a function of the pressure in the nozzle. From the equations for ideal flow, the ideal nozzle exit velocity, iv_2, and mass flow can be found as a function of nozzle pressure, and the ideal impulse computed, F. From these computations a ratio of measured force F_R to ideal force F, can be used to express the effectiveness of each surface. Then these ratios can be plotted as a function of the ideal exit velocity, iv_2.

FIG. 14-5 NOZZLE VELOCITY AND IMPULSE FORCE FOR FIVE IMPULSE SHAPES

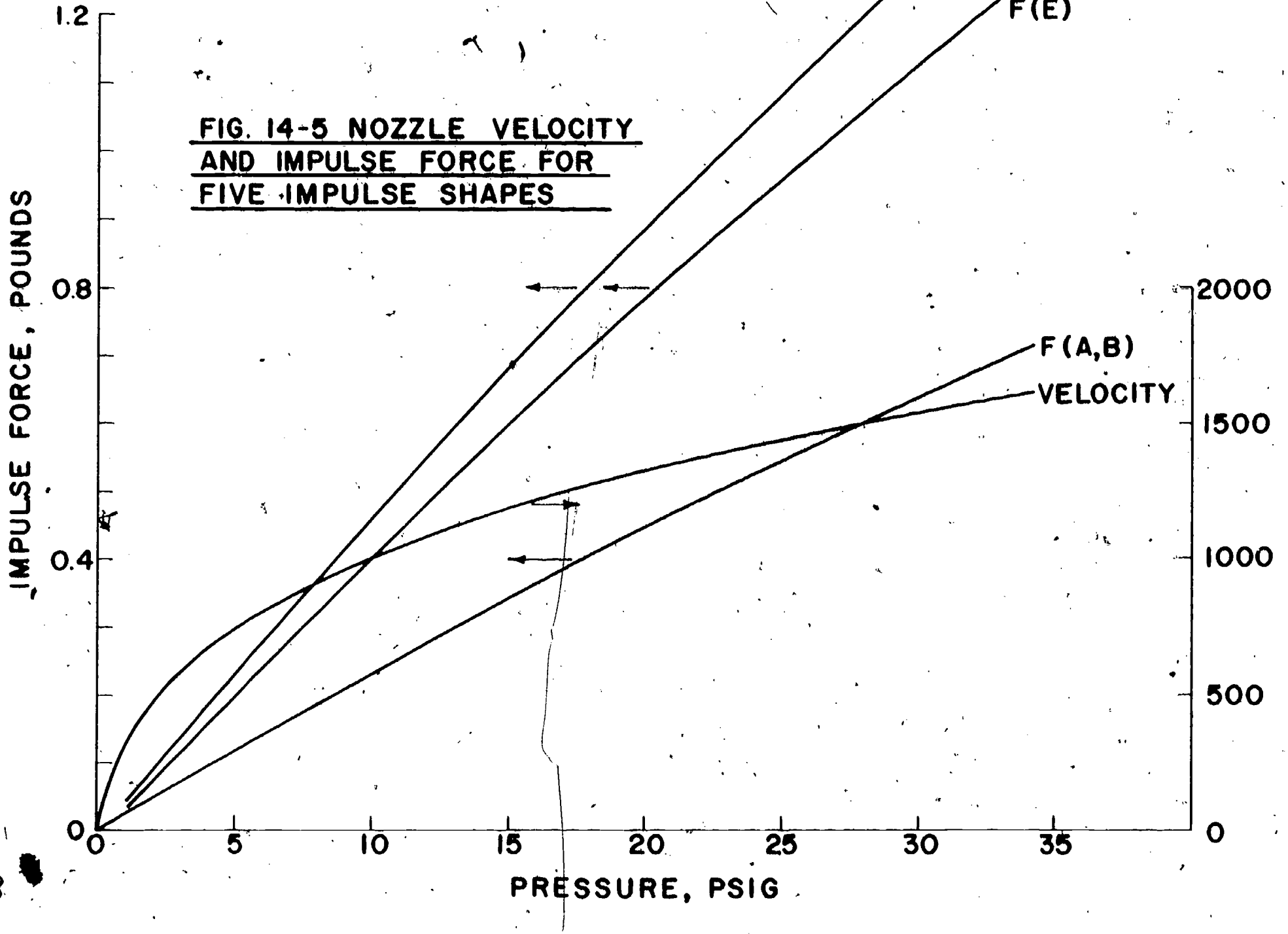

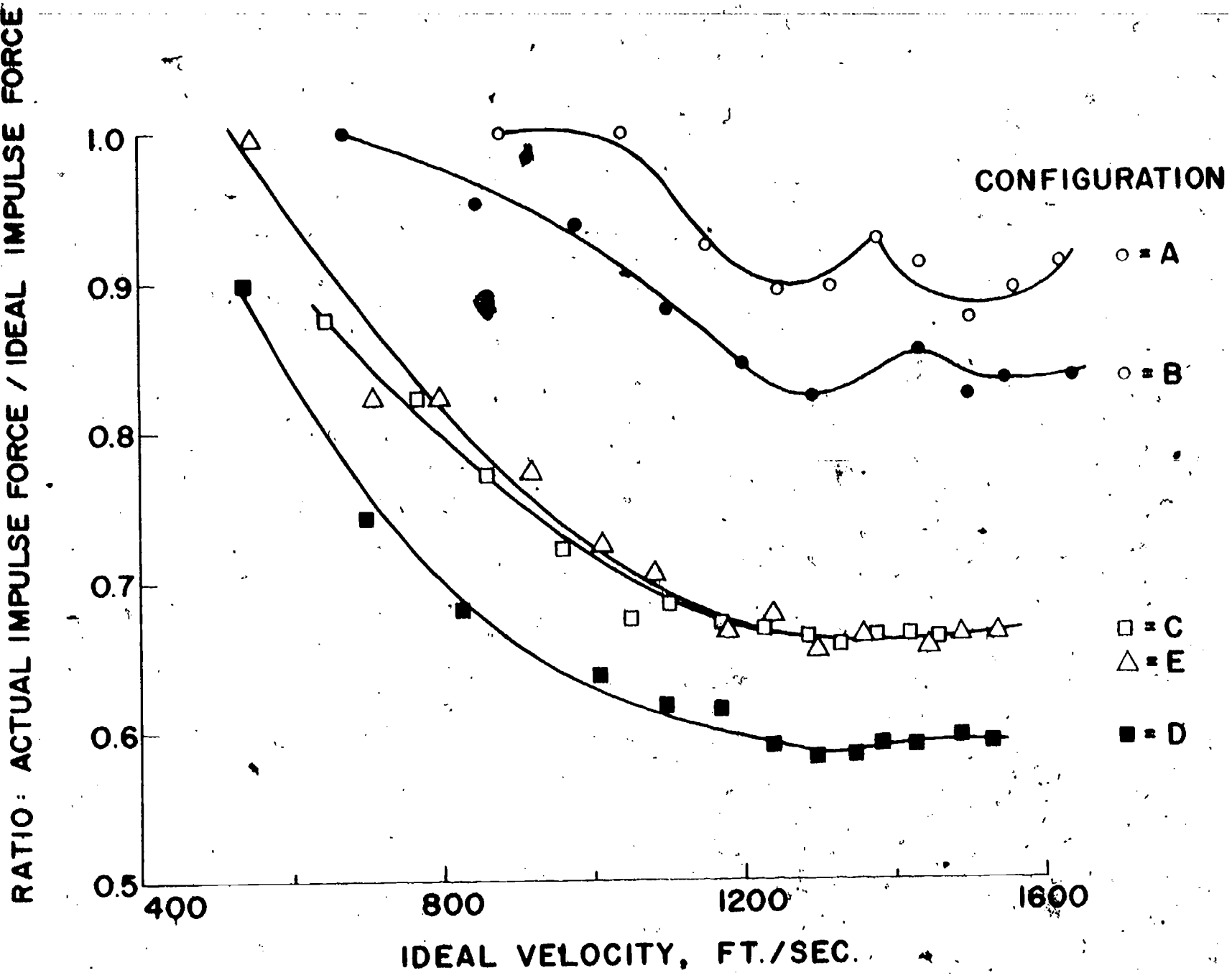

FIG. 14-6 CURVES OF VELOCITY COEFFICIENTS FOR FIVE IMPULSE DEVICES

Sample results

Experiments were run using the 0.125 in diameter nozzle, and the five shapes shown in Fig. 14-4. As the temperature in the nozzle remained nearly constant it was possible to generate curves of ideal exit velocity and impulse force as a function of nozzle pressure and surface shape. Curves of impulse force for the five shapes and ideal exit velocity for the nozzle are shown in Fig. 14-5. For each experiment, the ideal impulse force was taken for the measured nozzle pressure from the appropriate curve of Fig. 14-5. This was then compared to the measured force in the ratio F_R/F. Using the ideal velocity taken from the curve in Fig. 14-5, this ratio was plotted to produce the points in Fig. 14-6.

These data are from a student conducted experiment, and no attempt is made here to evaluate the results. However, there is consistency among data for each surface, and it is evident in every set that there is an increase in effectiveness near v_2 = 1400 ft/sec. Consequently, this inflection was incorporated in the "[illegible]ed" curves drawn through the data. It is more pronounced for cases A and B.

Experiment 14B

Distribution of a Free Jet in Air

> The object is to measure the shape of the plume of a jet of air into air.

Using the nozzle system of Experiment 14, it is possible to map the distribution of the jet in a room of still air. With a simple hot-wire system, velocity can be measured in planes aligned normal to the nozzle axis and at different distances from the nozzle exit. This provides a three dimensional distribution of velocity in the plume of the jet. Maps showing lines of constant velocity can be constructed.

A simpler version of the above, can be done by constructing a square about 4ft x 4ft of light piping, mounted on a portable stand. Twine is then attached across the piping to form a square grid as shown in Fig. 14-7. At the intersection of the cross strings, small tufts of light yarn are fastened. When the air jet is started some of the tufts on the frame will be affected by the air movement. By moving the frame along the axis of the jet, a qualitative distribution of the jet plume can be constructed.

In each of the cases, the nozzle pressure can be changed and the jet distribution mapped as a function of the nozzle pressure.

Experiment 14C

Noise in a Jet

> The objective is to measure the sound level and distribution of sound level in a jet plume.

Another experiment was run with the nozzle to determine the distribution of sound. The nozzle was run in free air, and the room probed with a small microphone and a sound level meter. From the readings maps were prepared to show the level of sound in the jet and in the room. The distribution of sound was then compared to the distribution of jet velocity. A line of maximum sound intensity was found starting at the nozzle center line

and spreading conically, until at a distance 24 ft. from the exit plan, the cone radius was 9 feet. Sound level maps were prepared in two dimensions for a nozzle pressure of 33 psig.

In addition, two mufflers were constructed, applying 2 inches of fibreglass insulation to wire cloth. One muffler was cylindrical, 3 feet long and 22 inches inside diameter. The second was conic, 33 inches long, with an inside diameter of 4-1/2 inches on one end and 19-1/2 inches on the other. Sound suppression was disappointing, and the velocity patterns were altered by both suppressors. At the exit of the conic muffler sound levels changed, periodically. It was also observed that the flow as observed by a hot-wire trace on an oscilliscope changed from laminar to turbulent to laminar as the sound level changed.

Experiment 14 D

A Simple Shadowgraph

The objective is to view a compressible jet using a simple shadowgraph.

When a gas flows at a high speed, the density variations in the gas become sufficiently large to affect the index of refraction. In fact density variation due to temperature differences cause changes in the index of refraction so large that nearly everyone has observed them. These are the distortion waves seen rising from a road on a hot day, or the waves that can be observed rising from the shadow of your hand in sunlight. This is the principle of the shadowgraph, observing the distortion as shadows cast by a source of parallel light. There are more sophisticated optical systems, for example the schlieren system or the interferometer.

A simple shadowgraph can be constructed to observe the wave patterns in a supersonic jet using a slide projector as a light source. Place the projector about ten to twenty feet from the nozzle jet with the light shining through the jet at right angles to it. Then place a ground glass or white paper close to the jet and in the light path. It may be necessary to put the paper 1/2 inch from the jet center line to get the shadow in focus. Now run the nozzle with nozzle pressures more than 1.9 times atmospheric to insure supersonic flow. A diamond pattern of shock and expansion waves will be observed in the shadow cast on the ground glass. Because the nozzle is small, the shadowgraph is small and faint, but it can be observed by magnifying it; photographed with a close-up lens; or displayed on a television monitor with close-up lens in the video camera.

Bibliography of Experimentation

Baird, D. C., Experimentation: An Introduction to Measurement Theory and Experiment Design, Prentice-Hall, Englewood Cliffs, N. J., (1962)

Beckwith, Thomas G. and N. Lewis Buck, Mechanical Measurements, Addison-Wesley, Reading, Mass., (1969)

Brighton, J. A., Fluid Mechanics Instruction Laboratory, Dept. of Mechanical Engineering, Penn State Univ., University Park, Pa., (1968)

Cook, Nathan H. and E. Rabinowicz, Physical Measurement and Analysis, Addison-Wesley, Reading, Mass., (1963)

Engineering Concepts Curriculum Project, Man Made World: Laboratory Manual, McGraw-Hill, New York, N. Y., (1968)

Holman, J. P., Experimental Methods for Engineers, McGraw-Hill, New York, N. Y., (1966)

Landis, F., J. T. Anderson, K. N. Astill, P. W. McFadden and W. C. Reynolds, Laboratory Experiments and Demonstrations in Fluid Mechanics and Heat Transfer, Dept. of Mechanical Engineering, New York Univ., New York, N. Y., (1964)

Lewis, H. Clay, Chemical Engineering Laboratory Problems, School of Chemical Engineering, Georgia Institute of Technology, Atlanta, Ga., (1957)

McFadden, Peter W. and Warren R. Stevenson, An Undergraduate Heat and Mass Transfer Laboratory, School of Mechanical Engineering, Purdue University, Lafayette, Indiana, (1967)

Moore, Mark B., Theory and Application of Mechanical Engineering Measurements, Van Nostrand, New York, N. Y., (1960)

Rabinowicz, Ernest, An Introduction to Experimentation, Addison-Wesley, Reading, Mass., (1970)

Schenck, Hilbert, Jr., Theories of Engineering Experimentation, McGraw-Hill, New York, N. Y., (1968)

Schenck, Hilbert, Jr., Case Studies in Experimental Engineering: A Programmed Approach, McGraw-Hill, New York, N. Y., (1970)

Shoop, Charles F. and George L. Tuve, Mechanical Engineering Practice, McGraw-Hill, New York, N. Y., (1956)

Ver Planck, D. W. and B. R. Teare, Jr., Engineering Analysis, John Wiley and Sons, New York, N. Y., (1954)

Young, H. D., Statistical Treatment of Experimental Data, McGraw-Hill, New York, N. Y., (1962)